A Destruction/Contraction Gradient Coordinates a Persistent and Polarized Global Actin Flow to Control Cell Directionality

Lawrence Yolland

A dissertation submitted in partial fulfillment

of the requirements for the degree of

Doctor of Philosophy

of

University College London

Department of Mechanical Engineering

University College London

September 2018

I, Lawrence Yolland confirm that the work presented in this thesis is my own. Where information has been derived from other sources, I confirm that this has been indicated in the thesis.

Signed……..

Abstract

Cell motility is hypothesised to be regulated by a step-wise series of events, beginning with leading-edge extension of the membrane. However, it is unclear how rapid leading-edge movements are capable of generating coordinated cell motion. Posterior to the leading edge is the flowing Actin network, which generates cellular propulsive forces. This flow is driven by a combination of Actin polymerisation pushing against the leading-edge, and myosin mediated contraction of the Actin network. Yet, it is unknown how this flow is organised and whether it is involved in controlling cell migration.

Through the development of novel computational tools, I show that Actin retrograde flow in developmentally dispersing Drosophila macrophages is highly coherent. Mathematical analysis of Actin flow within macrophages reveals distinct regions of network compression, which are highly persistent in time compared with the leading edge. This data also highlights super-convergent regions within the flow field that represent a sudden transition from retrograde to anterograde Actin motion, whose polarity with respect to the nucleus strongly correlates with cell motion. This unveils a structure and asymmetry to global Actin flow within migrating cells, which I hypothesise is responsible for driving movement through a ‘rear wheel drive’ mechanism of cell migration as opposed to the putative leading-edge mediated ‘front wheel drive’ mechanism of directing cell motion.

Impact Statement

In this thesis I outline my data regarding the underlying mechanisms of cell migration, which should be of interest to basic and translational cell biologists alike. In order to reverse engineer the process of cell migration, I have developed techniques that quantify and track the driver of migration, the Actin cytoskeleton. For this purpose, novel computational approaches and a convenient *in vivo* model system are used. The model system is the Drosophila embryonic macrophage, a genetically tractable cell type that is also highly amenable to imaging. Through analysis of these macrophages I have aimed to elucidate the biomechanics of these migrating cells during embryogenesis. This biomechanical approach could also be used in the study of other macrophage specific behaviours that rely on the dynamics of the Actin cytoskeleton, including but not limited to phagocytosis. As a consequence, this work represents a significant advance in the understanding of cell motion and the Actin cytoskeleton overall, which will be of interest to cell motility researchers as well as researchers invested in the translational component of cell biology. In order to gain insight into the underlying mechanisms of organism development or disease, a deep understanding of cell motility is required. Therapeutic strategies can be developed from this new understanding to address, for example, the mechanisms underlying invasive tumour cell migration or the dynamics of T cells in Rheumatoid Arthritis.

Acknowledgements

I would first like to express my gratitude to the BBSRC LIDo DTP for providing the financial support in order to undertake this study. I am especially grateful to this programme as it has fostered a brilliant community of talented researchers that I can call friends. I would like to thank my supervisors Professor Mark Miodownik at University College London and Dr Brian Stramer at King's College London for providing guidance and support throughout the last four years. I am also deeply indebted to my friends and family for their care and encouragement. Finally, I would like to express my gratitude to my girlfriend Gemma, who has been a constant source of inspiration, and with whom I have shared the ups and downs of my PhD journey.

Contents

Table of Figures

1 Literature Review

1.1 The Machinery of Cell motility

1.1.1 Actin: the fundamental building block of cell motility

Cell migration is thought to be a cyclical stepwise process that is initiated through the polarisation of the cell, defined by asymmetric extension of the cell boundary which defines the front of the cell, and as such the direction of cell migration (Ridley *et al.*, 2003). This migratory process involves a number of discrete, albeit highly integrated events to produce an inchworm effect (Lauffenburger and Horwitz, 1996; Mitchison and Cramer, 1996). These steps are (1) extension of a leading edge through the polymerisation of Actin filaments, (2) association of the Actin network to the migratory substrate through adhesions, (3) actomyosin contraction that pulls the cell body forwards, and (4) adhesions at the rear are disassembled and tail of the cell retracts. This process is facilitated by the dynamics of Actin and its effectors, such as; the contractile protein Myosin II; mediators of Actin assembly and disassembly, such as Profilin and Cofilin; and the focal adhesion complexes. Actin, its effectors and the ways they are currently understood to integrate into a complex migratory machine will be discussed here.

Actin is a 42kDa globular protein (G-Actin) that polymerises into helical filaments also known as F-Actin, and these two forms are in dynamic equilibrium (Blanchoin *et al.*, 2014). Here, Actin monomers associate to form dimers and then trimers, and it isn't until this trimer has been constructed that elongation of the filament is initiated (Figure 1.1). F-Actin is kinetically

polarised with one end, the barbed end, undergoing monomer addition at a faster rate than the pointed end (Pollard, 1986). Actin has three fundamental phosphorylated states: ADP-Actin, where Actin is bound to ADP; ADP-Pi-Actin, where Actin is associated with ADP and an inorganic phosphate (ADP-Pi-Actin); and ATP-Actin, which as the name suggests is Actin bound to ATP (Burnett and Carlsson, 2012). In the ADP-Actin state it dissociates from the filament (Bugyi and Carlier, 2010). Once Actin filaments have formed, they can be organised into complex arrays that provide structural support for cells and are utilised in a wide range of dynamic activities during cell migration (Figure 1.1).

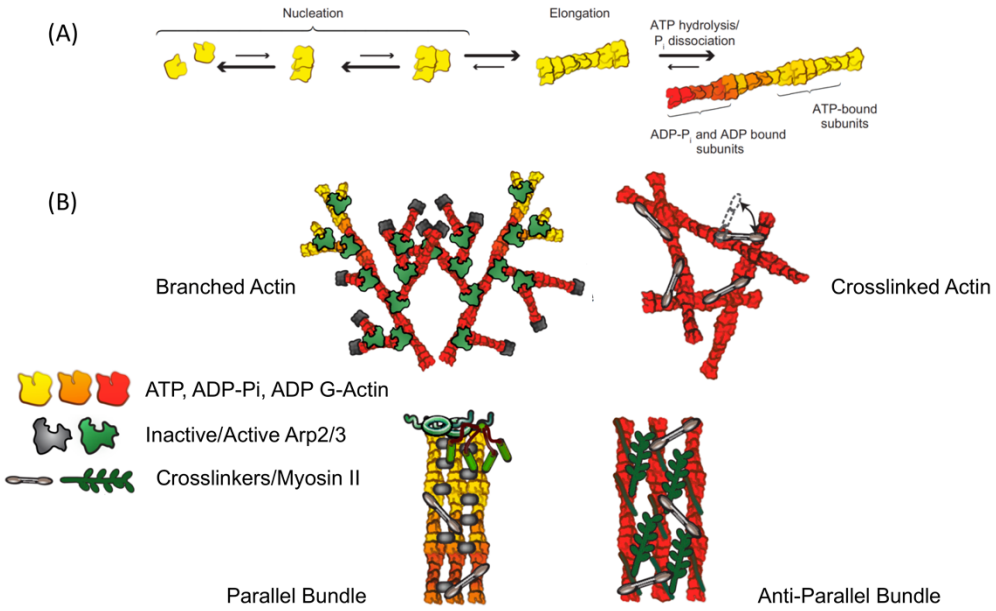

Figure 1.1: Schematics showing Actin filament assembly and the abundance of structures Actin can build. **(A)** The assembly of filamentous Actin (F-Actin) from monomeric globular G-Actin requires a nucleation step involving the formation of Actin dimers and trimers. **(B)** There are four Actin structures that are important in cell motility. The first (top left) are the branched

Actin structures mediated by Arp2/3 (green). Arp2/3 nucleates the formation of new filaments from extant ones. Filament lengths are limited through capping proteins (black). Crosslinked Actin structures (top right) feature Actin filaments with no specific polarity and are linked together by crosslinking proteins (grey rods). Parallel bundles (bottom left) are arrangements of Actin filaments in tight bundles, with a common polarity, facilitated by formins (the menagerie of structures at the tip of the bundles). Anti-parallel bundles (bottom left) involve the collaborative effort of crosslinkers and Myosin-II to bundle F-Actin. Schematics adapted from (Blanchoin *et al.*, 2014).

Extensions of the cell membrane via the growth of Actin filaments initiates a cycle of events are thought to direct cell motion. This process is dependent on the ability of Actin filaments to act as force generators against the membrane (Prass *et al.*, 2006; Heinemann, Doschke and Radmacher, 2011). The ability of F-Actin to produce force against a substrate is thought to be a result of a Brownian ratchet (Peskin, Odell and Oster, 1993; Mogilner and Oster, 1996, 2003a). In the Brownian ratchet, the thermal motion of Actin filaments reveals a gap between the tip of the filament and the object to be pushed which is subsequently occupied by an Actin monomer. When the filament returns to its lengthened state it forces the cell membrane (or bacterium of Actin comet tails) forwards (Mogilner and Oster, 1996).

Actin structures undergo constant remodelling which allows for a rapid response to the cellular environment, and remodelling is vital for cell motility. This remodelling is achieved on a larger scale by assembling and

disassembling the Actin network at the front and the rear of the cell respectively, and is known as treadmilling (Rafelski and Theriot, 2004). Actin filaments are capable of forming a dense meshwork in a branched formation and this is described by the dendritic nucleation model, and involves a number of accessory proteins, including Arp2/3, Cofilin, Arp2/3 Complex Activating Nucleation Promoting Factor, Profilin, and a barbed end capping protein (Nicholson-Dykstra, Higgs and Harris, 2005). The branched Actin network is located within the lamellipodia, a flat structure that is found at the cell periphery. The rate limiting step for network assembly is the concentration of free G-Actin monomers, as such a reservoir of these monomers must be maintained through accessory proteins. Profilin is deeply involved in Actin homeostasis, as it has the capacity to inhibit the production of new filaments by binding to G-Actin monomers. This sequestering behaviour of Profilin is supplemented by its ability to 'prepare' G-Actin for polymerisation by catalysing the exchange of ADP for ATP (Vinson *et al.*, 1998). ATP-Actin is now capable of being incorporated into the polymerisation machinery (Pollard and Borisy, 2003). Profilin renders G-Actin monomers unable to be added to the pointed ends of filaments, as such they are added to the barbed ends. The sequestered Actin that is associated with Profilin, binds at the barbed end of the filament and abuts the cell membrane. The cell membrane can extend here because F-Actin is kinetically polarised, with polymerisation predominantly occurring at this end of the filament which pushes the membrane outwards (Nicholson-Dykstra, Higgs and Harris, 2005). The barbed end is eventually capped, and the disassembly that is occurring at the pointed end continues, producing a large supply of monomeric G-Actin. The process of assembly and

disassembly is variable among filaments within an Actin array, with some filament lengths fixed through a variety of capping proteins at both poles, other filaments are allowed to extend against the leading edge, while others feature a capped barbed end and a disassembling pointed end (Mogilner and Oster, 2003b). The transformation of single Actin filaments into an organised array or meshwork is presumed to be in service of producing enough force to protrude the membrane.

The assembly of F-Actin into branched structures is partnered with the formation of Arp2/3 independent crosslinked Actin (Figure 1.1 B). This crosslinking behaviour allows for a greater diversity of Actin structures that can be produced, such as filopodia, or stress fibres (Kasza *et al.*, 2010). Unlike the branched arrays of Actin, crosslinked arrays are developed through extant filaments once polymerisation has ceased, for instance there is evidence to suggest that elevating F-Actin nucleation can halt the formation of crosslinked bundles (Falzone *et al.*, 2012). There are a number of other important crosslinkers which include but are not restricted to, Fascin, Fimbrin and Myosin II. Fascin for instance, a highly conserved protein has the capacity to form long parallel bundles out of individual parallel Actin filaments and is the core constituent of filopodia (Courson and Rock, 2010). Unlike Fascin, Myosin II crosslinks Actin in antiparallel orientation (Figure 1.1 B).

Myosin II is a member of the Myosin super family and is a motor protein responsible for contraction of the Actin network. Myosin II consists of three peptide units, which are the two 230 kDa heavy chains, two 17 kDa essential

light chains, and a pair of 20 kDa domains called the regulatory light chains (Vicente-Manzanares *et al.*, 2009). The catalytic activity that is essential for Myosin II's effective contractile ability is seated in its globular head domain which contains an ATP binding site. This head domain is associated with the two light chains, which act as a mechanical lever to slide Actin filaments. Myosin II slides filaments in an antiparallel fashion which results in contraction of the network (Reymann *et al.*, 2012).

1.1.2 Actin network destruction and disassembly

Contraction of the network has huge implications for cell motility but for now I will describe how contraction can result in the destruction of the network specifically. This section will take a detour away from how the Actin network is constructed to describe the remodelling mechanisms utilised in the context of destruction. Myosin II mediated destruction of the Actin network is a two-step process, which begins with the unbundling and splitting of Actin bundles into individual filaments and eventual buckling and breaking of those filaments (Haviv *et al.*, 2008). This was observed in self-organised Actin networks that were decomposed into Actin-Fascin bundles and then singular filaments, following the remodelling activity of Myosin II (Haviv *et al.*, 2008). This was subsequently followed by the severing of these 30-40 μm long filaments into fragments less than 1 μm in length (Haviv *et al.*, 2008). The rate of Actin filament severing is dependent on the concentration of Myosin II, and filaments are taken apart through filament buckling (Ishikawa *et al.*, 2003; Murrell and Gardel, 2012). Severing of Actin filaments appears to occur as a result of the curvature of the filament induced by Myosin contraction. This process of

breaking F-Actin into fragments releases free Actin barbed ends and pointed ends, which could have two consequences dependent on the local monomeric concentration. Which is to say that either broken down free filaments could act to stimulate polymer growth in the presence of an enriched G-Actin reservoir, or stimulate disassembly if the monomer concentration is low (Murrell and Gardel, 2012). Interestingly destruction of the Actin network may have a selective component, whereby filaments that are aligned with the direction of cell travel are under more strain, and thus are more amenable to buckling and disassembly (Adachi *et al.*, 2009).

The other proteins, which are more commonly associated with severing in the Actin network is the Actin Depolymerisation Factor (ADF)/Cofilin family. Cofilin is a 19 kDa protein that is widely distributed within the cell and is deactivated in its phosphorylated form while unphosphorylated Cofilin is activated for Actin filament severing. There is a variable spatial distribution of cofilin which is dependent on the phosphorylation state, with unphosphorylated Cofilin seemingly distributed near the leading edge (Song *et al.*, 2006). The localisation of 'activated' Cofilin near the leading edge is speculated to confine filament severing, which releases free barbed ends for polymerisation, and thus membrane extension (Ghosh *et al.*, 2004; Nishita *et al.*, 2005).

There are a number of mechanisms employed by Cofilin in order to break down F-Actin. The process of Actin severing is a timed process, as Cofilin cannot bind Actin subunits in the ATP state. However, once ATP

hydrolysis has taken place, Cofilin can associate with the filament, it then enhances the rate of dephosphorylation of ADP-Pi-Actin, and this promotes filament aging (Blanchoin and Pollard, 1999). Cofilin takes advantage of a combination of the mechanical and biochemical properties of Actin in order to sever filaments. When F-Actin is decorated with Cofilin there is a significant reduction in filament rigidity (McCullough *et al.*, 2008). Cofilin reduces filament rigidity by shortening the helical pitch of the filament, which results in a weakened structure that is more flexible (McGough *et al.*, 1997; Prochniewicz *et al.*, 2005; Tanaka *et al.*, 2018). The effect of filament weakening by Cofilin could be enhanced because Cofilin can only interact with ADP-Actin which is reportedly more susceptible to flexion (Isambert *et al.*, 1995). Combined with Cofilin's ability to alter the elastic properties of the Actin filament and Myosin's ability to impart stress and cause fragmentation, disassembly may be a complex interplay or feedback process between these two very different proteins. More research is required to confirm this, however results derived from studying Acto-Myosin rings are suggestive of a strong interdependence between disassembly and contraction, where Myosin is shown to be incapable of contracting a network in which depolymerisation is inhibited (Mendes Pinto *et al.*, 2012).

1.1.3 Actin flows and molecular clutches

Actin retrograde flow is a process by which the Actin network en masse, moves centripetally, away from the cell boundary and towards the centre of the cell (Welch *et al.*, 1997). There are two causes of Actin network flow described in the literature. The first is that polymerisation at the leading edge

not only extends the membrane forwards but also acts to push the network rearwards. The second mechanism is initiated through contraction of the Actin network through Myosin motor proteins (Lin *et al.*, 1996; Henson *et al.*, 1999; Maiuri *et al.*, 2015). Early in the study of Actin retrograde flows the polymerisation-based mechanism was dismissed. In experiments that inhibited polymerisation through Cytochalasin treatment, there was shown to be no obvious impact on the centripetal translocation of the Actin network (Forscher and Smith, 1988). As a consequence it was suggested that some other mechanism must be behind Actin flow, namely the activity of non-muscle Myosins, which have the capacity to produce a pulling force on the network (Forscher and Smith, 1988). However, with improvements in imaging technologies, and more advanced methods of flow tracking it has been determined that in many cell types both polymerisation and contraction are required for the instantiation of Actin flows. Interestingly, polymerisation and contraction control independent regions of the Actin cytoskeleton. The independence of these mechanisms was addressed in an analysis of the cytoskeleton of Sea Urchin leukocytes. During Cytochalasin exposure, polymerisation was inhibited but there was found to be Actin flows deep within the cell, towards the rear. The inverse was true during KT5926 (a Myosin Light Chain Inhibitor) exposure, where retrograde flow at the cell boundary was detected but flow towards the rear was arrested (Henson *et al.*, 1999).

For Myosin II dependent Actin flow, it's useful to consider how Myosin II is distributed throughout the cell. The spatial distributions of Actin and Myosin II are inversely related. The Actin network is most dense within the

lamellipodium at the cell front, whereas Myosin II is prominently localised towards the rear of the lamella (Svitkina *et al.*, 1997). There is also an evident band of Actin around the cell body that co-locates with labelled Myosin II, which suggests a region of compression induced accumulation of Actin, mediated by Myosin II prior to the Actin recycling observed in fish keratocytes (Svitkina *et al.*, 1997). With this said, the Actin network is pulled rearwards by a progressively increasing density of contractile Myosin II.

1.1.4 Tracking actin flows in cells

Before I extend any more attention to Actin flow it's important to understand how it can be tracked in order to make interpretations about the organisation of this flowing network. One early study described by the great cellular ethologist Michael Abercrombie highlighted that particles - either carbon from Gurr Indian Ink, Molybdenum Disulphate or cell fragments - that were loosely associated with the substrate, when in contact with a migrating cell were translocated towards the rear of the cell (Figure 1.2 B) (Abercrombie, Heaysman and Pegrum, 1970). This experiment was essentially recapitulated in a more controlled situation with the use of synthetic membrane-bound beads that were positioned on the cell membrane using optical tweezers (Figure 1.2 A) (Lin and Forscher, 1995; Lin *et al.*, 1996; Caspi *et al.*, 2001). Kymographs, a common tool in the study of cell dynamics, have also been utilised for Actin flow analysis (Figure 1.2 C). To produce a kymograph for Actin flow analysis, a fixed line that samples a narrow region of interest is used to extract Actin florescent intensity data from a time series. The regions of interest are subsequently aligned with respect to the temporal sequence in

which they are taken. This creates a new image which visually represents the passage of material through time. The axes of the image denote time (x-axis), and space (y-axis). With this new image, the rate of motion can be determined based on the slope of florescent intensity features, that trace a path through time. Examples of its use in Actin flow analysis can be seen in a number of studies (Jurado, 2004; Alexandrova *et al.*, 2008; Maiuri *et al.*, 2015)

Methods such as kymographs (Figure 1.2 C), or sparse single particle tracking (Figure 1.2 A-B), are limited in their ability to provide information that reflects the global dynamics of the Actin flow field (Figure 1.2 A-C). As a consequence, in order to build a comprehensive picture of the Actin flow field across the cell, different techniques must be used. The most common technique is that of florescent speckle microscopy (Figure 1.2 D). In a sense fluorescent speckle microscopy is at once a method of Actin labelling and the computational single particle tracking technique, known as quantitative fluorescent speckle microscopy (qFSM). Labelling in this method requires a low concentration of fluorescently labelled subunits such as tubulin or G-Actin. These fluorophores are stochastically incorporated into the filaments with the consequence being a speckle-like pattern, and thus trackable fiducial markers embedded within the filaments themselves (Waterman-Storer and Danuser, 2002).

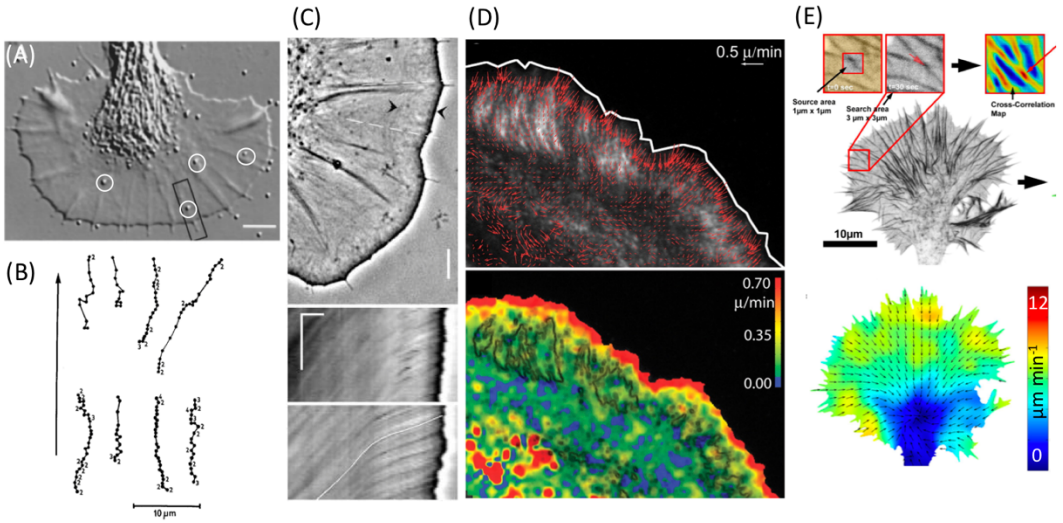

Figure 1.2: Image sequence showing the diverse range of flow tracking techniques. **(A)** Image of a motile growth cone with 200 nm synthetic beads placed onto the cell membrane, these beads move in the direction of Actin flow (adapted from (Lin *et al.*, 1996)). **(B)** Tracks derived from the motion of Gurr India ink particles on the migratory substrate, dragged by the flow of the network. The rear of the cell is at the top of the image (adapted from (Abercrombie, Heaysman and Pegrum, 1970)). **(C)** Kymographs are fixed lines, that sample flurescence intensity changes through time, when these line samples are stitched together the slope of the resulting image represents the rate of translation (adapted from (Alexandrova *et al.*, 2008)). **(D)** Stochastically bound Actin probes produce a speckle pattern throughout the Actin network that allows for the particle tracking capabilities in qFSM. The lower image is a heatmap denoting the speed of Actin flow (adapted from (Hu *et al.*, 2007)). **(E)** The upper image shows the velocity Particle Image Velocimetry workflow, where a region of the Actin network is cross-matched in the subsequent frame of the time-lapse movie. The lower image is a heatmap representing the speed

of Actin flow, with overlaid vectors denoting the local direction of Actin flow (adapted from (Betz, 2007)).

The qFSM tracking technique was introduced in Vallotton et al (Vallotton *et al.*, 2003). In this method there is an automatic screening process in place to select significant particles, these particles are then tracked through time (Figure 1.2 D). For more detail on this technique a comprehensive review of this tracking process is found in (Vallotton *et al.*, 2003). The other predominant method that allows researchers to understand global Actin flow is Particle Image Velocimetry (PIV) (Figure 1.2 E). PIV is utilised within this thesis and as such a detailed description can be found within section 2.3.1. For now, it is useful to note that it is a cross correlation-based technique that tracks the motion of sub-images, which in the context of Actin flow analysis are sub-images containing Actin fibres from time lapse images of cells (Westerweel, 1997; Raffel *et al.*, 2007; Zajac *et al.*, 2008; Betz *et al.*, 2009; Davis *et al.*, 2015). It also has the added advantage of being much less computationally intensive than qFSM. This technique has prominently been used in the study of Actin flow dynamics in neuronal growth cones, and in the study of Drosophila embryonic hemocytes undergoing Contact Inhibition of Locomotion (Betz *et al.*, 2009; Davis *et al.*, 2015) . It has also been used in the study of the Nematode Spermatozoa migration (Zajac *et al.*, 2008).

We now have a multitude of ways to analyse the flow of the Actin network, but what do we currently know about how flow assists in the migration of the cell? For a cell to migrate it must be able create traction forces between

itself and the migratory substrate. The mechanism that allows for a mechanical coupling of the substrate and the cell's Actin cytoskeleton is the Actin clutch (Elosegui-Artola, Trepat and Roca-Cusachs, 2018). This mechanism requires the association of the Actin network with focal adhesions that act to anchor the network to the substrate, this allows for force that was previously pulling the network rearwards to be transmitted into the substrate to allow for a cell to move forwards (Figure 1.3 A) (Beningo *et al.*, 2001; Giannone, Mege and Thoumine, 2009; Kanchanawong *et al.*, 2010). Clutches can be constructed out of a variety of protein constituents from Cadherins and Integrins, and have roles in mechano-transduction but also in the sensing of substrate stiffness (Beningo *et al.*, 2001; Bard *et al.*, 2008; Bangasser *et al.*, 2017). The reasoning behind the naming of this mechanism is an analogy to the mechanics of a clutch within a car. If the clutch is engaged, which is represented by the Actin network's association to focal adhesions, Actin flow slows down while Myosin II contractile forces are transmitted through this linkage into the substrate. When the clutch becomes disengaged, which is represented by the dissociation of the Actin network and focal adhesions, Actin flow speed increases and thus the Myosin II contractile forces are committed towards the rearward motion of the Actin network (Figure 1.3 A, B).

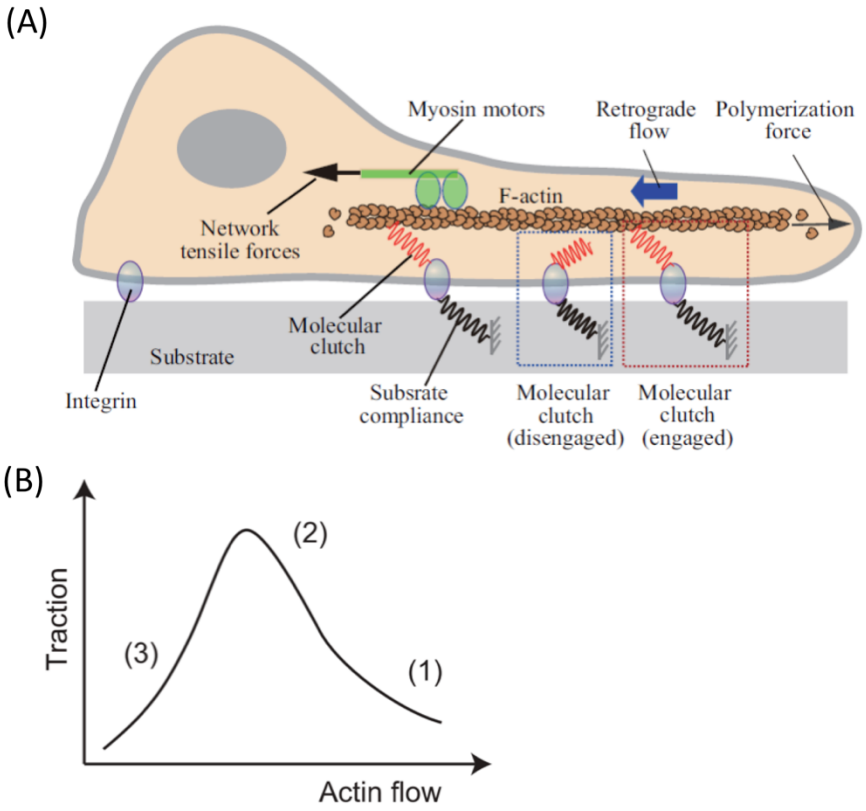

Figure 1.3: Schematic of the Actin treadmilling process that feeds into the molecular clutch. **(A)** Cross sectional schematic of a polarised migrating cell - this cell is moving towards the left edge of the page (adapted from (Okeyo, Adachi and Hojo, 2010)). Within the lamella treadmilling of the Actin network involves a dynamic interplay between polymerisation of Actin at the leading edge, the rearward motion of Actin facilitated by Myosin II, and the destruction of the network at the rear. The Actin network can associate with the migratory substrate through focal adhesions, and this association provides the traction force required for translocation. **(B)** The relationship between Actin flow speed and traction forces is biphasic in nature, as represented in this graphic (adapted from (Schwarz and Gardel, 2012)).

Through the Actin clutch the Actin network becomes coupled to the migratory substrate. This association with the substrate leads to the observation that Actin flow comes to a halt or slows from the perspective of substrate, which is thought to allow for progressive extension of the leading edge (Mitchison and Kirschner, 1988; Jurado, 2004; Barnhart *et al.*, 2011). It has been speculated that not all motion of Actin flow is transmitted into the substrate, which represents slipping of the Actin clutch system, and thus disengagement of the Actin network from the migratory substrate (Mitchison and Kirschner, 1988). There was later assessed to be two causes of retrograde flow in the context of the molecular clutch, which are; slippage of the network from the adhesions, which acts to reduce traction forces on the substrate; and slippage between the adhesions themselves and the substrate which elevates traction forces potentially through a raking process whereby the adhesion receptors are dragged over the migratory substrate (Jurado, 2004). Interestingly when comparing the magnitude of traction stresses and retrograde flow speed, a biphasic relationship was seen (Figure 1.3 B), whereby a positive correlation between traction and Actin flow speed was observed up to approximately 0.5 $\mu m\ min^{-1}$ (in migrating PtK1 epithelial cells). While beyond this flow speed threshold, traction forces decay in an inversely proportional manner (Gardel *et al.*, 2008)

Focal adhesions are a core constituent of the clutch system as they allow for the transmission of traction stress from the motion of the Actin network into the migratory substrate. As such, they are key components of the proposed motility cycle. Integrin based clutches are well characterised in the

literature (Schwarz and Gardel, 2012; Sun, Guo and Fässler, 2016), and the adhesion complexes that form around them allow for mechanical links to be established between F-Actin and the extracellular matrix. Adhesions that are located at the front of the cell are reportedly positioned by local membrane tension (Giannone *et al.*, 2007; Pontes *et al.*, 2017). Nascent adhesions allow for locally confined Actin assembly and reduction of Actin flow speed, however nascent adhesions also undergo a process of maturation where they can produce the contractile forces required for the retraction of the rear, as described by the motility cycle (Giannone, Mege and Thoumine, 2009). This maturation is a linear process which is mediated by Myosin II induced tension which initially causes an increase in nascent adhesion size (Giannone, Mege and Thoumine, 2009).

Initially, Integrins undergo a conformational change from a deactivated to an activated state when Actin retrograde flow associates with Talin, forming nascent adhesions which are associated with the migratory substrate (Jiang *et al.*, 2003; Tadokoro *et al.*, 2003; Case *et al.*, 2015). Paxillin recruits inactive Vinculin to the nascent adhesion, when Actomyosin contraction stretches Talin, Vinculin binding sites are revealed, which is a required step in the activation of Vinculin. Active Vinculin can associate with the flowing Actin network, and strengthen the linkage (del Rio *et al.*, 2009; Thievessen *et al.*, 2013). This process is reinforced through a positive feedback mechanism that involves Vinculin's ability to stabilise the elongated conformation of Talin, which in turn reveals more Vinculin binding sites reinforcing the adhesion site by further engaging the flowing Actin network (Case *et al.*, 2015). As such,

vinculin is thought to be the primary clutch component responsible for the transmission of traction forces into the migratory substrate (Ji, Lim and Danuser, 2008).

The utilisation of flow tracking techniques such as qFSM have revealed a number of intriguing 'topographical' descriptions of the flowing Actin network. For instance, analysis of newt epithelial lung cells, revealed four distinct regions of Actin flow, these are: a fast flowing region representing the lamellipodium; the slower retrograde flow region, determined to be the lamellum; a highly contractile convergence zone that acts as a demarcation between retrograde flow and anterograde flow; and a region of the network that flows in an anterograde fashion (Vallotton *et al.*, 2003, 2004; Ji, Lim and Danuser, 2008; Okeyo *et al.*, 2009). Using qFSM the kinetic and kinematic differences between these zones has been resolved (Ponti *et al.*, 2004; Vallotton *et al.*, 2004). For instance, with the observation that the convergence zone did not collocate with a region of elevated Actin florescence intensity, it was surmised that this region may play a role in network turnover. Specifically that the Actin network is taken apart within the convergence zones (Vallotton *et al.*, 2004). The opposite was true for the leading edge, which features elevated Actin network assembly. In the analysis of flow speed, the flow at the periphery, i.e. the lamellipodia, has been determined in a number of studies to be significantly faster than the flow speed within the lamella (Waterman-Storer and Salmon, 1997; Vallotton *et al.*, 2004). It should be noted that newt lung epithelial cells often used in qFSM (Vallotton *et al.*, 2003, 2004), are a relatively stationary cell type, restricted by cell-cell adhesions and as such,

much more Actin flow analysis in moving cells is required in order to understand how the organisation of Actin flows contributes to cell scale order and cell migration overall.

Through the study of Actin flows, the flows act as an antagonistic regulator of the cell boundary, countering edge protrusions. Early observations of Actin dynamics in growth cones, showed an apparent inverse relationship between the rearward motion of the Actin network and the forward progress of polymerising Actin at the boundary (Lin and Forscher, 1995). This was also supported in the analysis of Actin flow speed and edge extension rates in fish keratocytes (Jurado, 2004). This makes sense in light of the treadmilling model of Actin turnover, which describes a polymer that is added to at the front, pulled rearwards, and disassembled at the back of the cell (Rafelski and Theriot, 2004). Interestingly however, there is data to suggest that the fluctuations of the cell edge are independent of increases or decreases in Actin flow rates, with extensions and retractions occurring stochastically across the cell boundary (Betz *et al.*, 2009).

In order to study the effects of cell-scale cross talk between the cell boundary and the behaviour of the flow, new modelling efforts have been employed. In Mauri *et al.*, they set out to outline the Universal Coupling of Speed and Persistence (UCSP) model, which explains how cells exhibiting faster flows or faster migration speeds turn less frequently (Maiuri *et al.*, 2015). They argue that Actin flow has the capacity to advect away polarity cues from the edge and thus stabilise directional cell migration. This was also supported

with data that suggests that disruption of Actin retrograde flow through Myosin II inhibition resulted in a loss of cell shape asymmetry, whereby the cell rounds and protrudes radially (Lomakin *et al.*, 2015). This is a result of Actin flows no longer being able to advect away Myosin II from the cell boundary towards the rear of the cell.

1.2 **Cell polarity and steering**

Cell migration is principally considered to be a cyclical stepwise process, where a number of steps are required 1) Actin polymerisation driven membrane extensions at the leading edge, 2) an adhesion based process the allows for cells to build traction with the extracellular matrix, (3) actomyosin contraction that pulls the cell body forwards, and (4) adhesions at the rear are disassembled and tail of the cell retracts (Figure 1.4) (Ridley *et al.*, 2003). As previously described this theory of cell motility is initiated by the assembly of the Actin network which acts to extend the cell forwards in a polarised fashion. This assembly and the consequent pushing force can drive the network rearwards. This rearward motion is enhanced by the activity of Myosin motor proteins that act to contract the network. We have seen how the extension of the edge can induce the formation of new nascent adhesions which are associated with the migratory substrate. These associations promote further polymerisation through an engaged clutch-like mechanism. Nascent adhesions also undergo a stress dependent maturation phase which eventually fails and disengages the clutch, and the cell is able to progress its motion through another cycle (Chan and Odde, 2008). This process is framed

as being initiated by the extension of the leading edge and as a result much of the study of cell locomotion has been viewed through this lens.

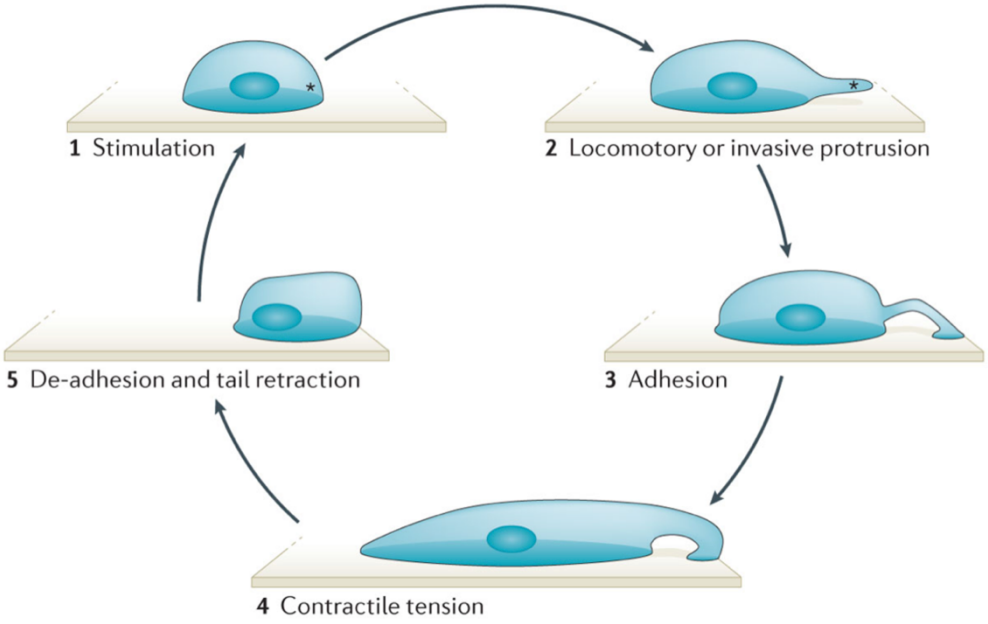

Figure 1.4: Schematic of the motility cycle. The stereotypical model of cell migration is that it is a stepwise cyclical process. This process is initiated by polymerisation activity at the leading edge. This is followed by a process of adhesions, Myosin II mediated cellular contraction, and finally a retraction of the rear of the cell. (Schematic adapted from (Bravo-Cordero *et al.*, 2013)).

1.2.1 The role of the edge in cell directionality

Despite the focus on the leading edge as a driver of cell motion, it is currently unresolved how coordinated cell motion over time can develop from fluctuations of the leading edge. The study of cell migration is compounded by the challenging notion of producing meaningful connections between events occurring at vastly different levels of spatial and temporal description (Rafelski

and Theriot, 2004). There are also experimentally distinct settings in which cell directionality may, to a more or lesser extent be regulated by the cell edge. For instance, cell's migrating towards a chemical cue (directed migration) are often noted to have an elevated migratory persistence and a more focussed leading edge (Petrie, Doyle and Yamada, 2009). While cell's migrating without the environmental influence of a chemical cue (random migration), are less persistent, a function of the environmental exploration that the cell is performing. This isn't just limited to chemical stimuli, as directed migration has been seen through changes in extracellular matrix topography (Park *et al.*, 2016) or a response to electric fields (Guo *et al.*, 2015). Establishing a leading edge during chemotaxis essentially derives from randomly generated protrusions, which are stabilised by chemotactic machinery within the cell which selects for optimal protrusions (Andrew and Insall, 2007). This results in the maintenance of protrusive activity in the orientation of the stimulus, and the fast retraction of peripheral protrusions. This suggests that effective chemotaxis could be considered a consequence of an accumulation and integration of biased 'decisions', that determine the fate of the cell edge (Andrew and Insall, 2007). They also suggested that the ability to induce protrusions was not externally influenced but was regulated principally by internal mechanisms. Migration in the absence of an external cue represents random migration and would be utilised in immune surveillance such as naïve T cells migrating in the lymph nodes seeking out antigen presenting cells (Krummel, Bartumeus and Gerard, 2016). The ability for cells to steer, and maintain polarity is fundamental to their migration, a cell reach a wound site, repolarise from contact inhibition, immune surveillance, or effectively following

developmental migratory pathways, without the ability to regulate its direction of motion. In the study of cell steering and re-orientation much attention has been paid to the role of Actin polymerisation at the leading edge and its capacity to direct cell motion (Krause and Gautreau, 2014).

The ability to switch between directed migration and random migration, or at the very least persistent migration and random migration, might be conferred by up- or down-regulating overall Rac activity in migrating cells and as such the frequency and location of protrusive activity (Pankov *et al.*, 2005). Rac is a member of the Rho GTPase family and is well studied in the context of cell migration (Ridley, 2015). Rac specifically interacts with a complex called WAVE, which in turn activates the dendritic nucleation of Arp2/3 and subsequently produces new lamellipodia. Four morphological and migratory subtypes have been characterised, that are dependent on the concentration of Rac. For instance, in cases of elevated Rac concentrations random migratory behavior has been observed, while a reduction in Rac concentration results in cells that are more capable of persistent migration. However, very low or very high concentrations of Rac result in cells that are unable to migrate. Interestingly, extreme levels of Rac produce cells with a circular and apolar morphology resulting from radially located lamellipodia (Pankov *et al.*, 2005). Characterisation of Rac levels may act as a useful guide in the context of directed migration as the current hypothesis suggests that migration occurs in alignment with the predominant protrusions. As such the finding that Rac knockdowns exhibit fewer peripheral lamellipodia, while the elevation of Rac promotes random migration through the formation of peripheral lamellipodia

that are distributed widely around the cell edge, provides insight into how directed and random migration is regulated by the location of edge protrusions (Pankov *et al.*, 2005). However, interestingly temporal cross-correlation analysis between the local activation of Rac and edge protrusion dynamics, have revealed that peak Rac activity is observed following protrusive activity – around 40 secs after the cell extends out, and is localised around 1.8 microns behind the cell boundary (Machacek *et al.*, 2009). As a consequence, Rac activity has been speculated to stabilise extant protrusions (Machacek *et al.*, 2009). This result has been further substantiated in investigations into the timed activity of Rac, where local Rac inactivation was preceded by local edge retraction and conversely local Rac activation was preceded by local edge extension, again by a 30+ second window (Yamao *et al.*, 2015). Other members of the Rho GTPase family that also increase in concentration locally, following protrusive activity include RhoA and Ras (Yang, Collins and Meyer, 2016).

Cdc42 is another member of the Rho GTPase family implicated in the protrusive activity of the cell, and cell steering, although its role is controversial. For instance, Cdc42 activity has been shown to be locally elevated prior to cell turning in a neutrophil chemoattraction assay (Yang, Collins and Meyer, 2016). However, it should be noted that in another study Cdc42 activity - like Rac activity - actually follows the extension of the cell edge, and it is as yet unclear how these two apparently contrary results are resolved (Yamao *et al.*, 2015). While *in vitro* studies have shown a dependence on Cdc42 for polarisation of the cell and directional migration, there is evidence that *in vivo*, Cdc42 is

dispensable for effective wound responses (Stramer *et al.*, 2005). Depletion of Cdc42 in Drosophila embryonic macrophages (hemocytes) have been shown to be capable of migrating towards a wound site and exhibit standard developmental dispersal patterns across the embryo despite disrupted cell migration behaviours (Stramer *et al.*, 2005).

One protein complex that is well studied in the context of cell persistence and cellular steering is Arp2/3 and Arpin its regulator (Nicholson-Dykstra and Higgs, 2008; Gorelik and Gautreau, 2015). The hypothesis of how Arp2/3 determines cell steering is dependent on its role in the dendritic assembly of the Actin network. The preferential local regulation of branched Actin network assembly results in localised protrusions that are reportedly required for effective cell migration (Pollard and Borisy, 2003). Evidence for the role of Arp2/3 in cell edge dynamics and migration suggests that disruption of the p21 subunit of the Arp2/3 complex in fibroblasts, results in a 'jagged' morphology and an inability to respond to wounding, despite remaining a motile cell type (Suraneni *et al.*, 2012). Negative regulation of Arp2/3 is through the inhibitor Arpin. Arpin activity is a part of an extended circuit of lamellipodial regulation, where Rac1 signalling activates Arpin which in turn inhibits Arp2/3 (Dang *et al.*, 2013). An increase in Arp2/3 activity has been shown to result in more directionally persistent cell tracks (i.e. they had a lower preponderance for turning), heightened migration speed, and an increase in environmental exploration (Dang *et al.*, 2013). While Arp2/3 inhibition, promoted through elevated activity of Arpin, reduces the number of peripheral lamellipodia. This finding was elaborated in further analysis of Arpin, where it was shown that

increasing Arpin activity, reduces cell speed and decreases cell persistence (Gorelik and Gautreau, 2015). However, it should be noted that the evidence for the Arp2/3 in cell migration is controversial and recent analysis has brought into question the effect of Arp2/3 and Arpin in controlling cell directionality. In one study cells lacking Arpin were shown to be as capable of migrating through a cAMP gradient as controls (Dang *et al.*, 2017). While in another study Arp2/3 was shown to be necessary in the formation of lamellipodia, but it was in fact dispensable for chemotaxis (Wu *et al.*, 2012). This by extension could suggest that lamellipodia themselves are not necessary for chemotaxis.

Cofilin a protein linked to F-Actin severing has also been associated with the regulation of cell directionality. For instance, Cofilin has been suggested as a regulator of cell steering, through the production of new lamellipodia (Dawe *et al.*, 2003; Ghosh *et al.*, 2004). The formation of new lamellipodia has been suggested to be regulated in synergy with Arp2/3 activity (DesMarais, 2004). The study of Cofilin in cell steering and cell migration more generally has revealed that depletion of Cofilin in non-metastatic tumour cells results in a decrease in cell speed, an increase in turning frequency, and a transformation from a unipolar morphology to a cell featuring many lamellipodia (Sidani *et al.*, 2007). The role of Cofilin was elucidated in an analysis that utilised photoactivatable Cofilin, whereby stimulation of Cofilin promoted the formation of new protrusions, and a new direction of cell motion (Ghosh *et al.*, 2004). The speculated cause of this was that the activation of Cofilin at the cell edge makes available free barbed ends which subsequently become the new sites for polymerisation and thus edge

extension. In this study, the cell's displacement vector (measured from the motion of the cell's centroid) was compared against the position vector of the photoactivation site, and it was revealed that during activation of Cofilin the alignment of the two vectors increased significantly. This sets up Cofilin, in the words of the authors as a core component of the "steering wheel of the cell" (Ghosh *et al.*, 2004). Interestingly while localised activation of Cofilin results in lamellipodia, that are presumed to be relevant for cell motion, increased Cofilin levels at the cell scale have been implicated as a negative regulator of edge protrusions, potentially by reducing the Tropomyosin concentration (Delorme *et al.*, 2007). Tropomyosin is a protein that stabilises the Actin network, by inhibiting Cofilin mediated severing (Ono and Ono, 2002). As a consequence, if Tropomyosin levels are reduced by globally elevated Cofilin levels, filament severing can increase in the lamella and focussed lamellipodia cannot be constructed (Delorme *et al.*, 2007).

There is significant evidence that events stimulating cell motion do not necessitate initial leading-edge activity. One study showed that cell fragments, could be stimulated into a migratory state by 'pushing' with a micropipette at the rear of the fragment. This activates deadhesion and Myosin mediated retraction of the rear of the fragment, and is thus a rear driven example of cell motion (Verkhovsky, Svitkina and Borisy, 1999). This also precedes a ruffling of the leading edge and an increase in protrusive activity, and thus cell polarity can be established not just by the effective polarity of Actin network assembly that extends the 'front' of the cell (Verkhovsky, Svitkina and Borisy, 1999). This supports earlier findings in Brown and Dunn (Brown and Dunn, 1989) and

Chen (Chen, 1979), whereby an increase in the activity of edge protrusions in fibroblasts was preceded by the retraction of the tail. It has also been shown that symmetry breaking, which is required to establish polarity of the cell is a Myosin II driven event in fish keratocytes, and that sustained retraction of the Actin network at the rear of the cell results in the transition of cells from a rounded morphology to the characteristic canoe-shaped morphology (Yam *et al.*, 2007). The Myosin II dependence was established through blebbistatin treatment, which resulted in only 10% of stationary keratocytes becoming motile. While treatment with Calyculin A, results in cells that undergo symmetry breaking and initiation of migration. Once cell polarity has been initiated persistent retractions of the rear and protrusions at the front then occur (Yam *et al.*, 2007). When flow driven symmetry breaking has been mathematically modelled a negative feedback loop between the rate of Actin flow and adhesion strength has been described (Barnhart *et al.*, 2015). Here stochastic fluctuations in adhesion strength and/or Myosin II contraction can result in a reduction in adhesion strength and an elevation of flow speed, eventually this rate reaches a particular threshold for retraction of the rear to take place (Barnhart *et al.*, 2015). Most recently a study investigating symmetry breaking in Dictyostelium discovered that the process can be dependent on the specific chemical stimulus, here cAMP activates a protrusion-first migratory response, while 8CPT activates a retraction-first migratory response (Cramer, Kay and Zatulovskiy, 2018).

Despite a preponderance of studies focussing on how assembly dynamics at the leading edge can contribute to cell motion, there is evidence

to suggest that the dynamics of the cell edge can actually disrupt coordinated migration. Efficiency as a descriptive parameter of cell migration was introduced in Dunn *et al* (Dunn, Weber and Zicha, 1997). It attempts to integrate the protrusive activity of migrating cells, with respect to the amount of the substrate that is covered during migration. Here, a perfectly efficient migrating cell would extend its membrane just once during one discrete displacement. While inefficient migration would involve many protrusions that lead to a high degree of environmental exploration (Dunn, Weber and Zicha, 1997). While another description of efficiency looks at the ratio between the distance the cell boundary advances in a protrusion and the distance the edge retracts (Delorme *et al.*, 2007). The general point here is that protrusions and retractions are connected to cell migration in some unresolved way, however it is unclear in the 'protrusion driven cell migration' paradigm, how cells can migrate effectively while exhibiting inefficient edge dynamics. Inefficient migration being represented by cells that feature protrusions that do not directly relate to either instantaneous displacements of the cell or the motion of the cell lagged by some time interval (Hermans *et al.*, 2013). Inefficient migration in this sense was experimentally revealed in the migration of leukocytes (Leithner *et al.*, 2016). This study highlighted that extensions of the leading edge are functionally important, for instance in the aiding of leukocyte invasion into complex matrix environments. However, what was interesting here is that cell migration itself was seemingly independent of the activity of the lamellipodia, reducing it to a sensory organelle rather than a driver of motion (Leithner *et al.*, 2016). The idea that lamellipodia and the leading edge are dispensable for the migration of cells was supported in Frtiz-Laylin *et al*.,

in a study of neutrophils (Fritz-Laylin *et al.*, 2017). This demonstrated that upon Arp2/3 inhibition turning frequency of the neutrophils was reduced, and there was a wide distribution of protrusions around the cell boundary, as opposed to control cells that had a primary large protrusion in the direction of travel. However, migration was largely unaffected. This again supports the notion of cell protrusions as organelles used to explore and sample the local environment, rather than being the predominant driver for motion

1.2.2 Actin flows can facilitate cell polarity

With the role of Actin polymerisation and the resulting edge extensions in cell motion explored, it is worth looking at Actin flows and its role in cell migration. Specifically, how Actin flows are utilised in the context of the Actin clutch and the transmission of traction forces into the extracellular matrix. It has previously been suggested that Actin flow speed is inversely proportional to the rate of advance of the lamellipodia, however the relationship between flow speeds and cell speeds is less clear (Lin and Forscher, 1995; Jurado, 2004). There have only been only a few studies that attempt to experimentally link these two parameters. For instance in Jurado *et al*., Actin flow speed was shown to be inversely correlated with cell migration (Jurado, 2004). However, the method of both 'tracking' cell motion and registering Actin flow rates is limited. Only small regions of the lamella were sampled for Actin flow measurements through kymography and did not consider global Actin flow rates. Cell motion itself was defined by the movement of the cell centroid. This can be problematic as centroid displacements are influenced by asymmetric extension of an object's shape, including cellular protrusions.

In another study which examined the process of symmetry breaking, the observation was made that an increase in Actin flow speed was coordinated with the initiation of motion (Yam *et al.*, 2007). In fact, during the symmetry breaking process, the rapid retraction at the rear and the coordinated fast anterograde flow of the network appeared to be aligned with the eventual direction of cell motion. They also noted that Actin flow speed at the front of the cell relative to the migratory substrate during migration was reduced which is an observation in alignment with the concept of the Actin clutch, which suggests that Actin flows will appear to slow in the laboratory reference frame when associating with the migratory substrate (Mitchison and Kirschner, 1988). However, this analysis appears to incompletely assess the relationship between flow speed and cell speed. The reason for this is that only a section at the front of the cell, that was aligned with the direction of travel was compared to cell speed. This acts to ignore other regions of network flow, such as the fast-moving lateral regions that are perpendicular to cell motion, or anterograde regions, that are observed in keratocytes, and are causes of a great deal of traction stress on the substrate (Lee *et al.*, 1994; Oliver, Dembo and Jacobson, 1999; Wilson *et al.*, 2010; Barnhart *et al.*, 2015).

Interestingly, attempts to compare the average of the flow speed across the lamella against the speed of cell migration have not been fruitful, in the context of the purported inverse relationship. In Wilson *et al* it was observed that there was no correlation between flow speed and cell speed, while the rate of the rapid inward flows from the sides of the cell were positively but weakly correlated to cell speed (Wilson *et al.*, 2010). Other attempts to connect

flow speed and cell speed are simply made through coincident observations, rather than making instantaneous comparisons between these two parameters. In one such study, keratocytes treated with Calyculin A, which increases retrograde flow rates, was observed to reduce cell speed (Okeyo *et al.*, 2009). While blebbistatin treatment which inhibits Myosin II activity and thus reduces Actin flow speed, results in slower moving cells (Okeyo *et al.*, 2009). This has also been observed in *in vivo* systems such as the Drosophila embryonic macrophages, where zygotic mutant embryos for the Myosin II heavy chain result in a reduction in Actin flow speed, and disrupted migration that results in deficient embryonic dispersal (Davis *et al.*, 2015). However, it is unclear how perturbing Actin flows, actually result in changes in cell motion, for instance the slow flows observed in cells treated with blebbistatin are not slow for the same reason that is relevant to the Actin clutch hypothesis.

Despite the relationship between the speed of Actin retrograde flow and cell speed remaining unclear, it has been used as a foundation on which to build links between other migratory parameters. One such comprehensive model is the 'Universal Coupling of Speed and Persistence', which attempts to explain observations that faster cells are capable of more persistent migration than slower cells (Maiuri *et al.*, 2012, 2015). In this model Actin flows act as an intermediary factor that co-regulates both the speed of cell migration and cell persistence. It was suggested that Actin flow speed was positively correlated with polarisation lifetime, a measure that describes how long a cell retains a specific morphology defined by the number of protrusions. Here an advection-based system was posited, where Actin flows transport polarity

regulators such as Arpin from the leading edge. This process would act to promote Actin branching at the leading edge. Actin flow also acts to increase the concentration of Myosin II at the cell rear which can stabilise cell polarity (Maiuri *et al.*, 2015). The overall principle here is that fast Actin flows are able to stabilise persistent cell migration through a preferential selection for unipolar cell morphologies. However, the use of kymographs limits the ability to make claims about the role that the global Actin flow field plays in migration. Another issue that arises is that for Actin flow to advect away polarity cues it must be moving, however in the laboratory reference frame the clutch hypothesis requires that this region of the network is actually stationary (or is at least slowly moving) with respect to the substrate and as such should not be able to remove these factors. It could however be the case that this model may be useful in describing not the advection of polarity cues from the front, but from the rear of the cell, as in this region the network is slipping from the substrate and thus moving fast enough to perhaps shuttle proteins away from the rear edge of the cell.

There have been a number of studies that have highlighted that other components beyond the assembling capacity of the leading edge should be implicated in cell turning. For instance, the motion of the Actin cytoskeleton has the ability to align focal adhesion complexes with respect to the local direction of Actin flows (Wu *et al.*, 2012). One study that investigated the alignment of Actin flows and the orientation of focal adhesion complexes found a high directional correlation between the velocity vectors of the flowing Actin network (derived from qFSM) and the traction force or stress vectors of the

substrate (derived from the displacement of substrate mounted beads) (Gardel *et al.*, 2008; Sabass *et al.*, 2008). This revealed that Actin flows may have a role in cell steering, which is the first experimental evidence that implicates something other than the leading edge in cell motion. An earlier study hinted at the ability of Actin flow dynamics reorienting a cell during migration (Suter *et al.*, 1998). Here, a fixed bead placed on the lamellae of growth cones locks the Actin network, allowing for directed polymerisation and focussed extension of the cell membrane. This results in a repolarisation of the lamella in the direction of the bead. In this case the bead acts as a strong clutch with which contractile tension is transmitted into the substrate, while polymerisation locally occurs in alignment with this region.

The directional alignment of adhesions and the flowing Actin network likely derives from the transmembrane nature of adhesion complexes, where a pulling force (such as Actin retrograde flow), may act to tilt and align the complexes in the direction of motion of the flow (Zhu *et al.*, 2009). In one study, the core constituents of focal adhesions; α-Integrin, FAK, Zyxin, Paxillin, Vinculin, Talin, and α-Actinin, were analysed with regards to how aligned their motion is with the flowing Actin network (Hu *et al.*, 2007). Here, they discovered that the constituents of the adhesion complexes that are most strongly associated with F-Actin (e.g. α-Actinin) move with a high degree of alignment with the local Actin flows. However, α-Integrin, which is found at the distal end of the adhesion complex, with respect to the Actin network, moves unaligned to the direction of local Actin flows (Hu *et al.*, 2007). In a recent study a new relationship between the direction of Actin flows and the

orientation of adhesions was experimentally shown (Swaminathan *et al.*, 2017). In this study, the orientation of the focal adhesions was actively determined by the direction of Actin flow and not as function of local F-Actin alignment. The hypothesis that resulted is that adhesions are selected based on their alignment and then activated based on a 'stress alignment preference' which would maximise mechano-transduction. Supplemental to these findings is analysis that has shown that there is a differential alignment of the integrin LFA-1, with a high degree of alignment to the direction of local Actin flow at the leading edge of the lymphocytes (Nordenfelt *et al.*, 2017). The alignment of LFA-1 to the direction of Actin flows decays as the distance from the cell boundary increases. The ultimate implications of this is that there may be a role in directional determination of cell motion, mediated by the flowing Actin network and the friction it can impart on the substrate. Adhesion alignment has been noted as particularly important in chemotaxis, as it would provide a means for directional sensing (Nordenfelt *et al.*, 2017). Cells that respond to external cues, such as those released to initiate an immune response not only have to migrate in the direction of the cue, but not be distracted by the inherent noise in the environment. In order to migrate effectively, cellular memory has been proposed. This allows for a cell to maintain a course that is aligned with respect to the source of a chemoattractant. Cellular memory requires an intracellular system that persists on a temporal scale that is long enough to 'experience' the varying environmental conditions, having been exposed to initial environmental conditions and the subsequent disturbances. There is now evidence to suggest that the stability of the Actin network make this a

good candidate to maintain cellular memory for this guidance system (Prentice-Mott *et al.*, 2016).

1.2.3 The effects of cell-shape on motility

The relationship between cell shape and cell migration has long been observed. For instance, in 1924 the observation was made that canoe cells (keratocytes derived from Minnow tissue cultures), consistently migrated along their minor axis (Goodrich, 1924). However, there is much diversity in the shape of motile cells, for instance growth cones are 'hand shaped' outgrowths of neurites, responsible for neuronal pathfinding (Betz *et al.*, 2011). Fibroblasts are elongated cells, responsible for deposition of extracellular matrix, and feature multiple lamellipodia (Herant and Dembo, 2010). While fish keratocytes, common in the study of cell motility, migrate rapidly, are directional persistent, and have a stable fan-like or canoe-shape morphology (Euteneuer and Schliwa, 1984; Herant and Dembo, 2010).

One common feature between many of these cell lines is a definable front and back, which as we have seen is necessary for effective motion, despite the underlying mechanisms of migratory polarity being unresolved. In a comprehensive study of keratocyte morphology, Keren *et al* described two distinct phenotypes, coherent and decoherent (Keren *et al.*, 2008). Coherent cells are defined by: 1) a large radius of curvature at the front of the cell, which contributes to the canoe-like nickname of these cells, 2) a high aspect ratio value, where the cell's major axis is much larger than the minor axis, 3) a smooth front edge of the cell. Decoherent cells are defined by the opposite

morphology, with a rough leading edge and low aspect ratio, in which the cells are more squared/rounded than elongated. They found a correlation between cell speed and the aspect ratio of the cell, demonstrating that in the case of keratocytes, cells that are wider than they are long move faster (Keren *et al.*, 2008). However, while other cells may still obey this rule whereby, they move faster if there is a significant difference between the lengths of the major and minor axis, what is not accounted for is whether it is relevant along which axis the cell migrates. As mentioned, keratocytes migrate along the minor axis, however growth cones would exhibit migration in the direction of the major axis (Betz, Lim and Kas, 2006; Keren *et al.*, 2008). In one study it was shown that faster moving leukocytes were more elongated than their more rounded, slower moving counterparts (Leithner *et al.*, 2016). This was achieved by comparing the leukocyte's 'shape factor' - a measure of roundness where a value of 1 denotes a circular morphology, while a value 0 is a cell of indefinite elongation - and cell speed, where they revealed that the two parameters were weakly negatively correlated (Leithner *et al.*, 2016). This data suggests that the specific axis along which a cell migrates may not be as important for cell migration as whether the cell is elongated and stable through time (Keren *et al.*, 2008; Leithner *et al.*, 2016). For Keren *et al* cell shape can be defined on a continuum of elongation which is suggested to be regulated by membrane tension (Keren *et al.*, 2008). The role of membrane tension in defining cell polarity is described in the 'Actin protrusion in an inextensible membrane bag' model. Here, Actin assembly pushes the membrane forwards and the cell membrane produces inward tension in response across the cell boundary (Keren *et al.*, 2008). Further analysis has suggested that this response is

delayed by approximately 40 seconds (Ji, Lim and Danuser, 2008). The pushing force of the Actin network is proportional to the Actin density in that region, as such the front of the cell extends more than at the sides. In fact, as a result of this Actin density dependent edge extension, the lateral regions of the cell edge are unable to protrude the membrane and assembly stalls here. Following this the Actin network is broken by the tension of the membrane in regions of low Actin density i.e. at the sides and rear, and this causes retraction of the cell rear. This is indirectly supported in the finding that in instances of where Actin monomer concentration is limited, migrating cells narrow due to an increase in Actin density at the front, and a decrease in density at the sides causing anterior stretching and medial contraction (Allard and Mogilner, 2013).

The relationship between cell speed and shape, was further investigated in one study that examined how cell speed changes with the distance between the lamellipodia and the rear (Ofer, Mogilner and Keren, 2011). Despite this analysis being carried out in fragments of keratocytes, these cells remarkably recapitulate the whole-keratocyte relationship to speed and shape, with slowing cells that progressively round up with their front to back distance increasing; and faster cells that take on a canoe-like morphology, with their front to back distance decreasing (Ofer, Mogilner and Keren, 2011). In this study the concept of a disassembly clock was developed, which accounts for previous observations that the distance between front and rear remained constant during stable migration (Keren *et al.*, 2008; Ofer, Mogilner and Keren, 2011). The disassembly clock describes the time taken for the network to be taken apart and the rear to retract, following network

assembly at the front (Mogilner and Rubinstein, 2010). These processes of assembly and disassembly are tightly integrated and result in the stability of the cell's area and a constant distance between the front and the rear. This model also establishes a mechanism by which the front of the cell is mechanically coupled to the rear of the cell (Ofer, Mogilner and Keren, 2011).

While the inextensible membrane bag model was effective in predicting cell speeds and shape, it ignores the rear of the cell focussing principally on the response to leading edge polymerisation, and specifically the behavior of the Actin network and the removal of adhesions which are known to be necessary in defining instantaneous cell shape. For instance, in keratocytes, the regions of greatest traction stresses occur at the most lateral ends of the cell; an increase in cell width results in far higher traction forces at the lateral sides of migrating keratocytes than of rounded cells; and ablating stress fibres at the side of keratocytes results in rapid asymmetric retraction of that specific side of the cell (Oliver, Dembo and Jacobson, 1999; Nakata *et al.*, 2016). In one study that investigated the determinants of cell shape, it was demonstrated that cell speed exhibited a biphasic response to migratory substrates of differing adhesive properties (Barnhart *et al.*, 2011). Here, cells migrated slower on substrates rated as high and low for adhesion strength, while intermediate adhesion strength produced faster moving cells. However, the shape of the keratocytes changed significantly. Cellular area increased with adhesion strength as did their left-right asymmetry. In the case of the aspect ratio of the cells, there was a biphasic relationship, where the keratocytes on the intermediate adhesion strength substrate took the

characteristic keratocyte shape, while the other two experimental conditions featured reduced aspect ratios, for instance cell rounding on low adhesion strength substrates. With the idea of morphological coherence in mind, an intermediate strength adhesive substrate promotes the most coherent morphology while decoherent morphologies are seen in low and high adhesion substrates to varying extents (Barnhart *et al.*, 2011).

1.3 **Why the fly? Drosophila embryonic hemocytes**

Complex three-dimensional environments are a tricky obstacle to overcome in the study of cell migration. Combined with the tremendously intensive computational requirements of assessing sub cellular Actin dynamics during migration in these *in vivo* environments it is no wonder why so much attention has been paid to developing one-dimensional, or two-dimensional *in vitro* migration assays. However, one model system that can circumvent these concerns is the migration of Drosophila embryonic macrophages. Also known as hemocytes, these cells migrate within a narrow acellular space called the hemocoel, so narrow in fact as to be effectively two-dimensional (Figure 1.5 B) (Matsubayashi *et al.*, 2017). Inferior to the epithelial layer on the ventral side of Drosophila embryos, hemocytes migrate within the hemocoel in superficial routes that make them particularly amenable to imaging. The benefits of this model cell system are compounded when you take into account the genetic tractability of Drosophila melanogaster (Weavers and Wood, 2016). Hemocytes perform a number of important functions for development as they play an integral role in Drosophila embryonic innate immunity as professional phagocytes, and are vital for morphogenesis through

their deposition of basement membrane proteins (Wood and Jacinto, 2007; Parsons and Foley, 2016). These responsibilities have led to hemocytes becoming renowned for their prowess at ‘multi-tasking’.

One vital morphogenetic event in Drosophila embryos that is inextricably linked to hemocytes occurs when one of the two fundamental constituents of the drosophila nervous system, the ventral nerve cord (VNC), undergoes condensation. Condensation being defined as a reduction in the volume of the tissue, with an increase in cell density. In the absence of hemocytes the VNC is unable to condense and that in nerve cords who are developmental disrupted inhibit the effective migration of hemocytes (Olofsson and Page, 2005; Evans *et al.*, 2010). Concomitant to the initiation of VNC condensation is the deposition of basement membrane proteins during hemocyte migration, which includes for example Laminin, Collagen IV and Perlecan (Olofsson and Page, 2005; Matsubayashi *et al.*, 2017).

There is also an apparent inter-dependence between basement membrane proteins and the hemocytes that deposit them as observed in where the integrin-dependent hemocyte migration along the VNC was disrupted in the absence of laminins (Urbano *et al.*, 2009). In Sanchez-Sanchez *et al*., they not only confirmed the critical nature of laminins to hemocyte VNC migration (98.3% of embryos observed, feature migration defects in LanB1 mutants) they also substantiated the idea that hemocyte essentially ‘pave their own road’ (Sánchez-Sánchez *et al.*, 2017). Here they utilised transplant experiments where hemocytes mutant for LanB1 (which

meant that these cells no longer autonomously release laminins) are transplanted into control embryos, they found that these cells migrated slower and had disrupted lamella dynamics - as shown from the reduced lamella area between transplant and control data.

There have been a number of studies that demonstrate that hemocytes respond to laser induced wounding of the embryonic epithelium (Stramer *et al.*, 2005; Moreira *et al.*, 2010). In Stramer *et al*., this response was determined to be highly Rac1 dependent, demonstrating the importance of hemocyte protrusion dynamics during wound response. This is in line with other findings that highlight the important role of Rac1 activity as key regulator of edge protrusions (Pankov *et al.*, 2005; Stramer *et al.*, 2005). Interestingly, while there's an evident wound response hemocytes are actually dispensable for the process of wound healing as embryos that lack hemocytes still undergo wound re-epithelisation. Their role is thus likely limited to an induction of an inflammatory response (Stramer *et al.*, 2008) and the clearing of apoptotic debris (Evans, Hartenstein and Banerjee, 2003).

In order to perform these roles, hemocytes must be able to migrate around the Drosophila embryo unencumbered. As such a number of migratory routes are utilised to effectively allow hemocytes to disperse throughout the embryo (Figure 1.5 A). Embryonic dispersal of hemocytes occurs between 10 and 13 hours into embryogenesis (by stage 14), and complete embryonic dispersal is achieved by stage 17 after leaving the head mesoderm at stage 10 (Tepass *et al.*, 1994; Wood, Faria and Jacinto, 2006). Hemocyte migration

originates from the head mesoderm, and as they leave this region they utilise four routes (Tepass *et al.*, 1994; Holz *et al.*, 2003). These routes are summarised below:

1. Along the ventral side of the embryo, sandwiched between the epidermis and the nerve cord
2. Along the dorsal surface of the nerve cord
3. Along the gut primordium
4. Along the dorsal boundary of the epidermal primordium

It is pathway 1 and the cell migratory behaviour exhibited within, that is of interest and exploited in the analysis featured within this thesis. Pathway 1 has been studied extensively as the pattering of hemocytes on the ventral surface during embryonic development is of great interest to developmental and cell migration biologists alike (Davis *et al.*, 2015; Matsubayashi *et al.*, 2017).

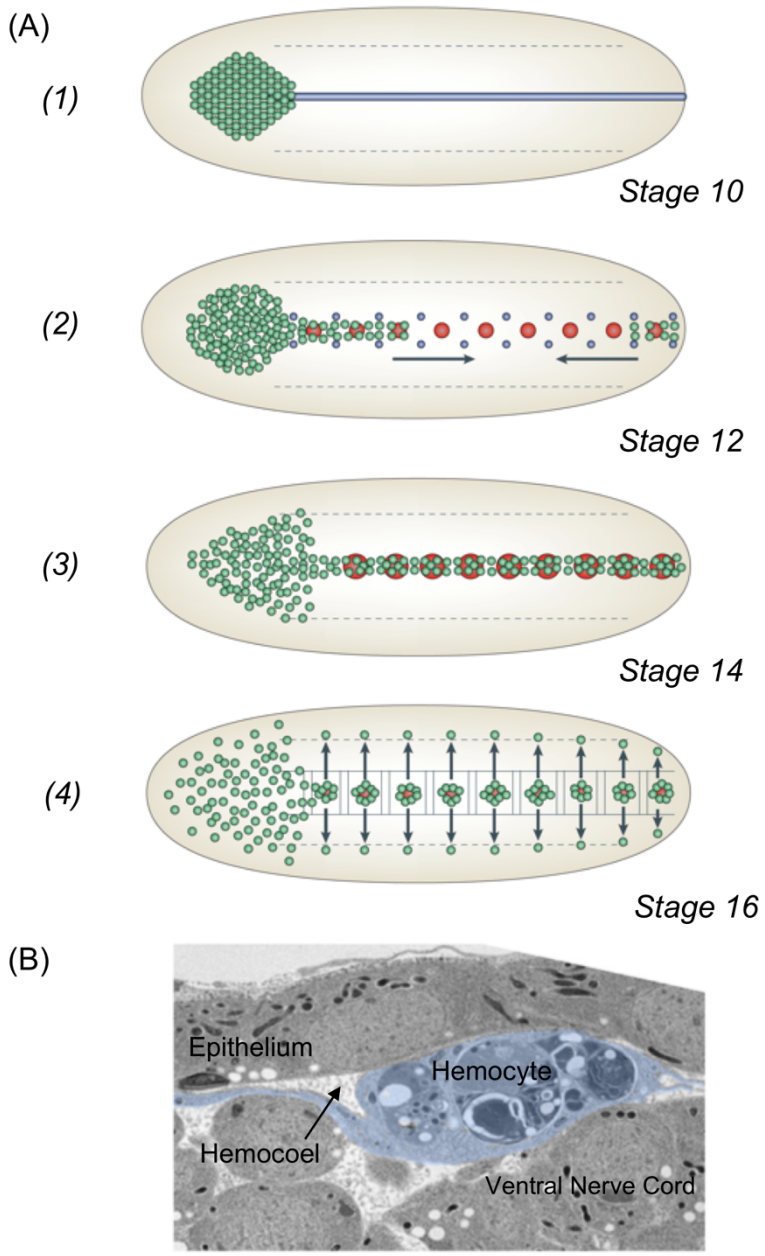

Figure 1.5: Schematic showing the embryonic migration of Drosophila macrophages (hemocytes). **(A)** Hemocytes (green circles) migrate along the ventral surface of the nerve cord. *(1)* Hemocytes originate in the head mesoderm, prior to migration there is a distinct localisation of Pvf3 (blue strip) along the ventral midline. *(2)* Hemocytes migrate down the ventral midline of the nerve cord, in response to Pvf3 and Pvf2 (red circles). *(3)* Hemocytes,

have now fully occupied the ventral midline, signalling changes have also occurred at this stage with Pvf3 depleted here, while the concentration of Pvf2 is elevated. *(4)* Hemocytes migrate laterally, filling the available space. (Schematic adapted from (Wood and Jacinto, 2007)). **(B)** Transmission electron micrograph of a migrating hemocyte (blue shading), within the narrow acellular space of the hemocoel. (Image adapted from (Matsubayashi *et al.*, 2017)).

Hemocytes that are migrating down the ventral nerve cord originate from the poles of the embryo. They migrate along the ventral midline, and once this region is occupied, hemocytes undergo a process of lateral migration to form the characteristic three-line pattern (Tepass *et al.*, 1994; Wood, Faria and Jacinto, 2006). There is a morphological change that has been characterised between hemocytes during the early stages of embryogenesis as they perform midline migration, and lateral migrating during the latter stages of embryogenesis. At stage 12 of development hemocytes feature a small number of Actin based protrusive structures, and only a few obviously identifiable lamellipodia, while later on at stage 16, hemocytes had both filopodia and lamellipodia (Wood, Faria and Jacinto, 2006). Hemocytes also produce peripheral protrusions during lateral migration. This acts to establish that during lateral migration hemocytes have a persistent leading edge that form Actin based protrusions in the direction of migration.

Hemocyte migration during the latter stages of embryogenesis is often linked to either chemotaxis or is derived from mechanically driven cell-cell

interactions. In the chemotactic case PDGF / VEGF signalling is responsible for migration along the ventral midline, mediated by the hemocyte receptor PVR, a receptor for Pvf1, 2 and 3 (PDGF / VEGF ligands) (Brückner *et al.*, 2004). This dependence on PDGF / VEGF signalling is shared with Drosophila embryonic border cells (Duchek *et al.*, 2001). It has been shown to be specifically Pvf2, and 3 which guide hemocyte migration along the ventral midline, where expression of Pvf3 precedes the expression of Pvf2, and that inactivation of Pvf2 and 3 inhibits both ventral midline and dorsal vessel hemocyte migration (Wood, Faria and Jacinto, 2006). Following migration along the ventral midline there is also the characteristic lateral migration that gives rise to the three lined patterns of hemocytes on the ventral surface of the nerve cord. This process had previously been linked also to Pvf2 expression, specifically its down-regulation which seemingly coincided with lateral migration at stage 15 (Wood, Faria and Jacinto, 2006). This is to imply that Pvf2 retains hemocytes on the midline until the concentration reduces enough to no longer be effective as a chemoattractant. This temporal correlation is supported by evidence in Pvf2 overexpression experiments (using the midline UAS driver *single-mindedGAL4*), that show hemocytes delayed in forming the three lined pattern (Wood, Faria and Jacinto, 2006).

Recent evidence suggests that mechanical activity facilitated by contact inhibition of locomotion is the principle inducer of lateral migration away from the ventral midline and subsequently allows for the uniform dispersal of hemocytes on the ventral nerve cord (Davis *et al.*, 2012). Contact inhibition being a process that involves cell-cell interactions that result in repulsion and

repolarisation and the understanding of contact inhibition in hemocytes was developed in Davis *et al* (Davis *et al.*, 2015). In this study they showed that contact inhibition was critical for the developmental dispersal of hemocytes, and that this process is coordinated through the organisation of the flowing Actin network in the colliding cells. This organisation manifests into a physical coupling between colliding cells, facilitated by an inter-cellular adhesion, that acts as a molecular clutch. This clutch increases tension in the Actin network, and it is the subsequent release of this tension that mediates the repulsion and eventual repolarisation of the colliding partners away from the point of contact and thus each other. This analysis was performed using a novel combination of Actin tracking tools such as PIV, and kinematic analysis that allowed them to look at both motion of the cells and the intracellular dynamics, at high temporal resolutions, which is a feature afforded by the utility of hemocytes.

This is the jumping off point for the analysis to be discussed in this thesis. We currently understand how the Actin network is organised and changes during the collision of hemocytes. However, the question of how the Actin network flows and behaves in freely moving hemocytes (and any other migrating cell for that matter) is poorly understood, beyond the simple analysis of flow speed measurements. This Drosophila hemocyte system, with its genetic tractability, the ease and accessibility of imaging, the rapidity of cell motion, and the ability to track Actin flows over long time periods, provides one with an opportunity to address fundamental questions of how coordinated cell motion over time is truly achieved.

2 Materials and Methods

2.1 Drosophila genetics and preparation of drosophila embryos

2.1.1 Drosophila genetics

In this study we have employed a number of tools, taking advantage of the genetic tractability of *Drosophila melanogaster*. *Drosophila* embryonic hemocytes were targeted directly utilising the hemocytes specific promoters of Singed (Sn) and Serpent (Srp). Singed is a fascin orthologue, responsible for Actin bundling, while the GATA transcription factor Serpent promotes haematopoiesis (Cant *et al.*, 1994; Waltzer *et al.*, 2002). We also employed the Gal4-UAS transcription system in order to drive the expression of, for example, particular genes of interest, or florescent molecular probes, in the cell-types under investigation.

Many times, a genetic perturbation may be lethal or sterile in a homozygous animal and as such in order to maintain a fly stock a balancer should be implemented. A balancer is a genetically engineered chromosome that features a recessive lethal mutation and a looped inversion. The mutation allows for a fly stock to persist in a heterozygous state, while homozygous progeny perish. These inversions prevent crossover between chromosomes, and thus recombination. The predominant balancers utilised for these studies, are CyO and TM6B, second and third chromosome balancers respectively. Both of these balancers express a clearly defined phenotype in the adult (CyO

and TM6B) and larval (TM6B) stages of fly development. CyO for instance manifests as flies with ‘curly’ wings as opposed to straight; while the humeral marker on adult flies and ‘tubby’ appearance to larvae are distinctive of flies carrying TM6B. In the embryo however, it is not so trivial to identify which animal contains a given balancer. In this instance, transgenics can be exploited and flies generated with a balancer with an intrinsic florescence such as Dfd-YFP, can allow for appropriate screening of Drosophila embryos and in the case of Dfd-YFP this can be from stage 13 of embryonic development.

2.1.2 Fly stocks

In order to investigate the migration of Drosophila embryonic hemocytes, the red nuclear probe UAS-RedStinger was instrumental, for nuclear tracking. This probe had been recombined into lines that feature green labelled Actin via UAS-LifeAct GFP (Zanet *et al.*, 2012). UAS-RedStinger has been previously recombined into the second or third chromosome and as such genetic perturbations on either chromosome can be investigated whilst maintaining the ability to track the cells.

In order to assess the migratory characteristics of individual freely moving hemocytes, often the ectopic expression of UAS-CyclinA was utilised used to migratory space constraint on the VNC. CyclinA is a protein involved in cell cycle regulation, and the degradation of the protein is required for the mitotic exit. Overexpression of CyclinA results in a prolonged S-phase, and a reduction in the number of hemocytes migrating down the ventral midline. To label Myosin II of the purposes of colocalisation analysis, UAS-Zipper GFP

was expressed alongside UAS-Moesin-mCherry, a red Actin marker. Also in order to examine Actin flow organisational disruption, mutant lines *tsr*^{1} and *zip*^{1} which were available from the Bloomington Stock centre. *tsr*^{1} is a hypomorphic allele for the Drosophila gene encoding *twinstar*, the Drosophila orthologue to cofilin (Gunsalus *et al.*, 1995). *zip*^{1} is an amorphic mutation in the Drosophila genes that encodes the Myosin II heavy chain (Young *et al.*, 1993).

2.1.3 Mounting the embryos

In order to start the imaging process male and female flies were crossed in cages. The base of the cages are removable and are comprised of grape juice agar plates smeared with yeast paste, onto which the flies will lay their eggs. A bleach solution is poured onto the agar plate in order to remove the opaque chorion, covering the embryos. The embryos are loosened from the agar plate, and the solution poured through a cell strainer, and any remaining bleach washed away.

Embryos are now ready to be examined for the appropriate fluorescent markers and for selection of embryos at the required stages of development with the aid of a florescent dissection microscope. For the purposes of this investigation, embryos at developmental stages 15-17 are appropriate as the hemocytes have migrated away from the head mesoderm, down the ventral midline and have initiated the lateral movement phase. Selected embryos are placed ventral side up, on Lumox gas permeable membranes between two size 1 glass coverslips. A drop of 10s Voltalef oil covers the embryo and another coverslip bridges the two incumbent slips, secured by nail varnish.

2.1.4 *in vivo* imaging

A Perkin Elmer Ultra VIEW spinning disk confocal microscope was used for the majority of the imaging featured here. In order to image the cytoskeletal dynamics, and the kinematics of hemocyte migration we used a 63x Zeiss oil immersion lens and the time step used for imaging at these high magnifications was approximately 5 seconds, over a period of 3-4 minutes. Lower magnification imaging, using 20x air objectives and 40x oil immersion objectives were also employed to assess the developmental dispersal patterns of the hemocytes in wild-type control, mutant, and wound response scenarios. In these situations time steps are noted in the specific figure legends. We have also implemented a Zeiss LSM 880 with fast Airy scan capabilities for high resolution imaging of hemocytes fluorescently labelled Actin (UAS-Moesin-mCherry) and myosin (UAS-Zipper-GFP) for colocalisation analysis. Epithelial wounding for the purpose of stimulating hemocyte wound response was performed on the aforementioned spinning disk microscope using a MicroPoint system

2.2 Image analysis

2.2.1 Automatic nuclear tracking

Hemocytes were tracked utilising fly stocks that feature a florescent nuclear marker (UAS-sn-RedStinger). Nuclear tracking was used as a proxy for cell locomotion. Tracking itself was performed automatically using a custom

algorithm in MATLAB (MathWorks™). This involves intensity thresholding of the nucleus and recording the co-ordinates of the nuclei centroid through time.

2.2.2 Measuring migratory persistence

Once the nuclear tracks are attained I have employed two commonly used measures of migratory persistence (Gorelik and Gautreau, 2014). At their core these methods describe slightly different processes that underlie the overall behaviour and activity of hemocyte migration, however they act together to build a comprehensive profile of the hemocytes migratory characteristics.

The first of these is the directionality ratio. Also known as the straightness index, this method compares the beeline distance of the cell's track, from start to end, to the summed displacements of the track. This is defined by $\langle {}^{d_t}/_{D_t} \rangle_C$, where, d_t is the beeline distance of the cell track, $D_t$is the length of the cell track, and C is the number of cells that are averaged over. This provides insight into how tortuous the trajectory a cell undergoes from the first time point to reach its final destination (in the context of the imaging session). This ratio can be displayed as a decay curve offering insight into the efficiency of migration through time, the often-reported directionality ratio value is typically the last value in the curve and it is always between 0 and 1. A directionality ratio of 0 would be derived from track exhibiting random, Brownian migration characteristics. A directionality ratio of 1 would be derived from a cell trajectory that was perfectly persistent.

The second method is the directional velocity autocorrelation of the cell tracks. This compares the cosine of the angle difference between cell displacements at all potential time lags. This method is particularly useful as it provides a decay curve that describes the propensity for turning that a cell exhibits. A trajectory whose autocorrelation curve decays rapidly to cos (θ) = 0 is one who turns more readily between time steps. While a perfectly straight track would exhibit a stable autocorrelation line at cos (θ) = 1. This velocity autocorrelation (v_{ac}) is calculated, as in (Gorelik and Gautreau, 2014):

$$v_{ac}(n) = \frac{1}{N-n}\sum_{i=0}^{N-n}\left[\frac{(x_i - x_{i+1})(x_{i+n} - x_{i+n+1}) + (y_i - y_{i+1})(y_{i+n} - y_{i+n+1})}{(\Delta t)^2} * \frac{1}{norm}\right] \quad \textbf{(2.1a)}$$

$$norm = \frac{1}{N}\sum_{i=0}^{N-1}|\vec{v}_i|^2 \quad \textbf{(2.1b)}$$

Where N is the cell track length, Δt is the smallest time step between points in the cell track, and n is the step size, and finally $\vec{v}_i$ describes the cell displacement vector described by the cell movement between (x_i, y_i) and (x_{i+1}, y_{i+1}).

2.3 Quantifying Actin flows in migrating hemocytes

2.3.1 Particle image velocimetry

Actin retrograde flow was tracked utilising Particle Image Velocimetry (PIV). PIV is a technique which retrieves quantitative information about a flowing material. In many cases PIV tracks particles seeded in a fluid, it is the motion of those particles that is used as a proxy for the flow of the fluid. PIV

here was used entirely on time-lapse images of hemocytes captured with a 63x oil immersion objective, with time intervals of approximately 5 seconds. PIV in this hemocyte system was established by Dr Andrei Luchici (Davis *et al.*, 2015) from algorithms and workflows developed by Dr Timo Betz (Betz, 2007).

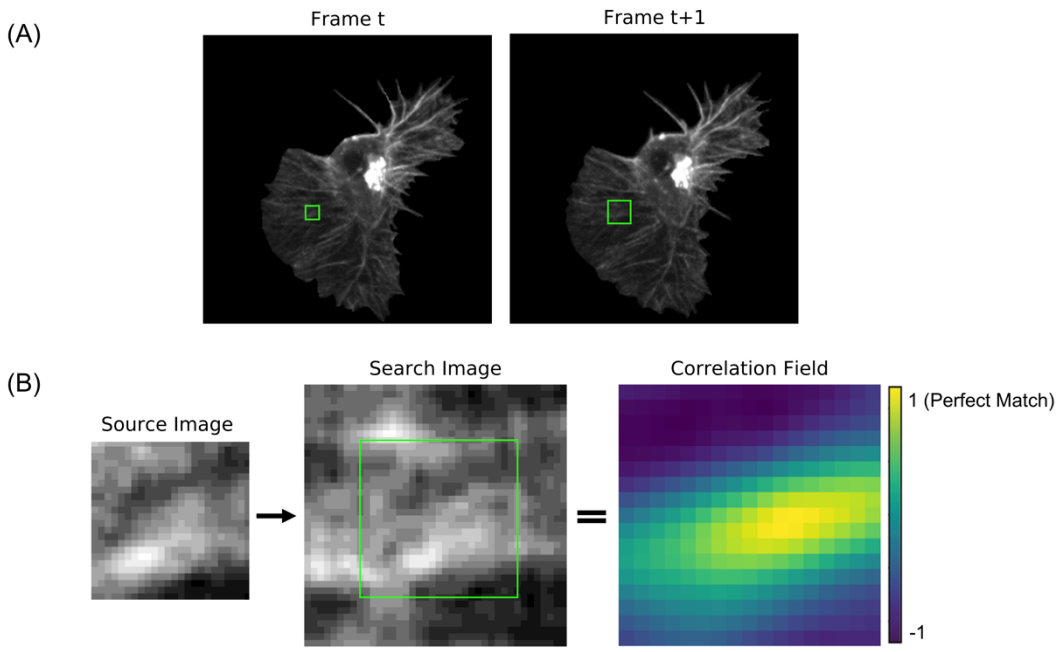

Figure 2.1: Example of the PIV tracking an Actin feature. **(A)** A small sub-image (green square in the left-hand cell) within the initial frame of a migrating hemocyte expressing UAS-LifeAct-GFP (Actin) and UAS-redStinger (nuclear marker), is compared within a larger sub-image (green square of the right-hand cell) of the consecutive time-lapse movie. These images recorded at 5 seconds per timepoint. **(B)** A schematic of the image-matching flow. The normalised cross-correlation function calculates the image similarity of the source image within the search image, producing a correlation field. Peaks within this correlation field are evaluated, with the coordinates of the maxima representing the estimated location to which the Actin features have displaced.

Briefly, PIV employs a 2D cross-correlation algorithm (Lewis, 1995), which is used to track Actin bundle displacement between time-lapse image frames. In this protocol a source image (fit to the size of a stereotypical Actin feature to be tracked), is compared with a search image (a sub-frame of the following image in the time-lapse) (Figure 2.1 A-B). In order to control for intensity variations within the template signal, the cross-correlation function is normalised. Without normalisation, regions with a higher frequency of bright particles can produce higher correlation values than lower intensity regions. The cross-correlation algorithm used to determine the value of similarity between the sub-images at each pixel is:

$$C = \frac{\sum_{x,y}\left[Search_{x,y} - \overline{Search}\right]\left[Source_{x,y} - \overline{Source}\right]}{\left\{\sum_{x,y}\left[Search_{x,y} - \overline{Search}\right]^2 \sum_{x,y}\left[Source_{x,y} - \overline{Source}\right]^2\right\}^{0.5}} \quad \textbf{(2.2)}$$

where C denotes the normalized cross-correlation coefficient between the source images and search images. x and y represent the position indices of a point within the given sub-image, while the overlined variables represent the mean of their respective images (*Source* or *Search*). The location of the maximum value of C denotes the end point of the feature displacement between time points. The vector of displacement is drawn from the centre of the *Source* image to the position of this maximum value of C. In our case the source size was 1.2 μm and the search size set at 2.0 μm. This correlation process is applied across the entire image, so that a quantitative measure of Actin flow in the hemocytes can be attained. A correlation threshold ($C_{threshold}$)

was used to screen and remove spurious tracking data, this was set at $C_{threshold}$ = 0.5.

Interpolation of the vector field was required to fill all pixels within the field for further analysis, this used a spatial convolution with a Gaussian kernel (σ^2 = 1μm), and a temporal convolution defined by a temporal convolution of 25 seconds. For all analysis in this thesis derived from the Actin flow field I have performed two steps to ensure that I am indeed examining the actual flow of the Actin. The first is that flow field analysis such as flow speed is assessed only within the region of the cell that acts as the intersection between time steps. This acts to remove spurious edge effects. The second process is that all velocity data within the cell body is discarded as there is no detectable Actin flow underneath in this region. This preserves only lamella flow in the data analysis. This process of excluding data points involved manually segmenting the cell body of the already segmented hemocyte image, creating a binary mask of this new image and only accepting flow values within this boundary. The algorithm for this PIV analysis was built and deployed in MATLAB (MathWorks™).

Prior to analysing flow images with PIV, it is recommended to validate the technique in order to reduce measurement uncertainty. For PIV the process of validation has been described in detail within (Raffel *et al.*, 2007). One useful validation method is to use fields of particles with known displacements. This can be from experiments whose flows have been previously validated, or by numerical Monte Carlo simulations. Simulations

have an advantage over experimental data sets as there is the ability to modify specific parameters that can influence the uncertainty of the PIV measurement. These parameters can include for example, particle density, particle size, and background noise. These constructed fields can then be used as a benchmark against which to validate the correlation parameters of the tracking method.

2.3.2 Quantifying flow speed

The output of the PIV software is a velocity field described by the x and y components of the displacement vectors of Actin features in time. In order to compute the speed of the flow field in local terms, the magnitude of the vectors was computed. In order to calculate the average flow speed, only data contained within the intersection of consecutive frames of the time-lapse movie was analysed. The reason for this is that hemocytes rapidly change shape during migration and this can have significant effects on the calculation of flow speed in these regions. Flow speed was calculated using $|\vec{v}| = \sqrt{x^2 + y^2}$ across all vectors within the flow field, where $|\vec{v}|$ is the magnitude of the displacement vector, and x, y are the components of the flow velocity vector $\vec{v}$.

2.3.3 Quantifying flow divergence

Divergence is a mathematical measure that describes whether regions of a flow field are sources or sinks for material. This measure looks at the summed gradient of the 2D velocity field. This spatial gradient is computed

using a central difference scheme on the two spatial dimensions of the PIV derived velocity field $\vec{V}$. This spatial gradient is summed to produce the flow field divergence:

$$\nabla \cdot \vec{V} = \frac{\partial V_x}{\partial x} + \frac{\partial V_y}{\partial y} \quad \textbf{(2.3)}$$

Divergence analysis of a velocity field produces a new signed scalar field. Negative values represent points in the flow field that take in more material than they release, i.e. a sink, and these regions can be described as convergent (they have also been referred to in the literature as compressive although that isn't necessarily the case (Vallotton *et al.*, 2004). Positive divergence values represent a point in the flow field that exudes more material to the environment than it takes in and is thus a source of material. Values of 0 are possible and this would represent a region of the network that displays no net flux of material (Figure 2.2).

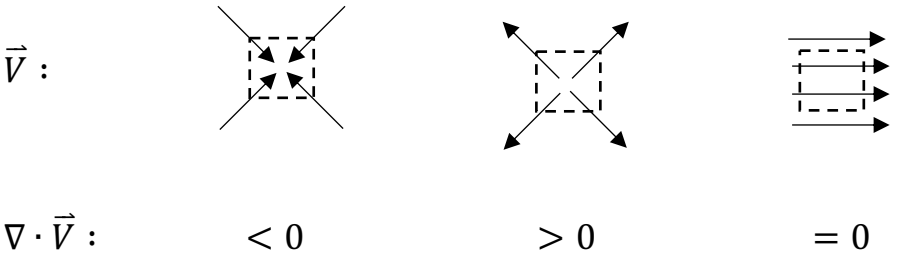

Figure 2.2: Schematic summarising flow divergence. The value of divergence ($\nabla \cdot \vec{V}$) is defined by the density change of a point in a velocity field.

This was implemented in MATLAB (MathWorks™), using the in-built *Divergence* function. For the purposes of visualisation an adapted implementation is used which allows for smoothing of the vector field and cleaner images, utilising a central difference scheme spanning 10 pixels. This version is written in MATLAB however in some instances a Python implementation was also used, which takes advantage of some specific plotting abilities within the *matplotlib* package.

2.3.4 Streamline descriptions of the flow field

Streamlines can be used as a descriptor for the global directionality of a flow field (Figure 2.3 A). The result of computing the stream function is a series of lines that are drawn tangential to each vector in the field. These lines are seeded from boundary of the cell. Within a velocity field, each point is represented by one velocity vector. As a consequence, each point along a streamline are also defined by a single velocity vector, specifically the tangent of that vector. This means that streamlines cannot cross, and the stream function becomes undefined which can give rise to stream sinks. Sinks are a result of the confluence of multiple streamlines at a specific point. This confluence of streamlines represents the same phenomena as a region displaying negative divergence. In order to capture whether we have stream sinks in our Actin flow field, the coordinates used to construct the streamlines were analysed. The termination coordinates of these lines were stored and binned into sub-images representing 2 μm^2 boxes (Figure 2.3 B). The quantity of streamlines terminating in a given box were then quantified and ranked. The reduction of multiple streamline 'end points' to a single representation of a

common termination point (the centre of the box) allows for more advanced analysis to take place such as the tracking of these sinks.

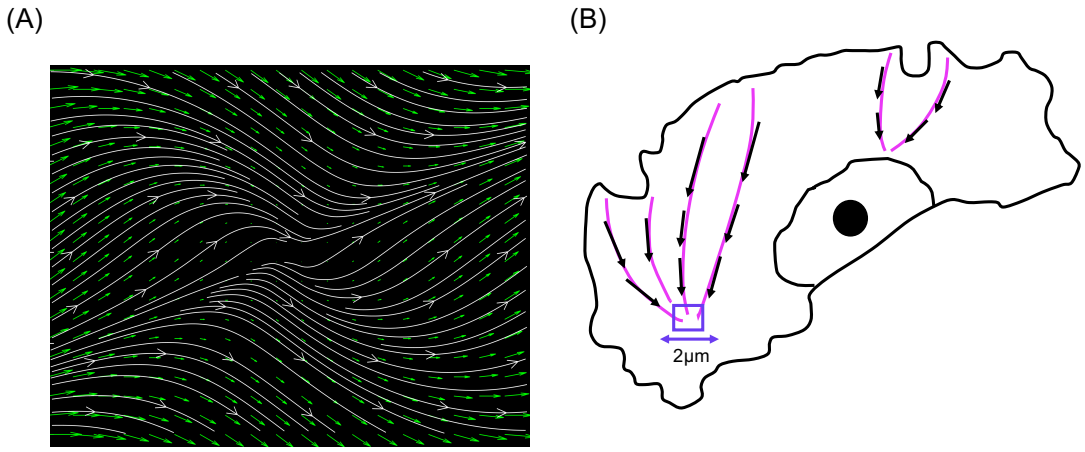

Figure 2.3: Example Image and schematic of the streamline analysis. **(A)** An example vector field (green arrows), has been analysed with streamlines to determine flow behavior, these lines are overlaid (white). A massless particle would follow the path of one of these streamlines. **(B)** An illustration of how the streamline sinks are determined. Here, regions of the network are sampled within 2 μm^2 boxes and the number of streamlines terminating there are counted.

In the images provided a display technique called the stream-slice is utilised which only provides a sample of the streamlines calculated, plotted at regular intervals for ease of visualisation. In actuality the stream function describes the entire flow field.

2.3.5 Turnover analysis

Treadmilling of the Actin network is considered to be a key feature of migrating cells, with addition off monomers allowing for leading edge growth,

the ‘rearward’ flow of the Actin network, and the destruction of the network at the rear. The ability of the Actin network to be recycled is necessary for effective cell motion and as such we have implemented an analytical method that computes the turnover of the Actin cytoskeleton (Vallotton *et al.*, 2004; Wilson *et al.*, 2010). This implementation provides us with insight into the assembly and disassembly characteristics of the Actin network. This process combines the local change in Actin florescence intensity (from UAS-LifeAct GFP probes), the time derivative of the network intensity, and the divergence of the Actin flow field to provide turnover of the Actin network (σ). If $\sigma > 0$ the meshwork density is increasing which can be considered assembly or accumulation, while $\sigma < 0$ represent a meshwork density decrease which would be disassembly.

$$turnover = \sigma = \frac{\partial I}{\partial t} + \big(I(\nabla \cdot V)\big) + \big(V(\nabla \cdot I)\big) \qquad \textbf{(2.4)}$$

The temporal derivative of the Actin network florescence intensity $\left(\frac{\partial I}{\partial t}\right)$ is computed from a forward difference scheme. The spatial gradients of flow velocity $\left(\nabla \cdot \vec{V}\right)$ and florescence intensity $(\nabla \cdot I)$ are computed using a central difference scheme. In earlier published analysis of flows, this method has been used to differentiate between Actin network contraction and network depolymerisation (Vallotton *et al.*, 2004). For the case of Actin network depolymerisation the Actin network intensity will decrease between frames and $\frac{\partial I}{\partial t}$ will be negative without an accompanying decrease in network divergence $\left(\nabla \cdot \vec{V}\right)$. Actin network contraction could be inferred by a decrease

in network divergence $\left(\nabla \cdot \vec{V}\right)$ and an increase in the spatial $(\nabla \cdot I)$ and temporal $\left(\frac{\partial I}{\partial t}\right)$ gradient of intensity. This increase in fluorescence intensity represents an increase in Actin density. As a result of the focus on the lamellae network for the Actin flow analysis, and the small amount of assembly seen within lamellae, only the disassembly data is shown, however both assembly and disassembly are included for within the analysis. For visualisation, normalised disassembly or divergence maps are shown, normalised to the maximum value in the field.

2.3.6 Principal strain analysis

With divergence illuminating where there are sources and sink regions in the Actin network, this specific strain analysis was employed to assess what kind of activity is occurring in those regions. Local deformation of the Actin network can be quantified by evaluation of the principal strains which are derived from local velocity changes derived from the PIV. The relative positional changes of points within a deforming body is initially described with a velocity tensor which is computed based on a central difference estimation over 5 pixels in both spatial dimensions.

$$V = \begin{pmatrix} \frac{\partial V_x}{\partial x} & \frac{\partial V_x}{\partial y} \\ \frac{\partial V_y}{\partial x} & \frac{\partial V_y}{\partial y} \end{pmatrix} \quad \textbf{(2.5)}$$

Decomposition of the velocity gradient provides a symmetric and antisymmetric component, with the symmetric part being the strain rate tensor.

This strain rate tensor is defined as $S = \frac{1}{2}(V + V^T)$. Decomposition of S yields the eigenvalues and eigenvectors of the deformation. Eigenvectors denote the principle axes of the deformation. The eigenvalues denote the principle components of the strain rate tensor, with their signs denoting compressive (negative) or tensile (positive) strain. We observe very little tensile strain inside the network along the major axis and as such for visualisation purposes, only the principal strain denoting compression are shown in figures, these are often normalised to be represented between -1 and 0.

2.3.7 Measuring the local organisation of the Actin flow field

While streamlines provide a visual description of the global Actin flow behaviour, another method that has been employed in this project is a description of the averaged local alignment of the flow field (Figure 2.4).

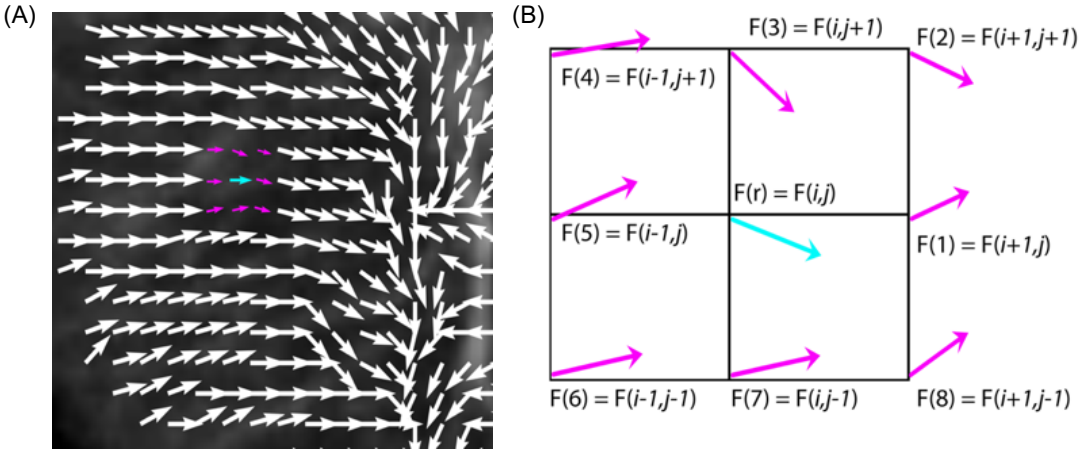

Figure 2.4: A schematic showing an example of the order analysis of Actin flow. The average cosine similarity between a reference velocity vector (cyan) $F(r)$) and it's 8 nearest neighbours (magenta) ($F(n)$) is calculated. This

local analysis of alignment is calculated for every vector in the field and averaged to produce the mean alignment for each genotype.

This allowed me to assess just aligned the flow vectors are and as such provides us with some insight into the coordination and organisation of the flowing Actin network. To compute the relationship between the orientation one vector and another and achieve an order parameter, the cosine similarity measure was employed. Specifically, the average cosine similarity between a reference velocity vector ($F(r)$) and it's 8 nearest neighbours ($F(n)$) is calculated (Figure 9). This local analysis of alignment is calculated for every vector in the field and averaged to produce the mean alignment for each genotype. The cosine similarity computes the cosine of the angle between two non-zero vectors and is derived by way of the normalised dot product. The result of this measure is a value in the range of -1 to 1. Values approaching -1 representing anti-correlation (vectors are anti-parallel); values approaching 0 display little to no correlation (vectors are approaching orthogonal); and values approaching 1 display positive correlations (vectors are orientated in the same direction).

2.3.8 Defining retrograde and anterograde flow regions

In order to further describe the behaviour of the Actin flow field I have developed a novel method that provides a functional definition of retrograde and anterograde flow. Previously when retrograde and anterograde flow has been described, these domains have been effectively made in reference to a notional polarity of the cell in question (Vallotton *et al.*, 2004; Okeyo *et al.*,

2009). Flow that moves from the front of the cell towards the rear of cell is considered to be retrograde flow. While anterograde flow is the region of the Actin network that flows from the back of the cell towards the front (Figure 2.5).

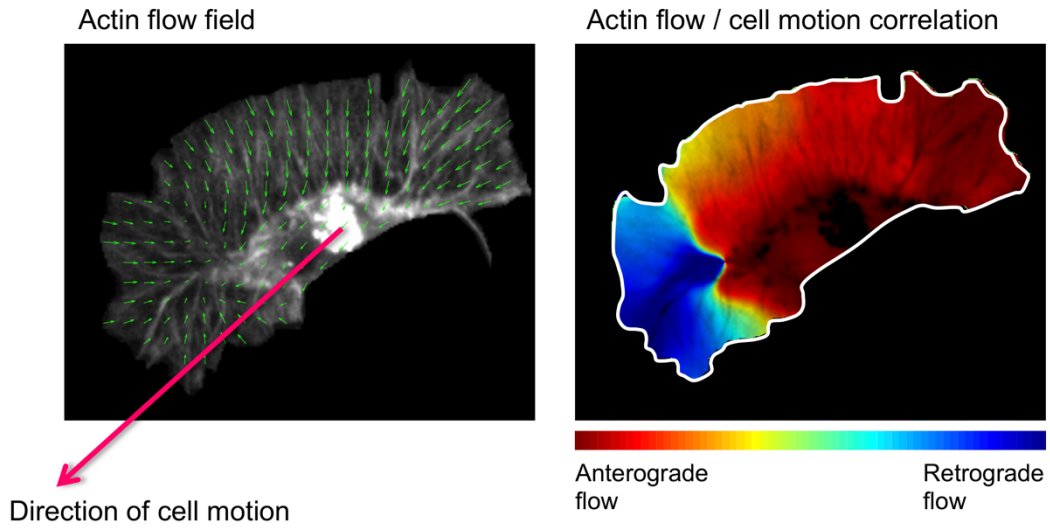

Figure 2.5: Graphical representation of the means of attaining retrograde and anterograde flows. The left side image shows Actin flow vectors output from the PIV analysis, with the direction of cell motion overlaid. These flow vectors are directionally correlation to the direction of cell motion, with the principle output being the right-side image. Here, regions in red are flow vectors parallel aligned with the direction of cell travel (anterograde flow), while regions in blue are antiparallel to the direction of cell motion (retrograde flow).

In the methodological design of this project I am defining retrograde flow as any part of the flowing Actin network that displaces in an antiparallel fashion to the displacement vector of the cell itself. The corollary of this is that anterograde flow is defined as the Actin network that flows in an aligned fashion with the directional of cell motion. This analysis also utilises the cosine

similarity measure, where, in this case the similarity is derived from a comparison between the cell's displacement vector and all velocity vectors in the Actin flow field. This analysis thus produces a new signed scalar field, representing the directional correlation values between Actin flow and cell motion. Any value in that correlation field that presents with a positive value is now to be considered anterograde flow, while negative values are to be considered retrograde.

2.4 **Analysing edge dynamics**

2.4.1 Extension and retraction analysis

In order to investigate the role of Actin cytoskeletal extensions in cell motion, we developed a technique that allowed us to identify regions of extensions and retractions. This method can be described as in Dunn *et al.,* in terms of sets (Dunn, Weber and Zicha, 1997).

$$Extension = \{C \mid \complement C_1 \cap C_2\} \quad \textbf{(2.6a)}$$

$$Retraction = \{C \mid C_1 \cap \complement C_2\} \quad \textbf{(2.6b)}$$

$$Intersection = \{C \mid C_1 \cap C_2\}\ , \quad \textbf{(2.6c)}$$

where C denotes pixels within a time-lapse image that are contained within the spread of the cell boundary between subsequent frames. C_1 represents an initial image while C_2 denotes the subsequent image. As an example, points in C_1 that are not found in C_2 (i.e. $\complement C_2$) are considered regions of the cell that have retracted between time points.

Here an initial image (C_1) of a hemocyte is a converted to a binary mask and subtracted from a binary mask of the subsequent frame of the time-lapse (C_2). This subtraction step reveals regions of that are shared between the two shapes i.e. the intersection (I), and regions that are only in one shape and not the other. This latter case is what is used to define extension and retractions for the analysis included here. This analysis can be initially viewed as something akin to a qualitative descriptor of edge dynamics. However, this has been developed and transformed into a method that is fundamentally quantitative in nature, through a number of techniques.

The first is that while understanding the overall dynamics of the cell boundary may be of interest, we were keen to develop a tool set to address the question of the role of the leading edge in cell migration. However, extensions appear throughout the perimeter of the cell boundary and it is not possible to assign an identity to the leading edge. One option could be to define any extension that occurs at the front of the cell to be a part of this, however this begs the question, in that in this definition the ‘leading edge’ is defined as the edge that ‘leads’ before we’ve established that that is indeed the case. The method I propose is that of a considered filtering of the cell extensions by size, removing all but the largest extension. This region would necessarily contain the most active polymerisation activity and so to address this question of edge extension in cell migration we should start with the largest protrusion and work from there. This processing probes the number of connected components of the extension ‘blobs’, labels them, and ranks by

pixel area. Following this next part of the analysis can be performed which will allow us to track that largest extension. This analysis is initially defined by the reduction of two image features, the cell nucleus and the large extension, to single coordinate points, these are: 1) the location of the nucleus' centroid at that time-point; 2) and the centroid of the extension. Using the nucleus as a base, the position vector of the extension is calculated. This provides us with a bearing of predominant cell protrusion which can be later compared to cell motion. This analysis can also be used to compare all cell protrusions across the cell boundary to cell travel.

2.4.2 Analysis of edge extension velocities

To evaluate edge dynamics, segmented time-lapse images of hemocytes were analysed using a Segmentation and Windowing package. Here cell edge extensions and retractions were calculated at each pixel along the cell boundary. Custom scripts implemented in MATLAB (MathWorks®) were used to calculate extension speed globally, and locally within specific regions of the cell boundary. For calculating the edge velocity in the direction of cell motion, the edge was segmented within a region bounded by a 25˚ cone that was centred about the direction of cell motion. For calculating the edge velocity within the largest extension, the longest uninterrupted region along the perimeter of the cell edge was segmented. For quantifying the net edge activity, velocities determined to be extension were positively signed while retraction were signed negative, and the average of this activity was calculated.

2.5 **Temporal cross-correlation**

Once the position vectors of the extension, and streamline sinks are derived I was interested in investigating whether there is any directional behaviour that precedes cell motion. This directly addresses the question of whether or not cell migration is indeed directed by leading edge migration. This analysis involves the directional correlation of the two vector parameters which are the position vectors of interest (representing the location of cell protrusions or primary streamline sinks) against the cell's direction of motion at all potential time lags. Directional cross-correlation has been used to resolve temporal hierarchies in a number of disparate fields from the study of the collective motion of pigeons (Nagy *et al.*, 2010); the synchronized flight of mosquitos (Shishika *et al.*, 2014); and relevant to this area of study is that this analysis has provided insight into the predictive power of Pi3K localization in cell migration (Weiger *et al.*, 2010). This directional cross-correlation function is described by $DC_{ij}(\tau) = \langle v_i(t) \cdot v_j(t+\tau) \rangle$ where, the time averaged scalar product of the normalised 'velocity' between parameter 1 (v_i) and parameter 2 (v_j) at time t and lagged time intervals ($t + \tau$).

3 The (mis)Leading Edge

3.1 Introduction

Cell migration is hypothesised to be a stepwise process that is led by a focussed extension of the cell boundary, driven through the process of Actin polymerisation (Ridley *et al.*, 2003). In this motility model, Actin polymerisation protrudes the cell membrane at the front of the cell. This is followed by the association of the Actin network with the extra-cellular matrix, and finally motor proteins contract pulling the rear of the cell forwards (Mitchison and Kirschner, 1988; Mitchison and Cramer, 1996). However, despite the prevalence of this model in the literature there are questions that have yet to be challenged. Firstly, it is unclear how coordinated cell motion over time results from the localised dynamics of the leading edge of the cell, and beyond that, it has also not been shown that cell migration is indeed a stepwise process. There is a growing body of evidence on the other hand, that the edge of the cell may actually be disruptive for cell motion. For instance a recent study showed that cells with many filopodia exhibit impaired migration (Leithner *et al.*, 2016).

In this chapter I directly address the role of the leading edge in cell migration. I show the findings from my investigations into the fluctuating edge of freely migrating Drosophila embryonic hemocytes. This begins with simple observations of the protruding and retracting cell boundary and moves onto the connection between edge behavior and gross cell movement. This was

achieved by the development of novel tools and the implementation of previously published methods of cell boundary tracking.

3.2 **Contributions**

Over the course of this project I have developed an analytical toolset to address questions concerning that of hemocyte edge dynamics. This includes the identification and tracking of edge extensions and retractions, and analysis of edge persistence and direction. A previous PhD student in the lab Dr Andrei Luchici and I have extended the utility of a cellular kinematics MATLAB package for the purposes of normalizing any position vector to any reference vector, that is utilized in the extension analysis (Davis *et al.*, 2015). The time-lapse imaging that has provided a library of freely moving wild type Drosophila embryonic hemocytes was performed by myself and a previous PhD student in the lab, Dr John Robert Davis.

3.3 **Results**

3.3.1 Hemocytes are Inefficient Migrators

In previous studies it has been reported that Drosophila embryonic hemocytes migrate persistently. For instance, the directionality ratio of hemocyte trajectories has been reported to be as high as 85.6% (Wood, Faria and Jacinto, 2006). This directionality ratio measure compares the straight-line distance of the cellular trajectory against the actual summed displacements of the trajectory, with results of 100% illustrating a perfectly

straight path. It remains unclear however, just how the persistence of hemocytes or any cells for that matter is maintained by the Actin cytoskeleton.

In order to analyse the processes governing hemocyte migration, the question of which marker would most reliably represent a cell's translation arose. It has been determined that the centroid of the labelled nucleus is an appropriate fiducial marker as the nucleus holds its shape robustly and doesn't move significantly independent of cell motion, as a result it can be tracked without much error (Davis *et al.*, 2012). This is in stark contrast to tracking of the cell's centroid. While the cell centroid is a common alternative for cell tracking, this approach can lead to tracks that are heavily biased in the direction of asymmetric shape change, a behavior that hemocytes exhibit very frequently. To illustrate this, I have shown an example of randomly migrating hemocyte, undergoing minimal whole-cell translation, despite the trajectory of the centroid positions suggesting a large amount of movement having taken place (Figure 3.1 A, Movie 1). This is very problematic given that this project involves assessing the relationship between cell motion and fluctuations at the cell boundary as large extensions will necessarily shift the position of the cell centroid without it being clear that this has caused real cell translation. In order to demonstrate the instability of the hemocyte cell boundary, I automatically traced the edge contours of hemocytes through time (Figure 3.1 B). This revealed that the edge is highly unstable, at the high temporal resolution of 5 seconds per frame.

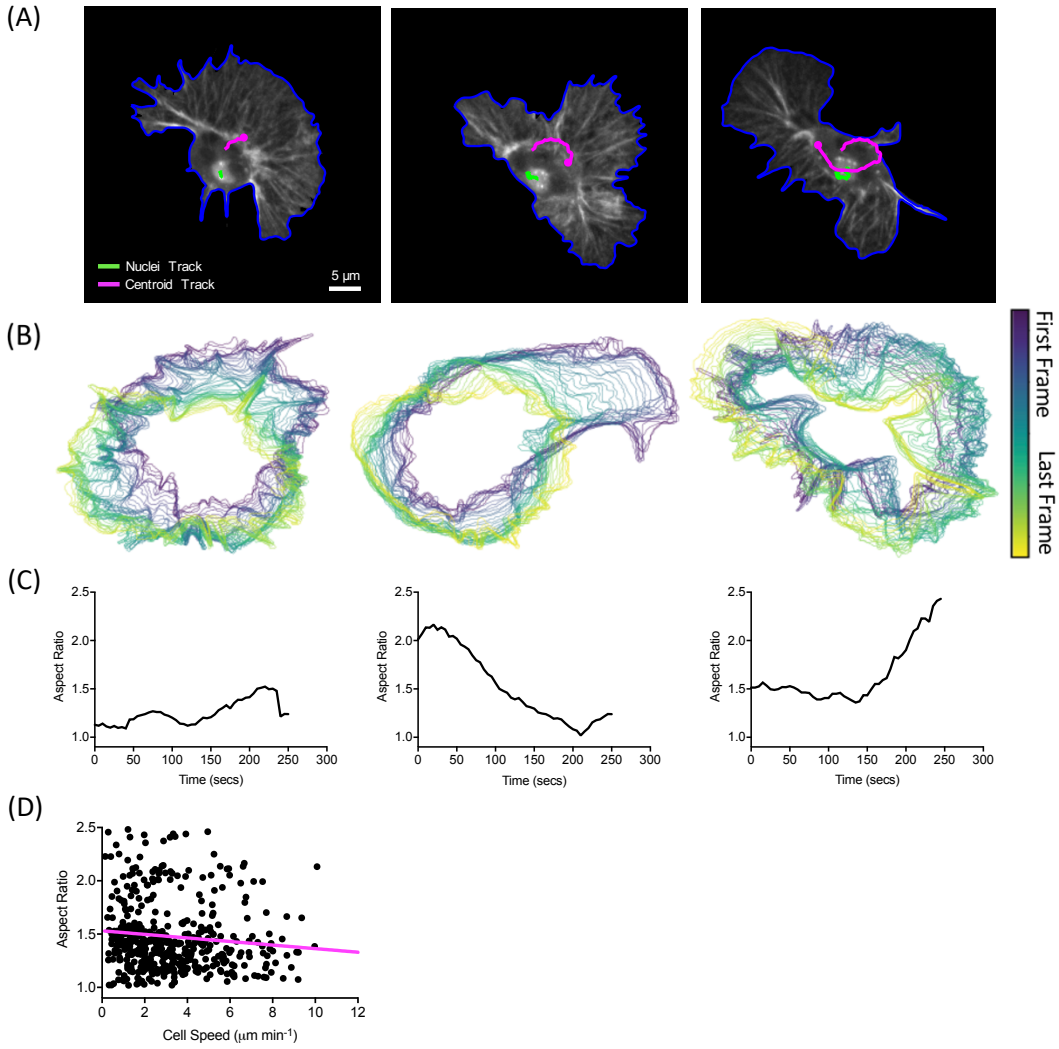

Figure 3.1: Hemocytes rapidly change shape readily during migration.

(A) Automatic tracking of a hemocyte comparing tracking of the cell centroid (magenta) and the nucleus (green). Note that in hemocytes at this temporal resolution (5 sec per timepoint) tracking the cell centroid reflects overall shape changes more than cell motion. In contrast, the nucleus represents a fixed fiducial within the cell that more accurately reflects cell movement. **(B)** Three example hemocyte edge activity maps where colour code spans from the first-time frame of the time-lapse to the last. Hemocyte edges fluctuate rapidly between time points, displaying many peripheral protrusions. **(C)** Three example time courses (analysed from the cells in **(B)**) which tracks the aspect

ratio of the cells through time. A value of 1 denotes a rounded morphology while values >1 denote indefinite elongation. **(D)** Scatter plot showing instantaneous hemocyte aspect ratio versus cell speed. This shows no correlation between these two parameters. R^2=0.01, n=443 data points, from 9 cells.

I was also interested in briefly examining the relationship of cell motion to cell shape in hemocytes. From this analysis I have ascertained that like other motile cell types such as fish keratocytes there is a preference to migrate in an elongated state, with an average aspect ratio (major axis length divided by the minor axis length) of 1.477 (data not shown). There is high variability in these hemocyte aspect ratio measures, and it can change significantly during migration, with cells occasionally transforming from a rounded morphology to an elongated morphology during migration and vice versa. (Figure 11 C). However, unlike in fish keratocytes these cells predominantly migrate along their major axis, rather than their minor axis (Keren *et al.*, 2008). I have examined this relationship by measuring the average angle difference between the vector of nuclear displacement that represents instantaneous cell motion and the major axis of the cell shape. This revealed an average angle difference of 37° which represents a bias of movement along this major axis (data not shown). I have also attempted to compare the speed of cell migration to the aspect ratio of the cell shape, with the hypothesis that the cell undergoes elongation during rapid migration, or that elongation facilitates faster migration, but interestingly I saw no such correlation, with an R^2 between these two parameters of 0.01 (Figure 3.1 D).

Through the use of a standard measure of cell persistence, the directionality ratio (Benhamou, 2004; Gorelik and Gautreau, 2014), I was able to quantify the propensity for turning that Drosophila embryonic hemocytes possess while migrating. The directionality ratio of these cells gives a median value of 0.71 (mean value of 0.59), supporting similar findings that show that hemocytes migrate persistently *in vivo* (Wood, Faria and Jacinto, 2006).

3.3.2 Edge extensions are poor predictors of cell directionality

3.3.2.1 Analysing the angular distributions of edge extensions

The behavior of the leading edge has been assumed to play a significant role as the driver of cell migration (Ridley, 2011), however recently there have been indications that peripheral protrusions can distract and disrupt the migration of cells. In order to analyse the behavior of the cell edge, I developed a method that determines the angle between the vector of cell displacement and the position vectors of all regions of extensions in that time frame. This involves the identification of cell edge extensions through a 'blob' detection method, which is used for all extensions, and for the largest region of extension (Figure 3.2, Movie 2). This process involves a normalisation step that rotates the position vectors to a common frame of reference which is the vector of nuclear displacement (fixed along the *OX* axis). This allowed me to probe the distribution of edge extensions and for the first time attain

information about the instantaneous directional relationship between the edge and the trajectory the cell (Figure 3.2).

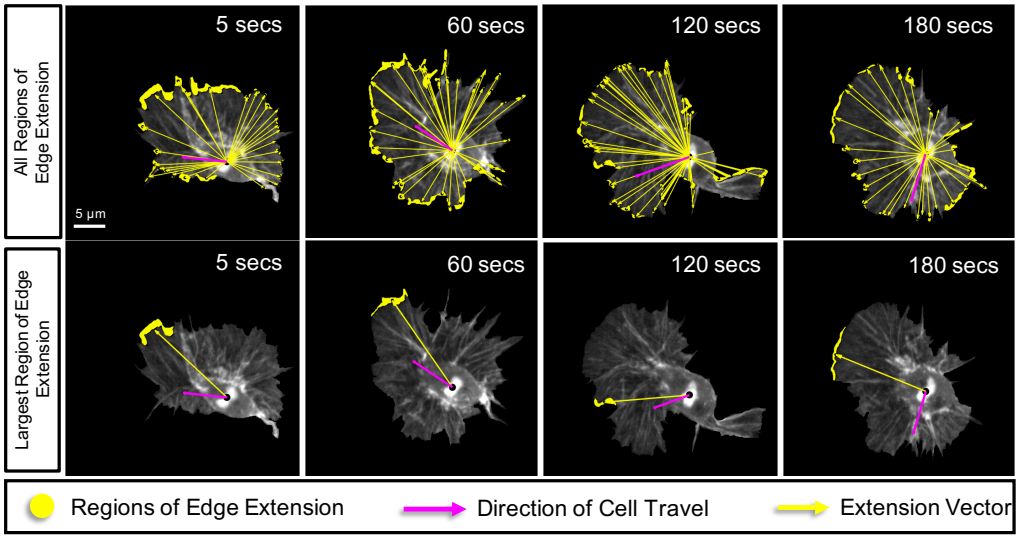

Figure 3.2: Tracking the regions of extension reveals weak connection to the direction of cell motion. Time-lapse sequence of a randomly migrating hemocyte in which edge extensions were automatically segmented. Vectors (yellow arrows) were then drawn from the nucleus to either each individual extension (top row) or the maximum extension defined as the largest contiguous area of extension (bottom row) while simultaneously tracking the cell's direction of travel (magenta arrow).

What becomes apparent from this analysis is that the cell edge is fluctuating in its protrusion dynamics in all directions. This highlights that despite the persistence of hemocytes it is clear that their migration is inefficient, in so much as these cells expend 'effort' in producing protrusions that contribute little to the motility of the cell (Figure 3.3 A). Rose plots that of the angle distributions of all edge extensions reveal a demonstrate a radial distribution around the cell boundary with a subtle bias in the direction of cell

travel (Figure 3.3 B). I was specifically interested in whether a directionality bias increases when filtering for the largest region of cell extension. Defined by the largest contiguous area of Actin network extension between frames, the angle of the position vector of the centroid of this large extension appears to be much more aligned with the cell trajectory, with a peak in the angle distribution within 60° of cell displacement, as shown through rose plots of the angle distributions (Figure 3.3 C-D). This highlights that there is indeed a greater amount of Actin polymerisation in the direction of travel. However, it is as yet unclear whether this is a coincidental relationship or whether it is the case that the leading edge is actually providing a directional influence on the cell's motion. However, often there are many instances where large extensions are produced in direction uncorrelated with the direction of cell motion (Figure 3.3 C-D).

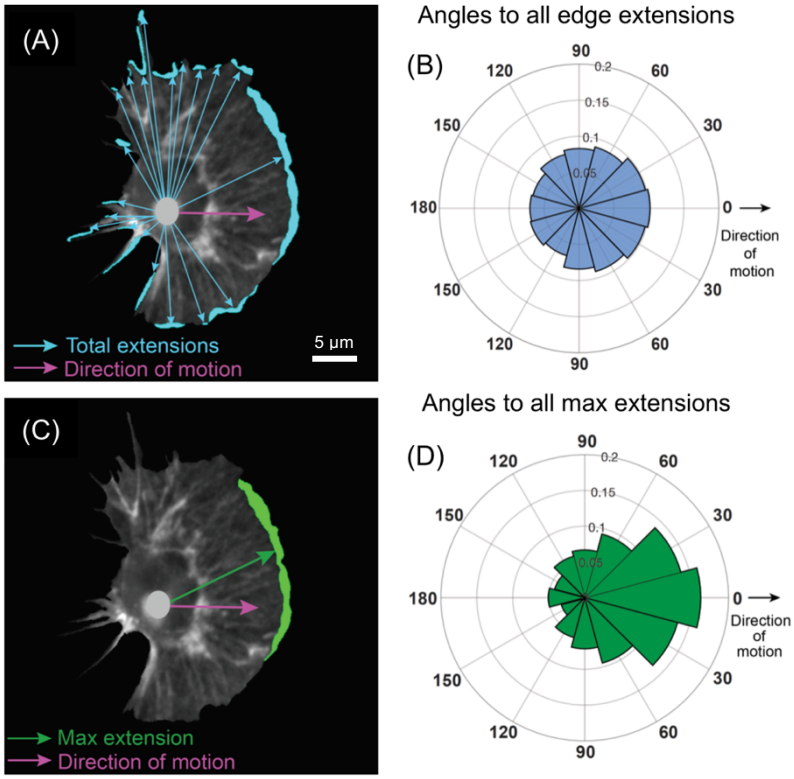

Figure 3.3: Leading edge fluctuations are a weak predictor of cell directionality. **(A)** A representative snapshot of a randomly migrating hemocyte with edge extensions automatically segmented. Vectors are drawn from the nucleus to each individual extension (blue arrows) and correlated with the direction of cell motion (magenta arrow). **(B)** A rose plot showing the direction of all extension vectors normalized to the direction of cell motion (0°). n=443 data points, from 9 cells **(C)** A representative snapshot of a randomly migrating hemocyte with maximum edge extensions automatically segmented. Vectors are drawn from the nucleus to the maximum extension by area (green arrow) and correlated with the direction of cell motion (magenta arrow). **(D)** A rose plot showing the direction of the maximum extension vectors normalized to the direction of cell motion (0°). n=443 data points, from 9 cells.

3.3.2.2 Correlating Edge Velocity Vectors to Cell Directionality

Through observation of migrating hemocytes it is clear that the edge rapidly fluctuates, which was examined by plotting the cell contours (Figure 3.1 B) and through edge tracking (Figure 3.4 A, B). Dynamic activity of the cell edge appears to be generated throughout the cell boundary with little relationship to the direction of motion. I wanted to develop this further and was interested in quantifying the stability of the cell extensions during migration and the locations in which they occur. The concept of inefficiency may be relevant here, which is a concept that considers a system that expends 'effort' on edge activity that doesn't get translated into cell motion (Dunn, Weber and Zicha, 1997; Hermans *et al.*, 2013). A cell that exhibits a high degree of migratory efficiency for instance would exhibit a reduced number of wasteful

protrusions while maintaining a similar amount of displacement. In order to test this motility efficiency in another way, I calculated the instantaneous cosine similarity between the position vectors of the largest contiguous region of extension and retraction to the direction of cell motion. This quantified the alignment of the direction of travel with significant edge activity (Figure 3.4 A-B).

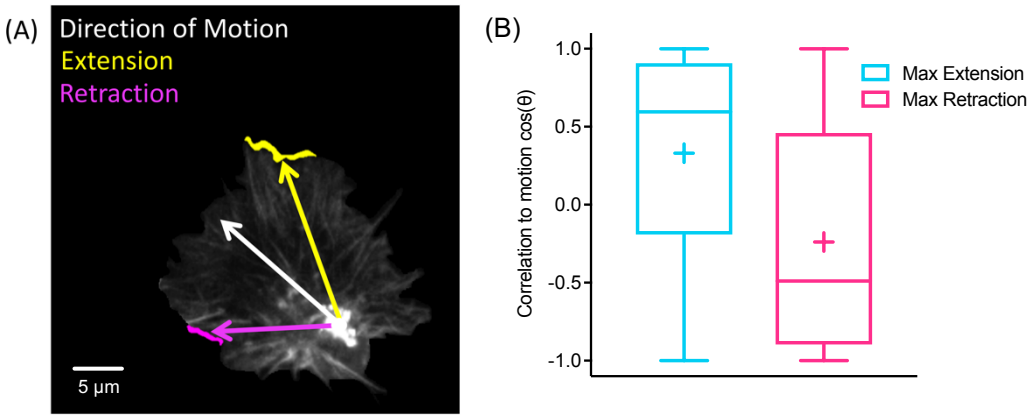

Figure 3.4: The largest regions of extension and retraction are weakly correlated to the direction of cell motion. **(A)** An example hemocyte frame showing the automatically segmented regions of largest extension and retraction (yellow and magenta respectively), their position vectors, as well as the instantaneous direction of cell motion (white arrow). **(B)** Boxplot showing the distribution of instantaneous correlation values (cosine of the angle difference) between the position vectors of the largest extension or retraction and the direction of motion. Units are in cos$\boldsymbol{\theta}$ where positive values approaching 1, represent parallel alignment, while negative values approaching -1 represent antiparallel alignment. n=443 data points, from 9 cells.

This revealed that the largest extension region, is weakly correlated with cell travel, with a mean alignment value at $\cos\theta$ = 0.33, and a median alignment value of $\cos\theta$ = 0.59. While the largest region of retraction has a mean alignment value at $\cos\theta$ = -0.24, and a median alignment value of $\cos\theta$ = -0.49. This highlights that the largest region of polymerisation is strongly disconnected from the direction of cell motion. Having analysed the angular distributions of the extensions with respect to the position of the nucleus, I was interested in examining how the direction of edge displacement velocity vectors aligned with cell motion. In order to do this the cell boundary was identified and tracked throughout the duration of the time-lapse movie using a technique developed for the purposes of studying leading edge dynamics (Machacek and Danuser, 2006). With the edge detected and the protrusions and retraction velocity vectors computed, I developed further methods of segmenting specific regions of the edge that are calculated from this edge morphodynamic protocol. For instance, not only can I access global edge extension dynamics (Figure 3.5 A), but in a similar process of filtering seen earlier in this chapter I have been able to derive the largest contiguous area of edge velocity vectors from the images (Figure 3.5 B). This morphodynamic analysis provided a velocity vector-based description of edge dynamics, and as such I wanted to investigate the overall directional bias of hemocyte protrusions. To achieve this, I analysed the resultant of the components of the extension velocity vectors and its correlation to cell motion. Which provided the overall direction of edge protrusion velocities, and as such this measure will give a direct indication of how efficiently the protrusions are formed with respect to cell motion. If protrusions are oriented in the direction of travel, then

the resultant of the protrusion vectors will be positively aligned with the cell's displacement vector and it would be reasonable to state that the protrusions are efficiently produced. However, deviation away from the direction of travel would highlight an expenditure of 'effort' generating protrusions that are not contributing to cell motility.

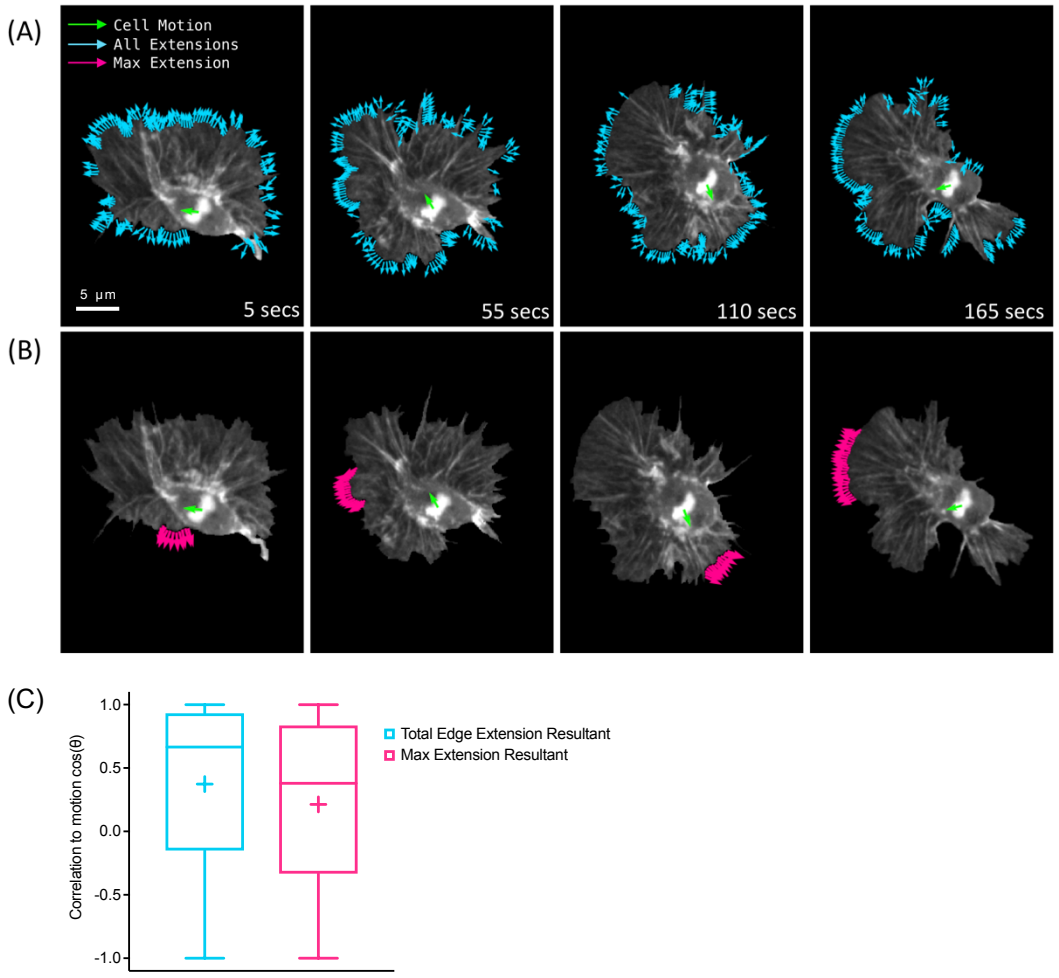

Figure 3.5: The direction of edge protrusion weakly correlates to cell motion. **(A)** A time-lapse sequence showing all protrusion around the cell boundary (blue vectors). These vectors are summed to give the resultant protrusion vector (not shown), which is correlated to the direction of cell motion (green vector). **(B)** A time-lapse sequence showing the dynamics of the edge

extensions, contained in the largest contiguous extending region (magenta vectors). These vectors are also summed to give the resultant protrusion vector (not shown), which is correlated to the direction of cell motion (green vector). **(C)** Box plot showing the distribution of correlation values when comparing the instantaneous directional correlation of the direction of cell motion and the resultant vectors of all edge velocities, and the velocities in the largest contiguous extension, and cell motion. A directional correlation value of 1 denotes that the resultant velocity vector is perfectly aligned with cell motion. n=443 data points, from 9 cells.

I have found that the resultant vector representing the summed velocity vectors in the largest region of extension is weakly oriented with respect to the direction of cell travel (Figure 3.5 B, C). This supports earlier evidence in this chapter showing that the 'leading edge' (as represented by the largest region of edge extension), is minimally contributing to cell directionality. Interestingly, the resultant of all edge extensions is also positively correlated with cell motion (Figure 3.5 A, C). This suggests a mechanism of global edge regulation, that appears to holistically contribute to cell motion.

3.3.2.3 Hemocyte Edge Dynamics are Less Persistent Than Cell Motion

Following from the earlier observation that large regions of protrusions are produced inefficiently with respect to the direction of cell motion, I wanted to quantify the positional stability of the largest extension. This was achieved by employing directional autocorrelation, a persistence measure used in many migration studies inside and outside of the cell migration literature (Gorelik and

Gautreau, 2014). This was applied to position vectors of the largest region of extension in a similar fashion to the correlative analysis seen in Weiger *et al*., where directional autocorrelation was used to analyse hot spots of Pi3K (Weiger *et al*., 2010). Persistence of position vectors through the directional autocorrelation method could be thought of as an analysis of positional stability. In the context of analysing the stability of the cell edge, this was only used on the region of maximum extension, as it provides a common identity with which we can group the position vectors in a form representing a meaningful trajectory. The directional autocorrelation was also computed for cell trajectories (from displacements of the nuclei) and the resulting curves were compared (Figure 3.6 A). The intriguing result here is that the directional autocorrelation curve for the region of largest extension decays at a faster rate than the directional autocorrelation of cell motion. The rate of decay of the autocorrelation curve is the measure of persistence, with a faster decay representing lower persistence and thus a greater preponderance for turning, an autocorrelation curve with a slope of zero would be representative of a perfectly persistent series of displacements with no turning observed. This finding in the autocorrelations is surprising, specifically because protrusions at the leading edge are thought to guide cell migration. However, in this analysis the positions of the largest extensions are less stable than the cell they are purported to direct. From this data it is difficult to understand how cell directionality could emerge from unstable dynamics of the edge.

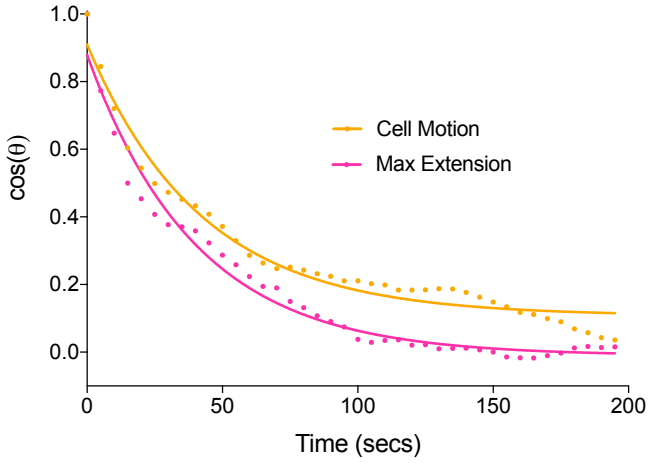

Figure 3.6: The leading edge is directionally impersistent. Directional autocorrelation comparing the persistence of cell motion and maximum edge extension showing that the maximum edge extension is less persistent than overall cell motion. Dotted lines are real data and solid lines are fits to an exponential decay.

3.3.2.4 Edge Extensions do not Precede Changes in Cell Directionality

Following the finding that the edge in hemocytes is not directionally persistent, I was interested in addressing whether directional changes in the position vectors of the cell extensions precede cell turning, which would suggest that the edge guide cell directionality (Figure 3.7 B). This was achieved by comparing the cell translocation vectors against the position vectors of the leading edge – specifically a vector constructed from the nucleus to the centroid of the largest extension – at varying time lags. This analysis would be considered to be a form of temporal cross-correlation, with a peak at a specific time lag representing the delay time between the cell edge protruding along some given axis and the nuclear displacement matching that orientation. This analysis revealed no specific temporal hierarchy, with the

cross-correlation curve peaking at zero-lags. This suggests edge extensions are not predicting the axis in which the cell turns. This challenges the implied temporal hierarchy of the stepwise model of cell migration.

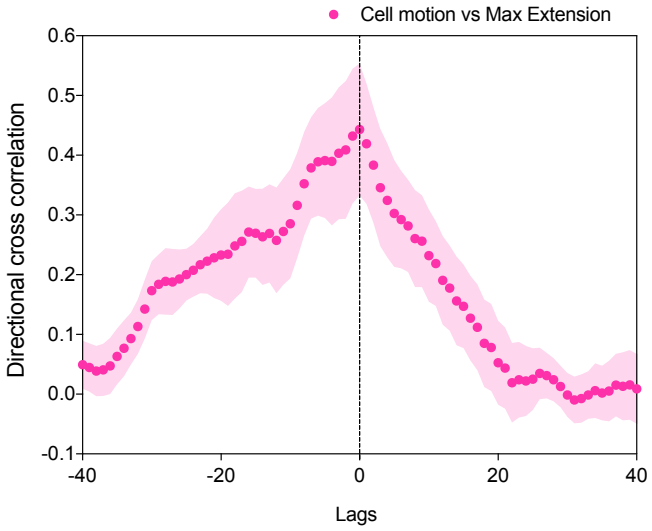

Figure 3.7: Edge Extension activity does not precede cell directional changes. Temporal directional cross-correlation comparing the direction of cell motion and the maximum edge extension which reveals a peak correlation at zero-lag (dotted line) showing no obvious temporal hierarchy in this migratory parameter. Error bars = SEM.

3.3.3 Analysing the rates of edge extension

The analysis featured up to this point has described the angular distributions of extensions, and the localised direction of edge extension. Consequently, I was interested in developing this analysis to incorporate the rates at which extensions are produced. This data was also attained from edge velocity vectors, around the cell boundary, restricted within a narrow cone that describes the direction of travel, and the largest contiguous region of edge extension (Figure 3.8 A, C, E). I also examined the net protrusive activity by

isolating edge displacement vectors that can be categorised as extensions or retractions depending on whether they are orientated outside of the cell, or inside the cell respectively (Figure 3.8 B, D). When analysing net protrusion speeds across the cell boundary I discovered that the average is essentially zero (-0.09 ± 0.04 μm min^{-1}) which reveals that hemocytes are able to maintain their cell area very effectively through the activity of the cell boundary. However, net speed calculated from the edge velocities in the direction of travel highlight an increase in speed (1.5 ± 0.2 μm min^{-1}), denoting a bias towards protrusive activity in the direction of motion.

I have also found that hemocytes develop protrusions in the direction of travel at an average rate of 5.4 ± 0.15 μm min^{-1} (Figure 3.8 D,F), while the region of largest extension has an average extension rate of 6.3 ± 0.16 μm min^{-1} (Figure 3.8 B, 17 E,F). I have also calculated the speed of hemocyte migration, calculated from the displacements of the nucleus, which revealed an average of 3.3 ± 0.1 μm min^{-1} (Figure 3.8 F). When comparing cell speed against the rate of edge extensions I observe a highly significant difference. This difference is observed in comparisons between cell speed and extensions in the direction of travel, and the largest region of extension (Figure 3.8 F). This rate comparison, like the earlier analysis into the angle distributions and directional correlations of the max extension, highlights a disconnect between the activity of the cell boundary and cell motion.

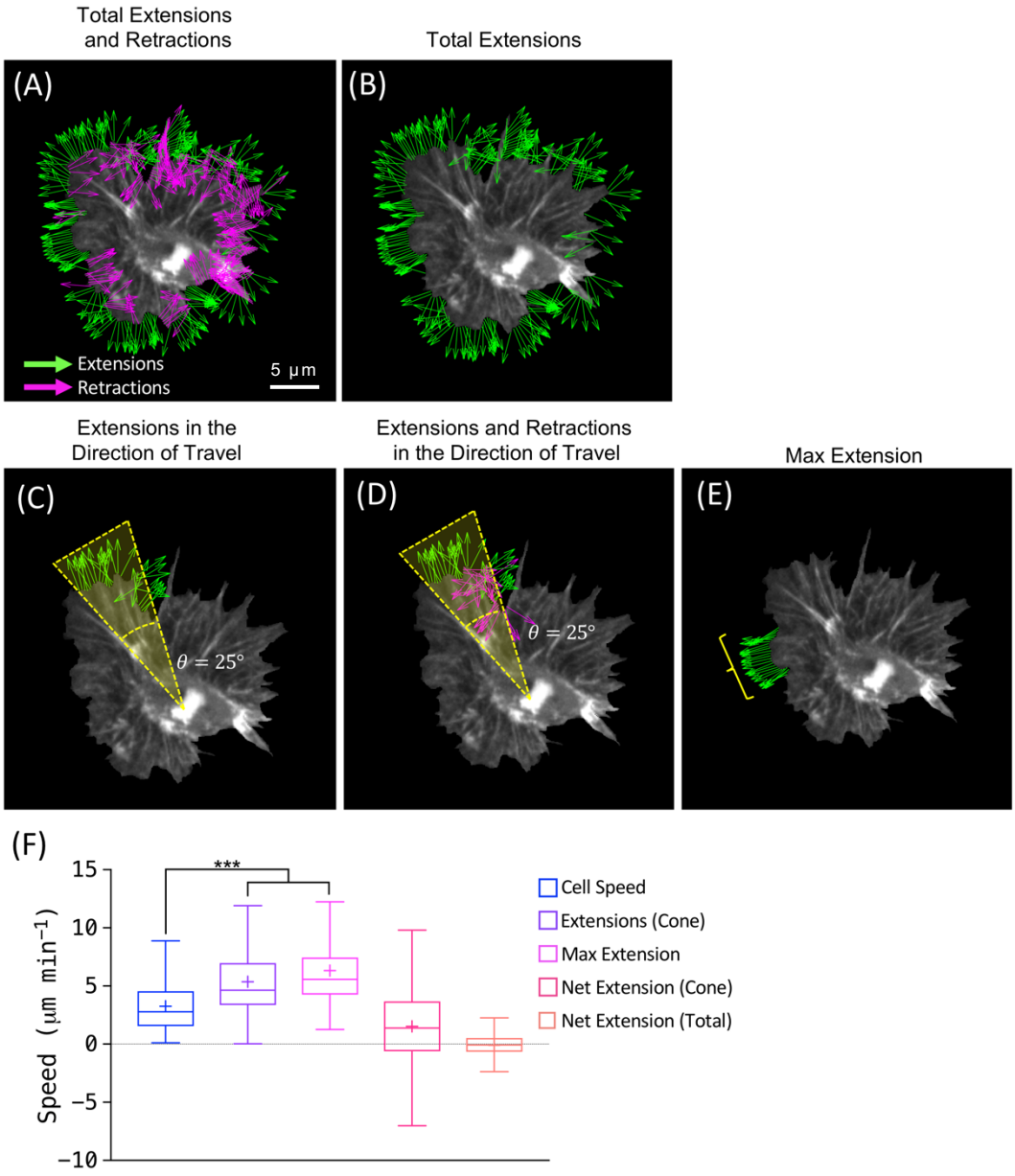

Figure 3.8: Like the direction of protrusion, the rate of protrusion is also disconnected from cell motion. **(A-E)** Example hemocyte with edge dynamics displayed with respect to the specific parameter of interest. **(A)** shows all edge extensions and retractions while **(B)** only highlights extension velocities around the cell boundary. **(C)** shows all extension velocities within a narrow cone (25°) in the direction of travel, while **(D)** shows velocity vectors of both extension and retraction in this coned area. **(E)** represents the largest contiguous area of extension velocities along the cell boundary. **(F)** A boxplot

denoting the speed of the hemocyte edge fluctuations. There is a significant difference between the speed of cell motion and the rate of edge extension in the direction of travel and in the largest extension, showing a disconnection between these parameters and cell speed. Also shown is the net protrusion speed in the direction of travel and across the cell boundary - extension are defined with a positively signed speed, while retractions are assigned a negative sign. There is a bias towards extension in the direction of travel, while the net extension across the cell is ~0 μm min^{-1} which demonstrates the active management of constant cell area. n=443 data points, from 9 cells.

3.4 **Discussion**

In this chapter I have shown that Drosophila embryonic hemocyte migration could be defined as an inefficient or wasteful process using the criteria of Hermans et al (Hermans *et al.*, 2013). This is because hemocyte edge extensions occur in wide distribution around the cell body and appear to minimally contribute to the directionality of cell motion. These cells migrate persistently, independent of the activity at the cell boundary. This brings into question whether the activity of the edge translates to migrational changes at the cell scale in freely moving hemocytes. To perform the analysis in this chapter, hemocyte nuclei were automatically tracked to define the motion of the hemocytes in the embryo.

Much attention has been paid to the leading edge as the fundamental driver of cell motion with migration itself often described as a cyclical process initiated by protrusion of a cell's leading edge (Ridley *et al.*, 2003). However,

through a novel combination of cell tracking and edge morphodynamic analysis I have challenged this concept directly in freely moving hemocytes. Firstly, the nucleus was used for cell tracking. In hemocytes the nucleus maintains its shape well and moves minimally during migration (independent of whole cell translocation), even during dramatic repolarisation events (e.g. contact inhibition of locomotion). Nuclei tracking compares well to other robust mechanisms of hemocyte tracking including tracking of the hemocyte cell body (Davis *et al.*, 2012). However, it should be noted that in other cell types the nucleus moves significantly and would not to be a reliable proxy for cell motion (Gomes, Jani and Gundersen, 2005). In many studies the movement of the cell centroid is used to represent cell motion. Tracking the cell centroid however, can introduce significant errors along the axis in which large regions of extensions occur. This effect is especially present at the high temporal resolution I have been imaging at, and importantly noisy centroid tracking has also been noted using 10 second intervals for the imaging of fish epithelial keratocytes which are noted for their shape stability (Keren *et al.*, 2008). Cell motion has also been measured through the summation of edge activity, inclusive of edge extensions and retractions (Yamao *et al.*, 2015). This however doesn't appear to be an appropriate measure in hemocytes as when examining the average combined velocity of extensions and retractions the value is approximately zero. An alternative mechanism of cellular tracking which is not liable to error through the activity of the edge involves a cross-correlation approach that computes the rotation and translation of the cell between frames (Wilson and Theriot, 2006; Keren *et al.*, 2008; Wilson *et al.*, 2010; Barnhart *et al.*, 2011). This method however is limited in its applications

beyond robust cell tracking. For instance, in this chapter I have introduced edge tracking techniques utilising position vectors constructed between the nucleus and for example the region of largest contiguous extension. All of the edge tracking methods featured here require two easily definable and identifiable sets of coordinates that acts as the head and tail of the vectors, this would not be possible using the cross-correlation method. However, one way this method could be utilised in this project is in discarding the small Brownian displacements of the nucleus away from the estimated cell trajectory. For instance, the calculation of cell speed could be improved by tracking the nucleus in the moving cell image (the laboratory reference frame) and tracking the nucleus in the cell image that has had its translation and rotation removed (the cell frame of reference). If the cell reference frame trajectory is subtracted from the trajectory calculated in the laboratory reference frame, any subtle motion of the nucleus would be removed.

In order to understand the relationship between cell extensions and cell. motion, I compared position vectors computed from the centroid of cell protrusions against the direction of cell motion at that specific time-point. This established that extensions are produced across the perimeter of the cell with but a subtle bias in the direction of travel. This is reminiscent of inefficient motility model described whereby the contributions of extensions and retractions contributed minimally to cell motion (Hermans *et al.*, 2013). However, while the role of the extending membrane in migrating cells may not be particularly informative of cell travel, the region of largest extension did appear to be often in the direction of travel, however through directional

autocorrelation analysis, it was observed to be directionally impersistent. This was confirmed by employing a morphodynamic profiling technique (Machacek and Danuser, 2006). Which demonstrated that protrusions are produced across the cell boundary, at speeds far higher than that of cell motion itself. This analysis also revealed that that the resultant velocity of the protrusion vectors was only weakly correlated with the direction cell travel, further suggesting that many protrusions are made that do not obviously contribute to cell directionality. Given this data, edge extensions in randomly migrating hemocytes exhibit exploratory behaviour. I was also unable to find any obvious preceding behavior when comparing the direction of cell motion and the direction of edge extensions. This not only addresses the edge centric model of cell migration but brings into question that cell migration is a stepwise process.

4 Actin Flows are Highly Organised During Hemocyte Migration

4.1 Introduction

This chapter outlines the analysis performed to quantify Actin flows in hemocytes, and the novel tools developed for this purpose. Specifically, I analysed how Actin network is organised as it flows within Drosophila embryonic hemocytes. This organisation includes but is not limited to; areas of compression and destruction, directionally distinct regions of the Actin flow field, and some more generic measures such as the rate of Actin flow. Principally I have used this information to examine how this organisation correlates to the motion of Drosophila embryonic hemocytes at high spatial and temporal resolutions.

There have been a number of attempts to probe how the flowing Actin network is organized, through various methods of analysis. For instance the Actin network in some cultured cells can be defined by two distinct domains, the lamella and lamellipodia which are "*kinematically, kinetically, molecularly, and functionally distinct*" (Ponti *et al.*, 2004). Other investigations into Actin network organisation have involved more complex analysis of the flowing Actin network utilizing the methods seen in fluid mechanics such the calculation of flow divergence to outline regions of Actin network turnover (Vallotton *et al.*, 2004; Schaub, Bohnet, Laurent, J. Meister, *et al.*, 2007; Okeyo *et al.*, 2009).

In one study (Vallotton *et al.*, 2004) four zones of which the Actin network are classified into, these are:

1. The lamellipodium
2. The lamellum
3. A region exhibiting anterograde flow of the Actin network
4. A convergence zone

In hemocytes there does not appear to be a distinctive lamellipodial / lamella separation, as such only Actin flow in lamellum (zone 2) will be analysed. Sites of anterograde flow (zone 3) and transition regions between directionally distinct domains of the Actin flow field (zone 4) have been identified in hemocytes through work performed for this thesis which will be discussed at length. In this chapter I will also discuss my findings on how the Actin network is organized, with specific attention paid to how that organisation persists in a system that is constantly flowing. I have also focused on trying for the first time to define the organisation of the Actin network in the context of the cell's motion.

4.2 **Contributions**

The development of the PIV pseudo-speckle method to measure Actin retrograde flow was developed in hemocytes by a previous PhD student in the lab Dr Andrei Luchici and adapted from work produced in the analysis of Actin dynamics in growth cones (Betz, 2007). I have designed and developed all the methods to probe flow organisation analysis seen here, with the exception of

the algorithms for principal strain and the analysis of flow turnover that was developed for this PIV system by Dr Andrei Luchici, from earlier flow analysis (Vallotton *et al.*, 2004; Wilson *et al.*, 2010). The process of computationally fixing a cell to change reference frames was utilised was developed for this hemocyte system by Dr Andrei Luchici from earlier migration studies (Wilson and Theriot, 2006). The wild type library of movies was produced by myself and Dr John Robert Davis.

4.3 **Results**

4.3.1 Analysing Actin flow rates in freely moving hemocytes

4.3.1.1 Tracking Actin flows through Particle Image Velocimetry

In order to probe the behavior of the Actin network during cell migration, tools had to be developed that provide a meaningful representation of its movement. This project has utilized particle image velocimetry (PIV) (section 2.3), which allows for the quantification of the global Actin flow field within hemocytes (Figure 4.1, Movie 3). PIV is a template matching technique rather than being a technique that tracks individual particles. PIV attempts to identify, through normalized cross-correlation (Lewis, 1995), the intensity distribution of a specific sub-image of an initial image, within a sub-image of a subsequent image of a time-lapse movie (Westerweel, 1997). This method has benefits over other tracking tools, PIV provides a global Actin flow field which is not possible in kymography and is less computationally intensive when compared to florescent speckle microscopy.

The analysis described here has utilized Drosophila embryonic hemocytes expressing UAS-LifeAct-GFP to visualise the Actin network (Figure 4.1, Movie 3). These cells are also expressing UAS-RedStinger, which is a probe for labelling the nucleus. These cells were manually segmented, and the PIV was only used on image information bounded within the cell mask (see section 2.3.1). All movies in this chapter were imaged at fast temporal resolution of 5 seconds/frame. For any analysis involving the quantification of the Actin flow derived from PIV, data contained within the cell body has been discarded as there is no obvious Actin flows in this region.

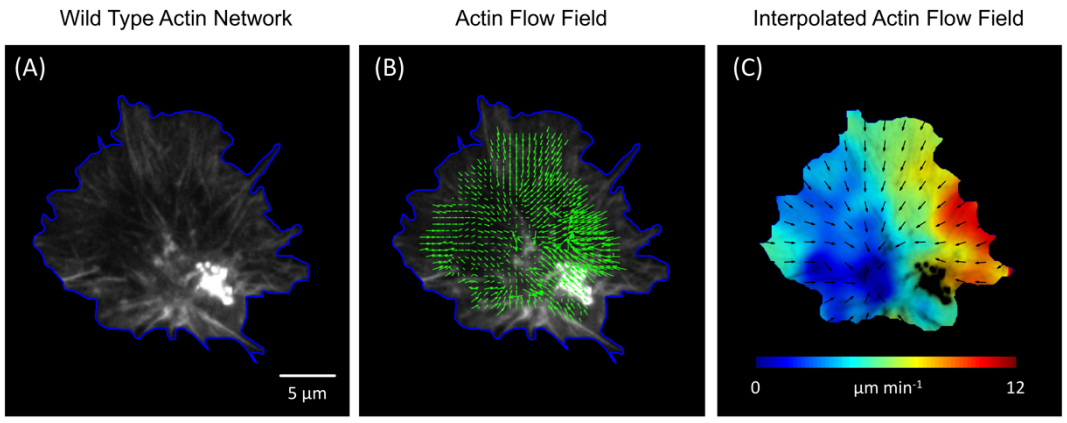

Figure 4.1: Actin flows in hemocytes can be effectively tracked using PIV. **(A)** An example hemocyte manually segmented, migrating on the ventral surface of the nerve cord. Actin is labelled with UAS-LifeAct-GFP, and the nucleus is labelled with UAS-RedStinger. **(B)** The raw and unfiltered displacement field of the Actin network in **(A)** tracked using PIV. Green arrows denote a displacement between time-frames of an Actin 'feature'. **(C)** An example of the interpolated velocity field of the Actin flow, the colour code denotes the speed of the Actin network flows, while the overlaid vectors are unit vectors denoting the direction of local Actin displacements.

4.3.1.2 There is no correlation between flow speed and the speed of cell migration

A qualitative assessment of the Actin flow field in hemocytes demonstrates a centripetal flow with an apparent speed gradient, with faster flows at the edge and slower flows as the network approaches the cell body. I have computed the average flow speed across 9 Drosophila embryonic hemocytes, which revealed a mean speed of 4.1 μm min^{-1} which fits with previous efforts to quantify Actin flow speed in these cells (Figure 4.2 A). One finding that was initially surprising and will require a more focused analysis is the relationship between flow speed and hemocyte migration speed. Previous studies that have become foundational to our understanding of this relationship describe a linear coupling between the speed of the Actin retrograde flow and the cell migrating (Jurado, 2004), which is characterised by the equation $v = \alpha V$.

This hypothesized linear (inverse) relationship between cell migration speed and Actin flow speed was supported by the descriptions of the Actin clutch, whereby the flowing Actin network slows down while gripping to the migration substrate, while the contraction forces used to pull the network rearwards are now driven into the substrate to provide a traction force for cell motion. However, in a recent study no correlation was observed between the speed of Actin retrograde flow and cell migration speed in the laboratory reference frame, which is the frame of reference in which the imaging and measurements were taken (Wilson *et al.*, 2010). Similarly, I have observed from comparing the instantaneous cell speed and the mean lamella flow speed

that there is no correlation between the two measures (R^2=0.06) (Figure 4.2 B). I do however observe a weak positive correlation in the cell's frame of reference when comparing the speed of Actin flow to cell speed (R^2=0.25) (Figure 4.2 C). This reference frame transformation has removed both the translation and rotation from cell motion and was achieved through published methods (Wilson and Theriot, 2006). The finding that there is no correlation to cell speed and the speed of Actin flows is surprising given the Actin clutch hypothesis. With the Actin clutch hypothesis slow flowing Actin represents the coupling of the network to the migratory substrate. This coupling results in elevated contractile tension that is driven into the substrate and results in an increase in cell speed. The observation of no correlation in the laboratory reference frame may be due to the observable regions of slow flow at the front and fast flow at the rear, which may simply cancel out, thus a more focussed analysis of the flow speed cell speed relationship might be required. As a consequence, the Actin clutch hypothesis is valid at small spatial scales, but it does not scale when considering global Actin flows.

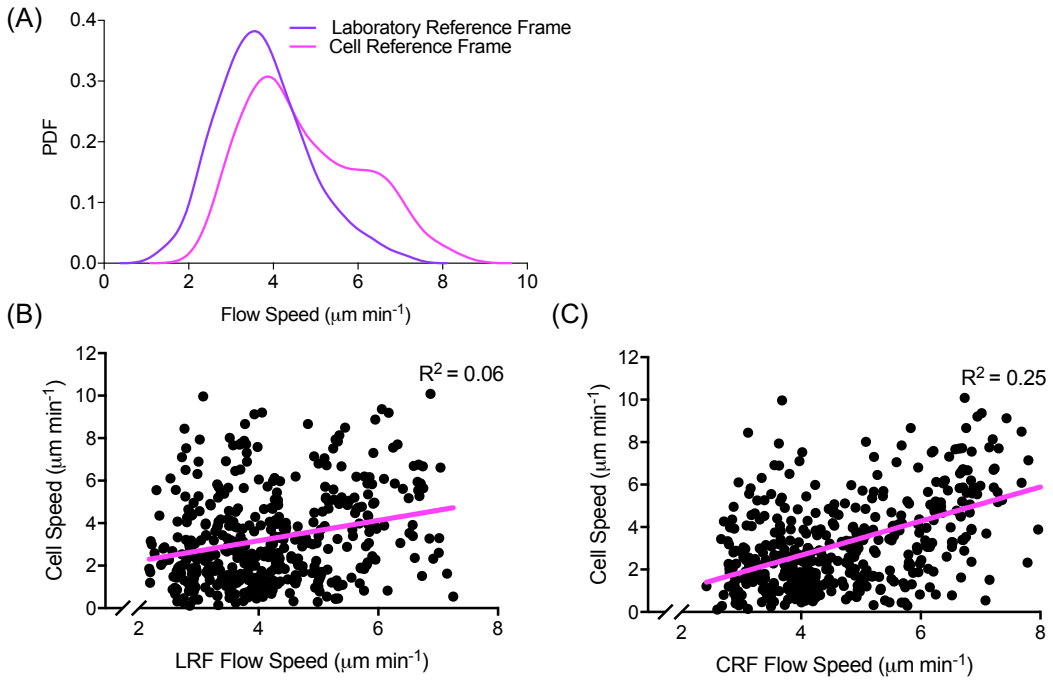

Figure 4.2: A linear relationship between flow speed and cell speed could not be detected in hemocytes. **(A)** Probability density function (PDF) showing the distribution of flow speeds in the laboratory reference frame (blue) and cell's reference frame (red). **(B)** Scatter plot showing the relationship between the average Actin flow speed in the laboratory reference frame (LRF) and cell speed. This shows there is no correlation between the two parameters (R^2=0.06). n=443 data points, from 9 cells**. (C)** Scatter plot showing the relationship between the average Actin flow speed in the cell's reference frame (CRF) and cell speed. This shows a very weak positive correlation between the two parameters (R^2=0.25). n=443 data points, from 9 cells.

4.3.1.3 There are Specific Regions of Actin Network Slipping and Gripping

In response to the findings that there is no correlation between cell speed and global flow speed, I developed a method to define specific regions of the flow field to make more specific comparisons. These regions are defined by the direction in which the network flows, with respect to the direction of cell travel. This allowed me to defined regions of Actin retrograde and anterograde flows. To achieve this, I used the alignment value between the Actin flow vectors and the direction of cell travel, the alignment value being defined as the cosine of the angle between each Actin flow velocity vector and cell's velocity vector (denoting cell motion). These alignment values provide insight into whether the flow is moving in the direction of cell motion, or not, i.e. whether the Actin network is flowing in a retrograde ($\cos\theta > 0$) or anterograde ($\cos\theta < 0$) manner, respectively (Figure 4.3 A). This was motivated by the

hypothesis that retrograde flow speed should be slower than anterograde given the adhesive activity occurring in these regions (Jurado, 2004; Swaminathan *et al.*, 2017).

The first examination of the flow speed in the context of these newly defined retrograde and anterograde regions was achieved by extracting the mean flow speed from each frame in the retrograde region. Specifically, I sampled the Actin flow rates in the highly retrograde region defined by velocity vectors that had an alignment value of $\cos\theta > -0.9$. I observed a significant difference between the average flow speed across the lamella in comparison to the highly retrograde region (Figure 4.3 B). This significant difference suggests that these retrograde regions are regions of increased friction whereby the network is associated with the migratory substrate.

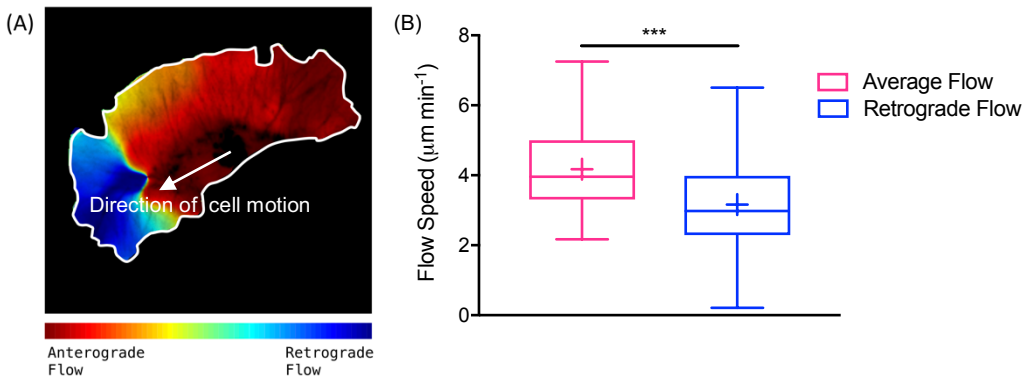

Figure 4.3: Directionally distinct regions of the Actin flow field are also distinct in magnitude. **(A)** A correlation map in which the direction of cell motion is correlated to the direction of every Actin flow vector within the cell. Note that a positive correlation highlights anterograde flow (red) while a negative correlation denotes retrograde flow (blue). **(B)** Quantification of the mean Actin flow speed in the entire cell versus the Actin flow speed in only the

region of the flow anti-correlated with cell motion (i.e. retrograde flow). Note that the Actin flow speed is significantly reduced in the retrograde region. ***P < 0.001, Mann-Whitney test. n=443 data points, from 9 cells.

I next moved onto analysing the flow speed in the direction of travel, versus a random orientation using line scans of the Actin flow field. This method would provide insight into the how the flow rate varies as a function of distance from the cell body. Broadly speaking I was expecting to observe a gradient of flow speeds, with low flow speeds recorded around the cell body, and increasing towards the edge as reported in hemocytes and other cell types such as fish keratocytes (Vallotton *et al.*, 2004; Yam *et al.*, 2007; Davis *et al.*, 2015). A gradient of flow speeds was observed for line scans drawn at random orientations through the lamella and line scans drawn in the direction of cell travel (Figure 4.4 A). However, the flow speed gradient is markedly reduced in the direction of travel, with overall speed levels reduced as well. This may highlight that only a narrow window of the retrograde flow is directly associating with the substrate enough to provide traction for the hemocyte to move. Specifically, that the hemocyte migrates along an axis defined by this slow flow corridor

With this data in mind, I was interested in examining what the average flow speed is, in the direction of travel compared to the average flow speed outside of the direction of travel. This was achieved by segmenting the flow field into two regions; the first defined by a narrow (25°) cone centred about the vector of cell travel, while the other is a narrow cone that captures Actin

flow information in a random orientation through the lamella. Analysis of the flow speed revealed that there is a significant difference in average flow speed between regions of the flow that are in the direction of travel compared to a random sampling of regions outside of this domain (Figure 4.4 B). However importantly there is no significant difference between retrograde flow speed defined by either the narrow cone of Actin flows, or their alignment value to the direction of cell motion (Figure 4.4 B). This again supports the notion that perhaps within this narrow corridor, the Actin network is tightly associated with the substrate through focal adhesions, while the rest of the network is, to use the terminology of Jurado *et al*., 'slipping' in an attempt to catch up to the rest of the network a during migration (Jurado, 2004).

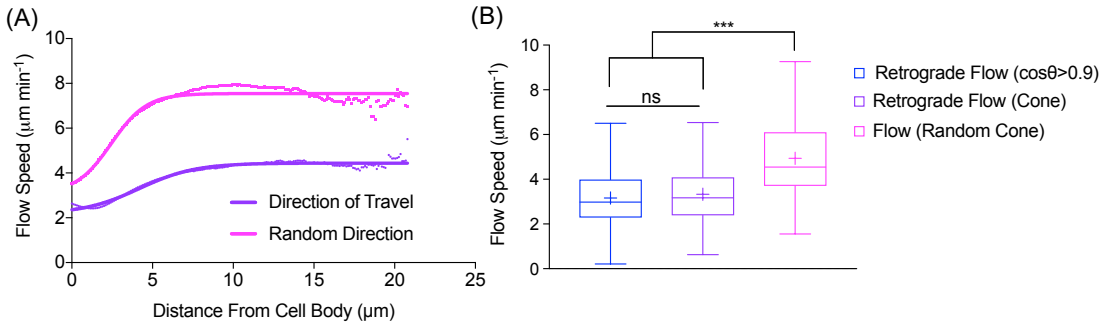

Figure 4.4: Actin flows slow in the direction of travel. **(A)** Actin flow speed data sampled from line-scans taken in the direction of travel and outside the direction of travel (randomly selected). The Actin flow field exhibits a sharp gradient, increasing in speed as a function of distance from the cell body towards the cell boundary. This gradient diminished in the direction of travel with much slower flow at all distances. **(B)** Boxplot representation of flow speed data sampled from regions that are highly retrograde to cell travel, in the direction of travel, and outside the direction of travel. There is no significant

difference between the direction of travel data set and the highly retrograde flow speeds. Both datasets were significantly reduced in comparison to the average cell speed randomly sampled from inside the lamella. ***P < 0.001, Mann-Whitney test. n=443 data points, from 9 cells.

I have determined that there was significantly different flow velocity characteristics of the Actin network in the direction of travel and the retrograde flow compared to the global average (and a random sampling from the lamella). I then investigated whether there was a correlation between the flow speeds in these two flow regions to the speed of cell motion. However, as with the comparison between average flow speed and cell speed (Figure 4.2) I was unable to detect any correlation between average flow speed sampled in the direction of cell motion and cell speed (Figure 4.5 A), or the average retrograde flow speed against cell speed (Figure 4.5 B).

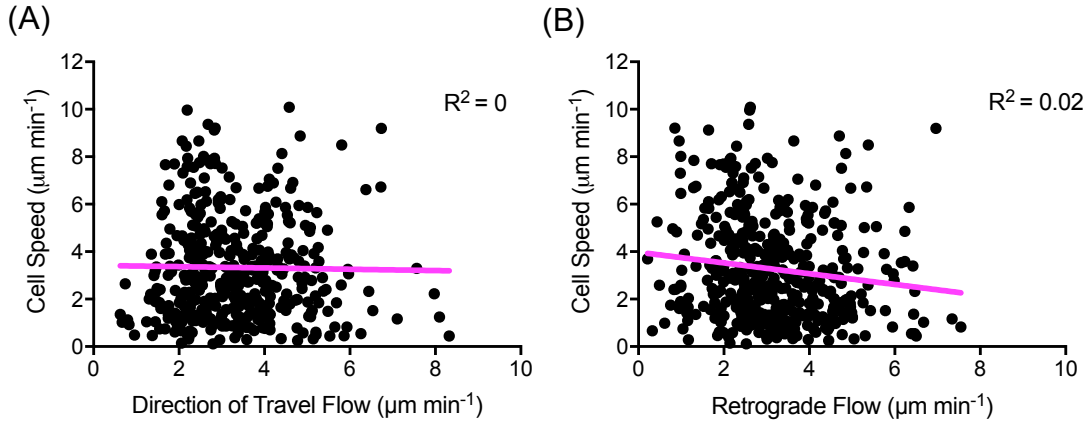

Figure 4.5: Speed of retrograde regions of Actin flow are also not correlated with cell speed. **(A)** Quantification of the average flow speed in the direction of travel against cell speed reveals no correlation (R^2=0). n=443 data points, from 9 cells. **(B)** As with the flow speed sampled in the direction

of travel, quantification of the average flow speed in the highly retrograde regions against cell speed reveals no correlation (R^2=0.02). n=443 data points, from 9 cells.

4.3.2 Divergence reveals time persistent organisation of the flowing Actin network

In order to investigate Actin network organisation, I looked at the divergence of the velocity field of Actin flow. This measure provides insight into the location of sources and sinks within the flow field. In a biological context, negative divergence values, which are sinks in the network have been hypothesised to be sites of Actin network compression and turnover where the Actin network is depolymerised (Vallotton *et al.*, 2004; Schaub, Meister and Verkhovsky, 2007). On initial observation of the divergence field I observed little positive divergence deep inside the Actin network, suggesting the absence of Actin sources inside the network (Figure 4.6 A, Movie 4). As a result, only negative divergence in the heatmaps within this chapter are presented. Divergence heatmaps reveal a distinct band of negative divergence surrounding the cell body (Figure 4.6 B). Another feature of these negatively divergent regions is that they appear to be have a degree of stability over time, with some regions of persisting on the order of a minute (Figure 4.6 B). The observation of time persistent sinks is notable given the behavior of the cell edge, which exhibits rapid fluctuating behavior. This finding supports previous studies on Actin flow divergence epithelial cells, in that regions of negative divergence or ‘compression’ are persistent on the order of minutes (Vallotton *et al.*, 2004).

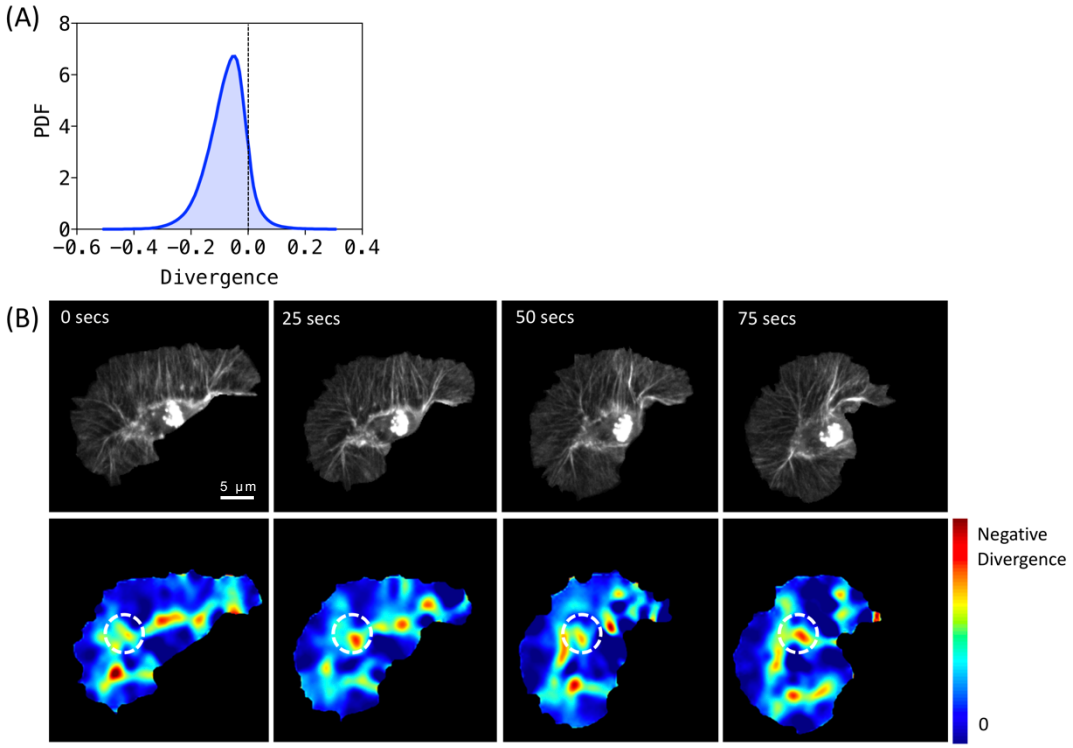

Figure 4.6: Divergence analysis of the Actin flow field reveals sinks in the flowing Actin network. **(A)** Probability density function (PDF) examining the distribution of divergence values within the Actin flow field. Note that most of the measured divergence within the Actin flow field is negative in value. **(B)** Divergence calculated from the Actin flow field to highlight sinks within the Actin network. In this image only negatively divergent regions are highlighted. The dashed white circle highlights a region of strong negative divergence that is persistent in time within the network.

From inspection of the Actin network at these regions of negative divergence I have also observed at sites of strong negative divergence occurrences of Actin network remodelling. For instance, during localised

spikes of negative divergence Actin fibres have been observed to reorganise (Figure 4.7 A, Movie 4).

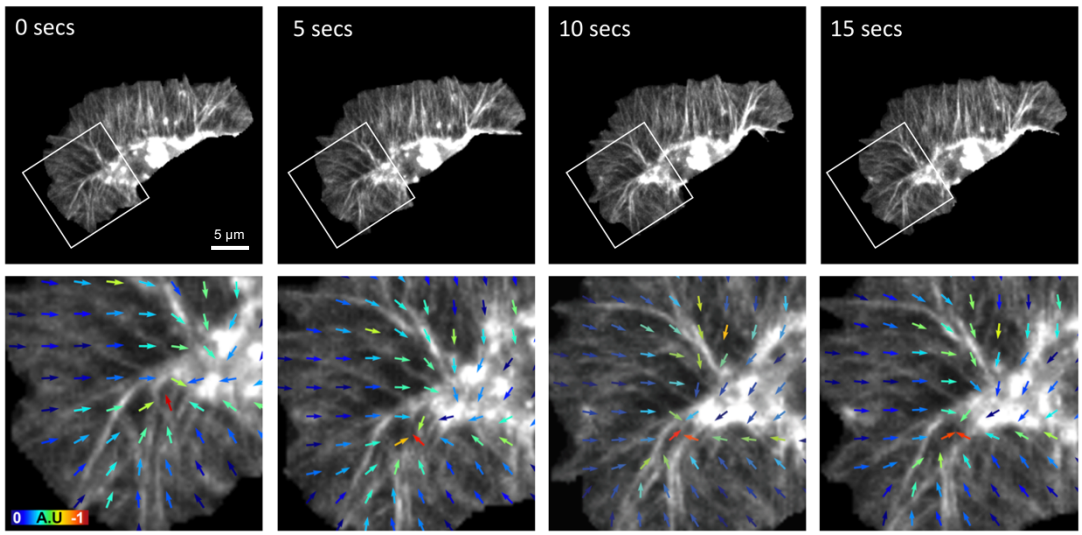

Figure 4.7: Sinks in the network represent regions of network deformation and remodelling. Time-lapse series of a LifeAct-GFP labelled hemocytes in Actin flow and subsequently divergence of the flow field were quantified. The bottom row is a high magnification image of the boxes in the upper row showing the direction of Actin flow (arrows) colour coded for the strength of the negative divergence. Note that in the centre of the flow field is a region of Actin network bending and bundling which correlates with strong negative divergence.

4.3.2.1 Negatively divergent regions denote sites of Actin network compression

The divergence analysis revealed negatively divergent regions of the network that could represent sites of compression and breaking or disassembly of the network. I was interested in probing these regions further to identify which mechanism is active at these sites, i.e. is there more

compression or depolymerisation. In order to approach this question, I computed the rate of strain of the flowing Actin network, which describes the amount of deformation that the Actin network undergoes. This was achieved by examining the eigenvalues that result from decomposition of the strain rate tensor (see section 2.3.6). Eigenvalues are signed scalars that denote whether the deformation is tensile (positive eigenvalue) or compressive (negative eigenvalue).

Once the compression values were computed, heatmaps of the compressive activity in the Actin network can be produced (Figure 4.8 A, Movie 4). These heatmaps revealed a spatial relationship between the areas of compression and of negative divergence. For instance, there are regions of intense compression that colocalises with regions of negative divergence (Figure 4.8 A). Following the observation that compression and negative divergence colocalise, I was interested in quantifying the extent of this spatial correlation. To achieve this, the divergence and principal strain fields were normalized to the maximum absolute value in their respective fields (to constrain the values to between -1 and 1). Once normalised, the pixel intensity of the divergence and principal strain fields were compared and the R^2 values determined (Dunn, Kamocka and McDonald, 2011). This process allowed me to determine how much of the variance of the divergence field could be accounted for by compression. This analysis revealed that there is a positive correlation between the principal component of strain and divergence, with a ρ value of 0.7 and an R^2 of 0.49 (Figure 4.8 B). This demonstrates that negative divergence is indeed constituted of compressive forces, where the

Actin network is put under intense strain. This compressive process would act to buckle the Actin network and make it more amenable to cutting and further buckling and breaking.

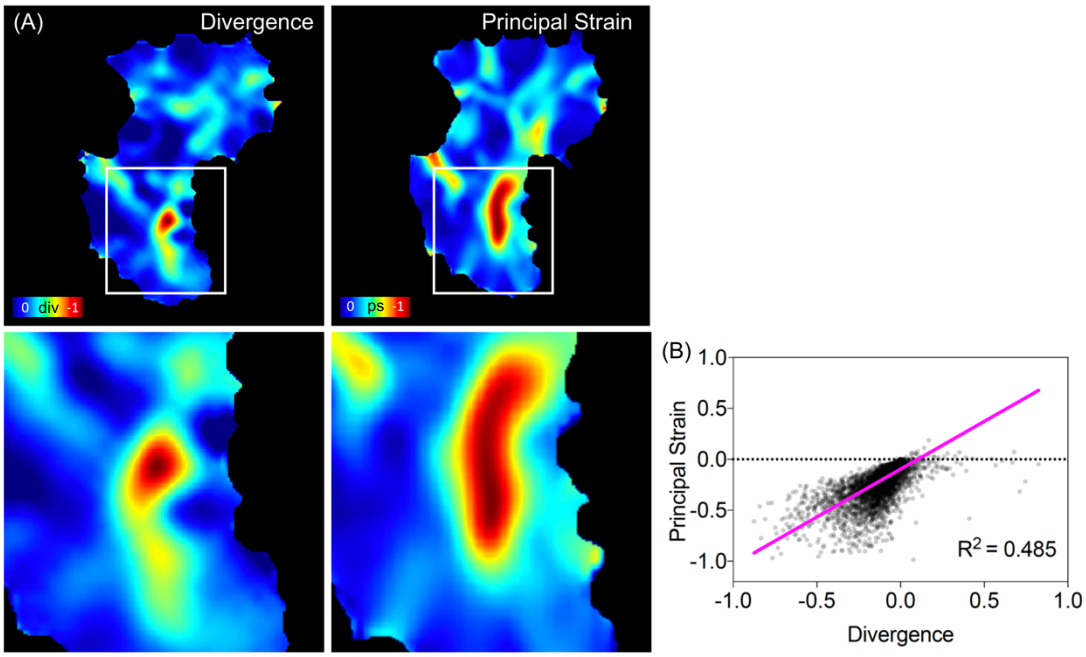

Figure 4.8: Negatively divergent regions of the Actin flow field represent regions of Actin network compression. **(A)** Heatmaps comparing the quantification of divergence (left panel), and negative principal strain (ps) i.e. network compression (right panel). Bottom panels are high magnification images of the boxes outlined in the upper panels. Note the partial overlap of these parameters. **(B)** Scatter plot comparing a random sample of points in the Actin flow field for divergence and principal strain. Note the relationship between the negative divergence and the negative values of the principal strain (i.e. compression).

4.3.2.2 Negatively divergent regions denote sites of Actin network disassembly

Previously I have calculated the contributions of compression towards the regions of negative divergence. I have found that approximately half of the variance (R^2 = 0.49) of the divergence field accounted by compression of the Actin network. Following this data, I was interested in looking at the role of disassembly of the Actin filaments in the negatively divergent regions as negative divergence could be linked network turnover as well as compression. Through observations of the Actin network in hemocytes it became apparent that there was not much accumulation of Actin at the rear of the lamella. Therefore, I hypothesised that there must be disassembly occurring. This disassembly would then provide new Actin monomers that can be recycled into the polymerization process. In order to trace the process of how the network is disassembled, I employed an algorithm that calculated the mass transfer of the flowing Actin cytoskeleton. This technique is designed to reveal where in the flowing network there is assembly and disassembly by examining the loss or gain of florescence intensity both between consecutive time-lapse images, and in the spatial gradient of florescence intensity (Vallotton *et al.*, 2004; Wilson *et al.*, 2010). Production of disassembly heatmaps reveals that there is a spatial overlap between the negative divergence and regions where the network is being taken apart (Figure 4.9 A, Movie 4). I observe that these negatively divergent regions are comprised to a significant extent of depolymerisation activity (R^2=0.463) (Figure 4.9 B).

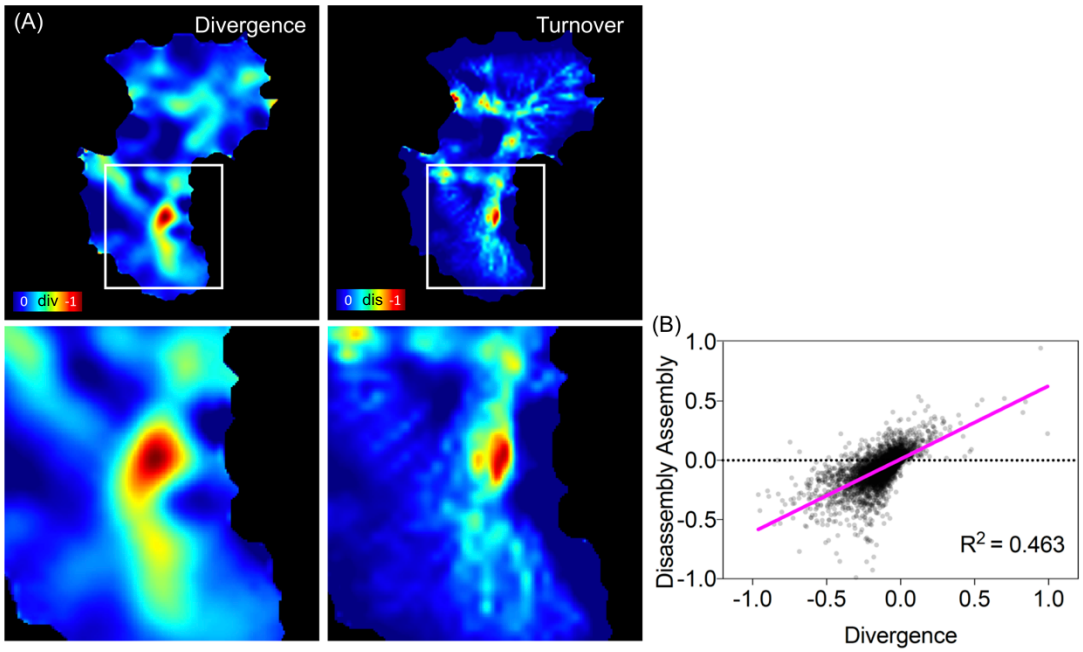

Figure 4.9: Negatively divergent regions of the Actin flow field also represent regions of Actin network disassembly. **(A)** Heatmaps comparing the quantification of divergence (left panel), and negative network turnover, i.e. disassembly (dis) (right panel). Bottom panels are high magnification images of the boxes outlined in the upper panels. Note the partial overlap of these parameters. **(B)** Scatter plot comparing a random sample of points in the Actin flow field for divergence and network turnover. Note the relationship between the negative divergence and the negative values of the turnover (i.e. disassembly).

4.3.3 Streamline analysis reveals global organisation of the flowing Actin network

While analysis of flow divergence has revealed stable organisation of the flowing Actin network, I was interested in exploring through other methods, the coherence of the cytoskeleton at the cell scale. To achieve this, I utilised

streamline analysis. Streamlines are a commonly used tool in fluid mechanics to describe the global organisation of a flow field. However, this technique has not been exploited in the study of cell migration and cytoskeletal flows. An individual streamline illustrates the path that a massless particle would take if it were to enter the flow field. Each point along the line is defined by the tangent of a single vector in a flow field and as such, streamlines cannot cross. In this project I have seeded streamlines around the edge of the cell which provides insight into the patterns of Actin flow behaviour and coherence across the lamella.

4.3.3.1 Streamline sinks represent asymmetries in the Actin flow field

Initial streamline analysis of the Actin flow field in hemocytes revealed that the network flows in a coherent manner, with the streamline retaining a stable line from their seed point at the cell periphery to their eventual termination (Figure 4.10 A, Movie 5). I also observed that these streamlines are highly confluent, with many streamlines terminating in a specific region of the cell in a streamline sink. I was interested in exploring the streamline data further by probing these sinks. I have found that there are often many sinks inside the network. However, during migration many streamlines terminate in a specific location forming a primary sink (Figure 4.10 B, Movie 5). This is an intriguing result, as it highlights a level of spatial organisation of the Actin retrograde flow field, which represents cell scale coherent behaviour of the Actin network. We observe that the region most densely populated with streamlines, appears to ‘lead’ the cell during migration. This may suggest an internal guiding mechanism that manifests out of the flowing Actin network.

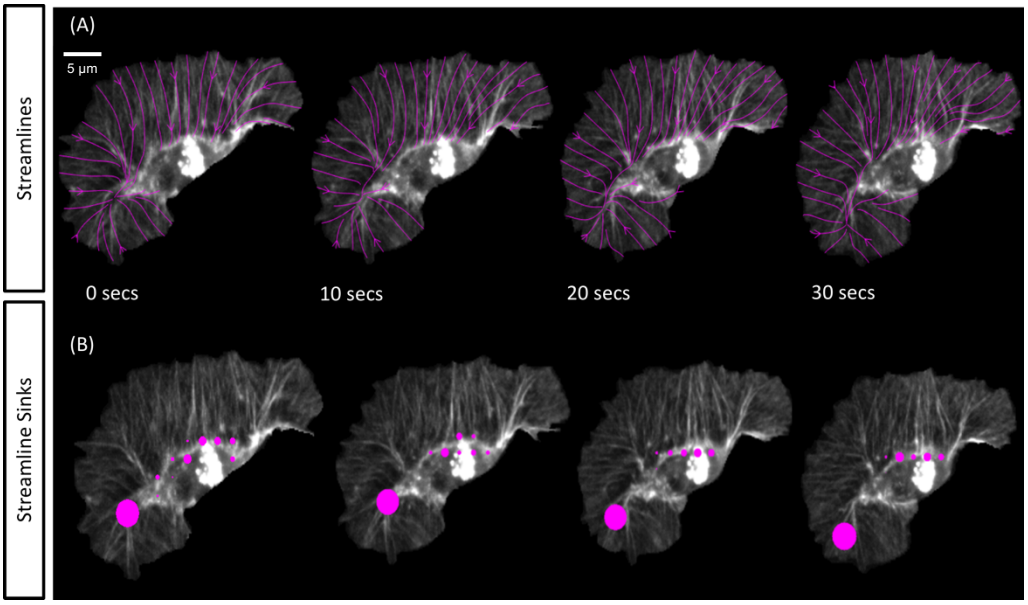

Figure 4.10: Streamline sinks reveal asymmetric behavior within the Actin flow field. **(A)** Streamlines calculated from the Actin flow field in which streamlines were seeded along the entire boundary of the cell, revealing the overall organization through the flowing network. **(B)** The confluence of streamlines quantified by calculating the number of streamlines ending in any one particular location within the cell. In this image, the size of the spots is normalized to the number of streamline sinks.

4.3.3.2 Streamline sinks colocalise with negatively divergent regions

I was next interested in comparing the localisation of the streamline primary sinks against the negatively divergent regions. Divergence is a measure that describes the extent to which a point in a flow field is a source of material. Streamlines on the other hand are a global measure that represent the directionality of the flowing Actin network as a whole. In order to examine this, I sampled the divergent values within a 2 µm x 2 µm box, centred about

the primary sink location, as well as more minor sinks. This analysis revealed that there was indeed a colocalisation which illustrates a degree of coordination across different levels of spatial description in the Actin network that has previously been unseen (Figure 4.11 A-B). I also found that the primary sink is strongly associated with the corridor of slow flow observed in

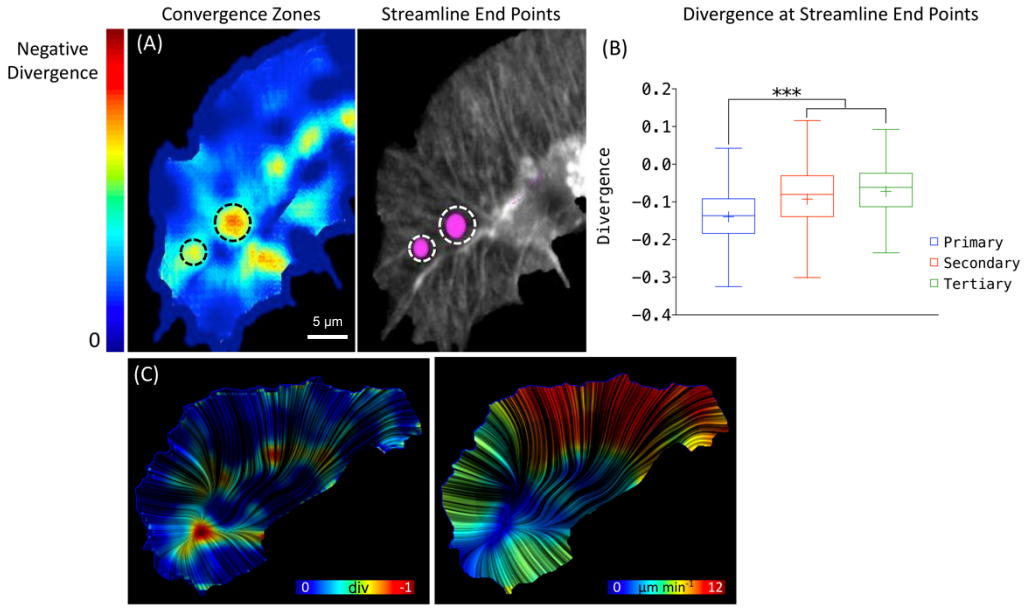

Figure 4.11: Actin retrograde flow is globally organized in migrating hemocytes. **(A)** Divergence (left panel) calculated from the Actin flow field to highlight sinks within the Actin network. In this image only negatively divergent regions are shown. The confluence of streamlines and thus sinks (right panel) quantified by calculating the number of streamlines ending in any one particular location within the cell. In this image, the size of the spots is normalized to the number of streamline endpoints. **(B)** Quantification of the divergence at the primary, secondary, and tertiary sinks. Here, many streamlines seeded at the cell boundary terminate at specific locations that are

sites of intense negative divergence. ***P < 0.001, Kruskal-Wallis test and Dunn's multiple comparison test. n=443 data points, from 9 cells. **(C)** Line Integral Convolution images of the divergence field (left panel) and the flow speed (right panel), highlighting how Actin network flows into specific regions of the network where the flows slows, compresses and disassembles.

4.3.4 Cell motion is directed by Actin flow asymmetries

4.3.4.1 Streamline sinks represent a transition between kinetically and kinematically distinct domains of the Actin flow field

Previously I have shown that the Actin network can be defined by the direction in which it flows. Specifically, I have been able to highlight regions of the Actin flow that moves in an anti-parallel alignment to the direction of cell motion. This region can be described as Actin retrograde flow, whereas regions of the Actin flow field moving with direction of cell travel is anterograde. Qualitative observations of these retrograde/anterograde fields suggest that there a sharp transition between these two regions (Figure 4.12 B). In order to highlight this transition, I computed the gradient of the retrograde/anterograde field (Figure 4.12 C). This highlighted the topography of the retrograde/anterograde field, showing that it is consistently flat everywhere except a sharp transition between directionally distinct domains of the flow (Figure 4.12 C). What was resolved was this sharp transition was consistently associated with the region where most of the streamlines were converging during cell motion (Figure 4.12 D). To confirm the colocalisation of streamline sinks with the maximum transition region, I have examined the average value of the gradient in the neighbourhood of the streamline sinks (Figure 4.12 E).

What this has revealed is that the primary sink indeed colocalises with the sharpest transition between retrograde and anterograde flow (Figure 4.12 E). This would highlight the streamline sink as a point of transition between regions of the network with highly different frictional characteristics. Whereby retrograde flow associating with the migratory substrate provides traction forces required for cell locomotion. The anterograde region on the other hand would be defined as an area of network slipping, whereby the molecular clutch is disengaged.

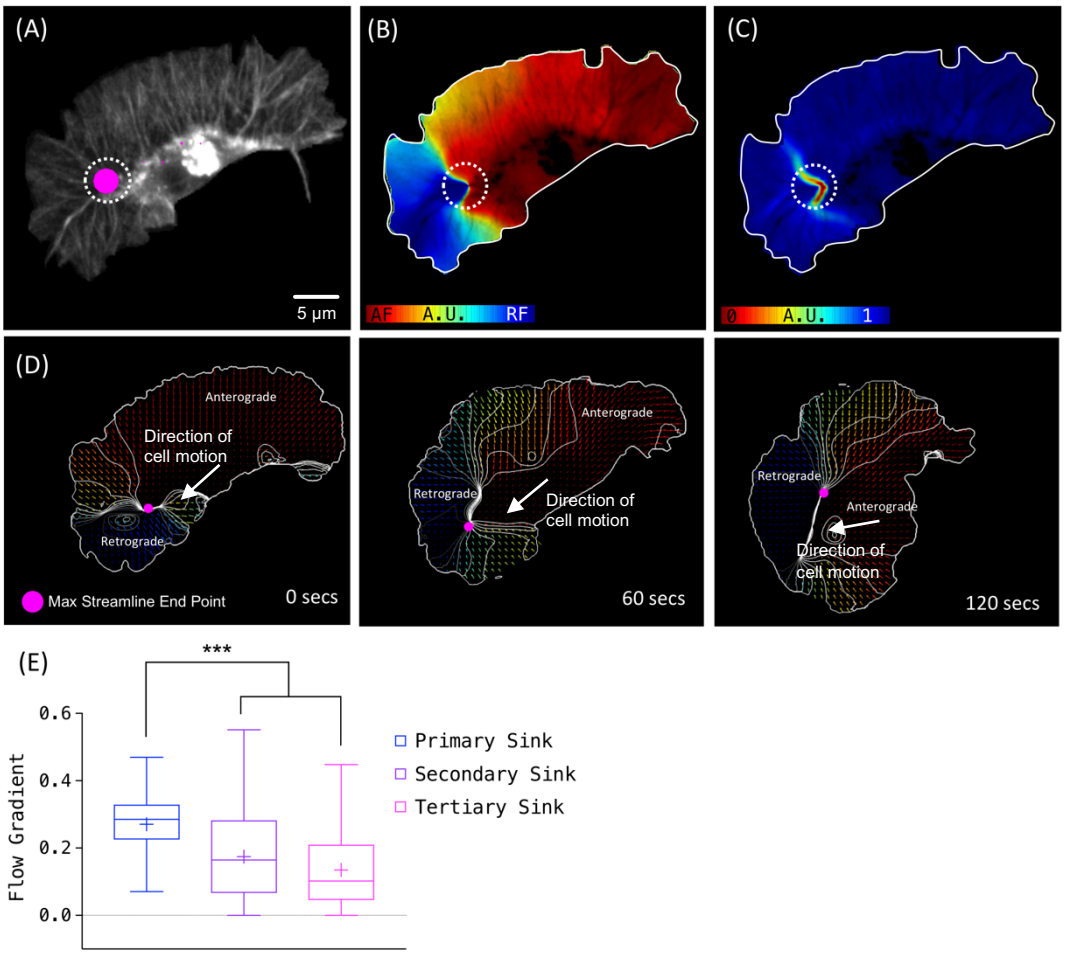

Figure 4.12: Primary sink represent a frictional transition region. **(A)** The confluence of streamlines is again quantified by calculating the number of streamlines ending in any one particular location within the cell. In this image,

the size of the spots are normalized to the number of streamline endpoints. **(B)** A correlation map in which the direction of cell motion is correlated to the direction of every Actin flow vector within the cell. Note that a positive correlation highlights anterograde flow while a negative correlation denotes retrograde flow. The dashed circle indicates the location of the maximum streamline endpoint. **(C)** Quantification of the gradient of the correlation map in '**B**' reveals sharp transition regions within the flow field. The dashed circle indicates the location of the maximum streamline endpoint. **(D)** Time-lapse of a representative hemocyte, with the flow vectors colour coded with reference to their polarity to the direction of travel (blue = retrograde flow, red = anterograde flow). A contour plot segmenting these regions is overlaid (white), while the primary sink (magenta spot) is plotted, showing its colocation with the retrograde/anterograde flow transition region. **(E)** Quantification of the gradient of the retrograde/anterograde flow correlation at the primary, secondary and tertiary sinks, which reveals that the primary sink represents a region of steep retrograde/anterograde flow transition. ***P < 0.001, Kruskal-Wallis test and Dunn's multiple comparison test. n=443 data points, from 9 cells.

4.3.4.2 Streamline sinks are highly correlated with cell directionality

I next wanted to investigate the streamline sinks in order see how effective they are as marker of polarity. I first correlated streamlines to cell motion is by calculating the cosine of the angle between the position vector of the most intense streamline sinks and the vector of cell displacement. I also used the same analysis with the position vector of the largest region of cell

extension and the location of sharpest transition in the flow field (Figure 4.13). The primary sink is as correlated with cell travel as the point of frictional transition (denoted as 'peak gradient' in Figure 4.13). This transition region is associated with frictional transition given the previous finding that Actin flow speeds are significantly different between retrograde and anterograde regions (Figure 4.3). The primary sink is significantly more correlated with cell travel than the second and third most significant streamline sinks. It was also significantly more correlated to cell travel than the region of largest extension (Movie 6). The high correlation to cell motion that the primary sink exhibits suggests that this region is an internal marker of polarity. This analysis has revealed a process of cell motion that appears to be guided by a well-defined point of Actin flow asymmetry within the lamella.

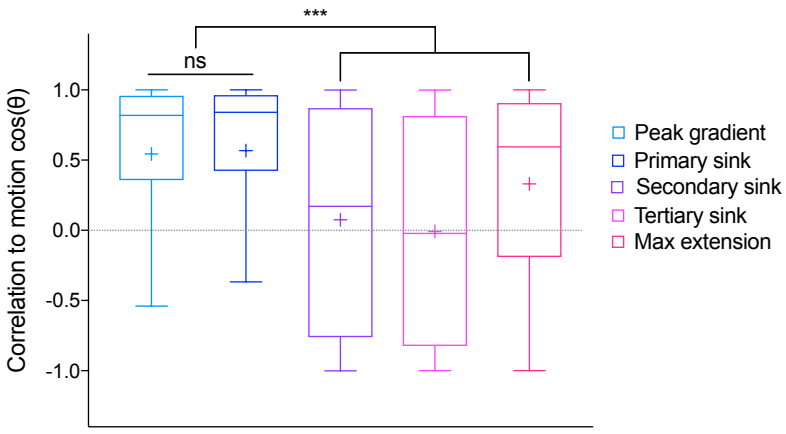

Figure 4.13. During random migration, the polarity of global Actin flow, unlike the leading edge, is highly correlated with cell directionality. Boxplot showing the migratory parameters and their directional correlation to cell motion. These regions include: the maximum, 2nd and 3rd streamline sinks; the position of the peak retrograde/anterograde gradient; and the maximum extension. The boxplot shows that the max endpoint and the peak

gradient are strongly correlated with the direction of cell motion compared to other measures. '+' denotes mean of the distribution. ***P < 0.001, Kruskal-Wallis test and Dunn's multiple comparison test. n=443 data points, from 9 cells.

4.3.4.3 Streamline sinks are directionally persistent

Having analysed the instantaneous correlations of the primary sinks and found them to be better associated with cell motion than the largest region of extension, I examined the cell track and position vector information to assess this difference (Figure 4.14 A). This further revealed that the primary streamline sink is tightly coupled to cell motion, whereas the position vectors of the extension display exploratory behavior, decoupled from the cell's trajectory (Figure 4.14 A). I followed this instantaneous correlation analysis with an assessment of the directional persistence of these migratory parameters. This analysis revealed that the primary streamline sink was the most directionally persistent measure (Figure 4.14 B). Cell motion was the second most persistent migratory parameter. While the least persistent migratory parameter was the area of edge extension. This could suggest that persistent hemocyte migration is a compromise between the coherence of the Actin flow field, and the exploratory behaviour of the cell boundary.

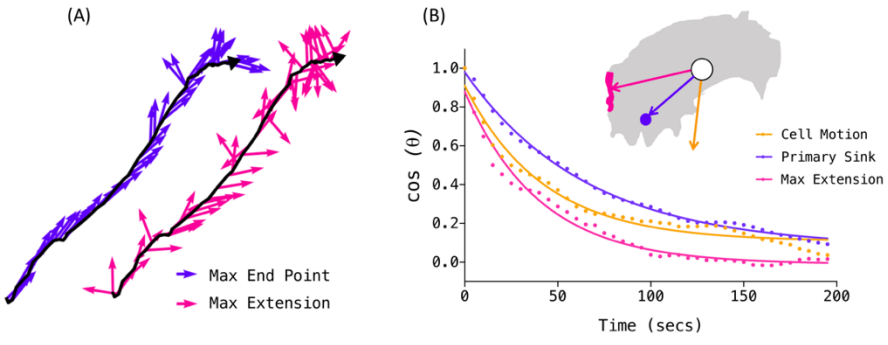

Figure 4.14: Actin flows are more persistent in time than the leading edge. **(A)** Example cell track (black lines) of a randomly migrating hemocyte in which the unit vectors of the max edge extension (purple) or the primary streamline sink are superimposed. Note that the direction of the maximum endpoint is better correlated with the direction of cell motion. **(B)** Directional autocorrelation comparing the persistence of cell motion, maximum edge extension and the maximum streamline endpoint during random migration. Dotted lines are real data and solid lines are fits to an exponential decay. Note that the autocorrelation of the max endpoint is compared with the autocorrelation for cell motion and max extension. n=443 data points, from 9 cells.

4.3.4.4 The temporal integration of Actin flows and edge dynamics represents a mechanical Coupling

The current conception of cell motion is that is a cyclical and step wise process. The cycle is thought to be initiated by extension at the leading edge of the cell and is followed by adhesion to the substrate and contraction within the cell that pulls the cell behind. However, as it was unclear how the rapid fluctuations of the leading edge can result in coordinated cell motion over time, it was equally unclear whether cell migration itself is a stepwise process at all. The steps of this hypothetical sequence are well described but the integration of these steps remains to be addressed. Having determined that the directionality of leading-edge extensions do not precede cell turning, I examined whether there was any temporal hierarchy considering the

directionality of the Actin network using the primary streamline sink. This was achieved by employing directional cross-correlation, a method that compares the position vectors of the primary sink against the set of displacement vectors that comprise cell motion, at all time lags. The result of this analysis is that all measures (primary sink and max extension) peak at zero lag. This data suggests that neither the primary sinks or the max extension predict cell directionality at this time scale (Figure 4.15 A). Interestingly given the tight coordination in time and the distances this information must be transferred over (primary streamline sink to nucleus = ~8.8 μm; edge extension to nucleus = ~17.9 μm) this coordination must be mediated by a mechanical coupling (Figure 4.15 B). The key difference between these different metrics is that the primary sink is better correlated across all time lags than the regions of largest extension.

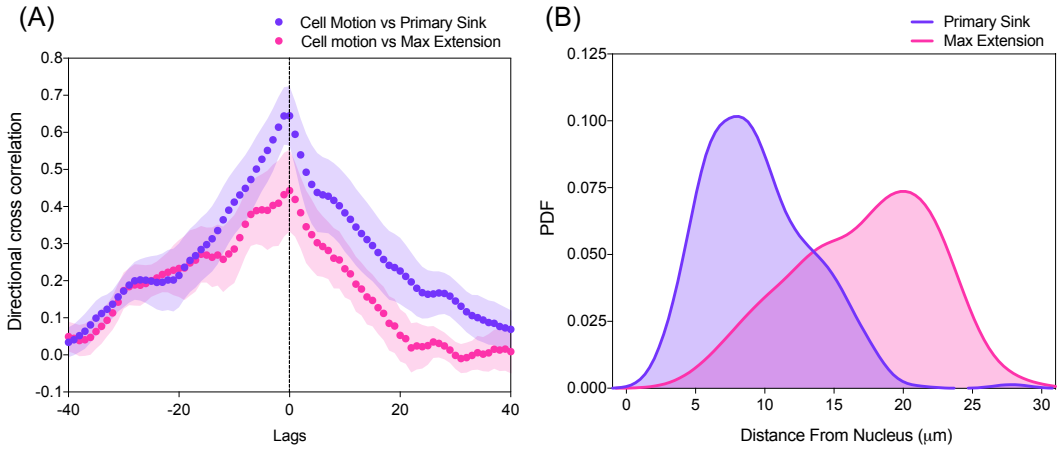

Figure 4.15: There is no detectable temporal hierarchy implying a mechanical linkage system. **(A)** Temporal cross correlation comparing the direction of cell motion, maximum edge extension and the primary sink. This reveals a peak correlation at zero-lag showing no obvious temporal hierarchy in these migratory parameters. Error bars = SEM. **(B)** Probability density

function (PDF) comparing the distribution of distances from the nucleus to the max edge extension and the nucleus to the primary streamline sink. These distances in light of the data in **(A)** suggest a mechanical coupling between the cell edge, Actin flows, and nuclear displacement.

4.4 **Discussion**

Within this chapter I have demonstrated that the flowing Actin network is highly organised and that this organisation is highly time persistent. Through novel methods of Actin flow analysis, I have shown that during hemocyte migration the Actin network has cell-scale polarity, with respect to cell motion. I have also shown that local Actin network organisation is defined by time persistent regions of Actin remodelling whereby Actin filaments undergo compression and depolymerisation.

Previous studies into Actin flows have predominantly focussed on the activity of the Actin network within a small section at the leading edge (Jurado, 2004; Koestler *et al.*, 2008; Maiuri *et al.*, 2015; Mendoza *et al.*, 2015). However, through the implementation of Particle Image Velocimetry (PIV), I have been able to attain and analyse a global Actin flow field. After attaining information of the full hemocyte Actin flow field, I was able to describe in detail the directional characteristics of the flow field, as well as investigate the variance of flow speeds seen within hemocyte lamella.

In the case of Actin flow speeds, I was interested in addressing a common assumption in cell migratory studies, which is that a linear relationship

between Actin flow speeds and cell migratory speeds exist (Jurado, 2004; Maiuri *et al.*, 2015). The hypothesis arises from the concept of a mechanical coupling of the Actin network to the migratory substrate through an Actin clutch (Mitchison and Cramer, 1996). Here, the slowing of Actin flows promotes an increase in cell speed, as more contractile tension is driven through adhesions in the engaged clutch state (see section 1.1.3 for more information on Actin clutches in cell motion). In the disengaged clutch state, the network is able to move, pulled by the contractile activity of Myosin II - and no lamellae forces are transmitted to the substrate. I have made a number of independent comparisons utilizing different measures of computing of flow speeds and I have not been able determine any obvious correlation between the rate of Actin flow and the speed of hemocyte migration.

Initially I attempted to compare the average global flow speed to cell speed which did not reveal the proposed negative linear relationship. I next transformed the time-lapse movie of my hemocytes to the cell's reference frame and recorded the Actin flow speed within 'computationally stationary' hemocytes using published methods (Wilson and Theriot, 2006; Wilson *et al.*, 2010; Maiuri *et al.*, 2015). This process of image transformation has been used in previous studies to directly compare flow speed and cell speed from the reference frame of the cell. However, I was not able to determine, like in the analysis of flows from the laboratory frame of reference, a strong inverse linear relationship. This result brings into question the proposed coupling of flow speed and cell speed, and supports recent analysis of global Actin flow speed,

that also showed no linear correlation between these two migratory parameters (Wilson *et al.*, 2010).

Further to this analysis of flow speed, I investigated a region of the network that was highly anticorrelated with cell travel (retrograde flow), as defined by a negative cosine similarity between the velocity vectors and the vector of cell motion. I also segmented a region of the Actin flow field that is captured within a narrow field of view centred about the direction of travel. Upon analysis of the flow speeds in the retrograde zone and flows in the direction of cell travel, I demonstrated that retrograde flows and flows in the direction of travel are significantly slower than the global average. Given the reduced flow speeds, I hypothesise that these regions, denote a very narrow corridor of the Actin network that is strongly associating with the migratory substrate. In the context of the Actin clutch model, it is possible to think of these flow domains as 'gripping' the substrate, while anterograde flows, which move in the direction of travel and move at a significantly faster rate, as regions of network 'slipping' (Jurado, 2004). However, when I compare the average flow speeds in the 'gripping regions' with the speed of cell migration I was unable to derive any meaningful correlation. In the case of hemocytes, I have used a temporal resolution of 5 seconds per timepoint. While in other studies in keratocytes that also failed to show a coupling of flow speed and cell speed, imaging was performed at 2 seconds per timepoint (Wilson *et al.*, 2010). As a result, I hypothesise that the linear relationship between flow speed and cell speed does not hold for data sampled at high temporal resolutions. It would be

interesting to examine this flow speed and cell speed relationship using larger time intervals, approaching increments of a minute or more in hemocytes.

Previous studies into the organisation of the flowing Actin network have reported findings of convergence zones deep inside the lamella (Vallotton *et al.*, 2004; Schaub, Bohnet, Laurent, J. J. Meister, *et al.*, 2007; Okeyo *et al.*, 2009). Convergence zones were revealed through analysis of the divergence of Actin velocity fields. Divergence is a mathematical operator that describes the extent to which a point in a velocity field is a source of material. In the context of the Actin network, regions where the network converges is described by negative divergence in this region, i.e. it's a sink within the network. I have implemented divergence analysis for the purposes of probing the topography of the flowing Actin network. Using divergence analysis, I have demonstrated that much of the divergence values are negatively signed, and that there is a distinct region of negative divergence (a convergence zone), surrounding the cell body in hemocytes. I also showed that these regions are highly persistent in time. When analysing the temporal stability of specific sinks in the network, I found that they could persist upwards of a minute and were static in position representing fixed regions of Actin network remodelling. This is in dramatic contrast to the what I observed for the cell boundary, where the leading edge was directionally impersistent, and the contours of the edge fluctuated rapidly (Figure 3.1 & 3.2). This temporal stability of Actin network organisation was noted in earlier studies of Actin flows, where kinetic and kinematically distinct regions of the flow field persisted over minutes (Vallotton *et al.*, 2004). The kinetic behaviour describes the differential turnover

characteristics of specific regions of the Actin network, whereby areas of the network undergo assembly or disassembly and significantly different rate. While investigations into the kinematics of the Actin network, have shown heterogeneities in flow speeds across the cell.

In this chapter I have also demonstrated that the activity within negatively divergent regions of the flowing Actin network is constituted by a combination of compressive strains and filament disassembly. There are a number of studies that have investigated Actin in both migrating cells, such as keratocytes, and stationary cells such as newt lung epithelial cells (Vallotton *et al.*, 2004; Schaub, Bohnet, Laurent, J. J. Meister, *et al.*, 2007; Wilson *et al.*, 2010). As in these earlier studies, my findings demonstrate that regions of negative Actin divergence colocalise with sites of network depolymerisation. I have also found that regions of negative Actin divergence colocalise with sites of compression. Often in the literature concerning cell migration and Actin network deformation, the terms compression and negative divergence are often used interchangeably (Vallotton *et al.*, 2004; Schaub, Bohnet, Laurent, J. J. Meister, *et al.*, 2007; Stam *et al.*, 2017). For instance, in one study compressive and tensile Actin network behaviour was defined as negative and positive divergence respectively (Schaub, Bohnet, Laurent, J. J. Meister, *et al.*, 2007). However, in my study I explicitly calculate principal strains in the Actin network, which has allowed me to determine that the lamellae undergo intensive compressive activity. The localisation of both compressive and disassembling forces around the cell body in hemocytes, is analogous to the localisation of the peak internal stresses in neuronal growth cones (Betz *et al.*,

2011). In growth cones, Actin network stresses peak between the central domain (the region nearest the axon, enriched with microtubules (Lowery and Vactor, 2009)) and the lamella in a region called the transition zone.

I have also been able to establish that on the cell-scale, the Actin network is polarised when considering the direction in which it flows with respect to cell directionality. I achieved this through the first implementation of streamline analysis used in cell migration studies. This method provides insight into the gross directionality of the flow field. The streamline representation of the flow field also highlighted a specific time persistent region of the network that denotes a sharp transition between anterograde and retrograde flows which is highly correlated with cell travel (the streamline sink). As such, I hypothesise that the primary sink is a transition between Actin flows 'gripping' and engaging with the substrate, and 'slipping' and disengaging from the substrate. It would be interesting to investigate this hypothesis and determine whether these regions are frictionally distinct through analysis of the traction stresses in the substrate. For instance, there may be greater traction stresses observed in the regions of Actin retrograde flow. It is notable that the primary streamline sink that represents a focus zone of Actin flows also features the greatest amount of negative divergence. This suggests that the organised and polarised global Actin flows, are mediated by compression and disassembly. Divergence is a local measure of flow behaviour describing how points in the flow field contribute to their environment, streamlines however describe global activity of the flow field. In the case of the Actin flow field, streamlines show that the network flows in a highly organised manner

from the cell boundary, until the network is disassembled within sinks. Divergence provides information about the intensity of those sinks, and the extent to which these specific regions can compress and disassemble the Actin network.

The finding that there is no temporal hierarchy between my migratory parameters (cell motion, streamline sinks, and the leading edge) was also very interesting. In the previous chapter I had shown that cell motility is not a process guided by the dynamics of the leading edge using temporal cross-correlation analysis. In this chapter I have shown that using temporal cross-correlation that no temporal hierarchy is detectable between the activity of the streamline sinks and cell motion. As such it is not possible to claim that the Actin flow asymmetry as represented by the streamline sinks predict changes in cell direction, despite being highly correlated to cell motion overall. This highlights that cell motion is not a stepwise process as previously described (Mitchison and Cramer, 1996; Ridley *et al.*, 2003). It should be noted that this level of temporal integration is particularly surprising considering the distance this information would have to travel between the cell boundary and the nucleus. My data suggests that instantaneous transmission is required for this, therefore I hypothesise a mechanical crosstalk between these distant parameters is responsible.

5 Global Organisation of Actin Flows is Mediated by Myosin and Cofilin

5.1 Introduction

In the previous chapter I have demonstrated that the flowing Actin network is highly organised, that it undergoes turnover, and that these sites of network remodelling are persistent in time. I have also provided detailed descriptions of the ways in which the Actin network is organised. I have also shown that there are organising centres which result in global directedness of the flowing network. However, what I have not established yet are the mechanisms by which these sinks arise and how global organisation of the flow field is mediated. What creates compressive regions? Which, if any, molecular components are responsible for taking apart the network to prevent accumulation of Actin at the rear? How is the organisation of the Actin cytoskeleton maintained through space and time? These are all questions I address in this chapter. I will discuss these through genetic manipulations of specific proteins involved in the contraction and destruction of the Actin network, namely Myosin II and Cofilin respectively.

5.2 Contributions

My contribution was to analyse the Actin flows in the mutants, as well as develop the line-scan assays to profile the gradients of the divergence, principal strain, and turnover. Dr Mubarik Burki contributed to the results within this chapter. Specifically, Dr Burki conducted all imaging in this section and

maintained the Drosophila lines required for hemocyte analysis. Dr Burki also performed the line scan analysis from software that I developed.

5.3 Results

5.3.1 Myosin II and Cofilin are required to drive Actin flows, and hemocyte migration

5.3.1.1 Hemocyte migration and Actin flows are dependent on Myosin II

The role of Myosin II in regulating Actin dynamics is well studied and it has been implicated in the cell-scale organisation of the cytoskeleton (Wilson *et al.*, 2010). My data in Chapter 4 suggests that global organisation of the network is driven by compression and disassembly. As a consequence, I was interested in investigating the hypothesis that Myosin II through its contractile activity mediates cytoskeletal coherence. This was achieved through producing time-lapse movies of freely moving hemocytes at a temporal resolution of 5 seconds per frame. Wild-Type control embryos and zygotic mutant embryos for *myosin II heavy chain* (*zip*^{1}) were analysed.

Initially in order to investigate the effects of the *zip*^{1} mutation, low magnification still images of the embryos were taken (Figure 5.1 A). This allowed me to assess the migratory defects of this mutant against control embryos. This analysis showed significant defects in migratory patterning at stage 16 of Drosophila embryonic development (Figure 5.1 A). These defects were characterised by large unoccupied patches of the ventral surface of the embryo by hemocytes, which corroborates earlier analysis of *zip*^{1} hemocytes.

In wild-type control embryos, hemocytes migrating down the ventral surface of the embryo and formed the characteristic three-line pattern. Following the low magnification confirmation that *zip*^{1} mutant hemocytes have migratory defects I next measured cell speed in high magnification time-lapse movies. Cell speed analysis was performed by first tracking the nucleus (Figure 5.1 B, D). This analysis highlighted that migration speeds in *zip*^{1} mutant hemocytes is dramatically reduced (3.3 ± 0.1 μm min^{-1} in controls to 1.1 ± 0.1 μm min^{-1} in mutants) (Figure 5.1 D). These findings in the *zip*^{1} mutant hemocytes highlight the requirement for Myosin II during hemocyte migration.

Analysis of *zip*^{1} hemocytes using Particle Image Velocimetry revealed a significant reduction in average Actin flow speed compared to controls (4.1 ± 0.1 μm min^{-1} in controls to 1.6 μm min^{-1} in mutants) (Figure 35 C, E, Movie 7). Upon qualitative analysis of the *zip*^{1} Actin velocity field, I observe disordered flow behavior, demonstrated by the velocity vectors of the PIV showing a high degree of directional variance (Figure 5.1 C, Movie 7). Controls however feature Actin flows that are highly organised, as the network moves centripetally away from the cell boundary (Figure 5.1 C, Movie 3 & 7).

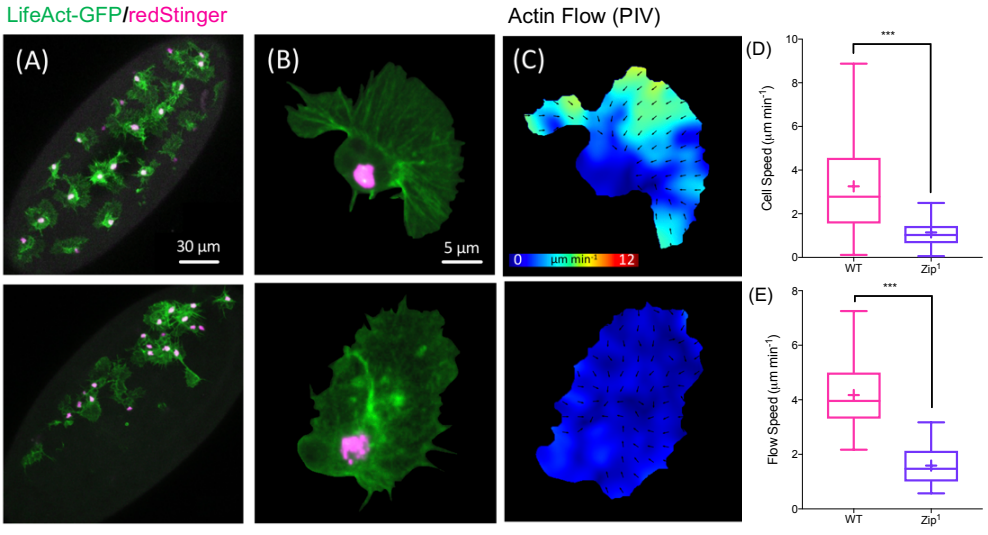

Figure 5.1: Loss of Myosin II leads to reduced Actin flow and cell speed.

(A) Images of hemocytes on the ventral surface of *Drosophila* embryos in *wild-type* and *zip[1]* mutant embryos. **(B)** High magnification images of *wild-type*, and *zip[1]* mutant hemocytes. **(C)** Representative PIV heat maps of Actin flow in *wild-type* and *zip[1]* mutant cells. **(D)** Quantification of mean cell speed in *wild-type* (n=443 data points, from 9 cells) and *zip[1]* mutant cells (n=219 data points, from 9 cells). Cell speed in *zip[1]* mutant hemocytes are slower than wild-type cells. ***P < 0.001, Kruskal-Wallis test and Dunn's multiple comparison test. **(E)** Quantification of mean Actin flow speed in *wild-type* and mutant cells. Actin flows in *zip[1]* mutant hemocytes are slower than wild-type cells. ***P < 0.001, Kruskal-Wallis test and Dunn's multiple comparison test.

5.3.1.2 Myosin II controls Actin flow coherence

The quantification of Actin flows highlighted disordered flow behavior in the *zip[1]* mutants, as represented by the scattered directions of Actin flow vectors (Figure 5.1 C). As a consequence, I was interested in using the streamline tools (described in section 2.3.4) to examine this further. Streamline analysis of the flow field can be used to describe the 'gross directionality' of a flow field, in the case of disordered flows it will highlight any regions of 'turbulence' in a qualitative fashion and represent them through disordered lines. The quantification of the *zip[1]* mutant flow fields through streamlines revealed that it is highly disordered compared to controls hemocytes, with a swirling and disrupted pattern (Figure 5.2 A, Movie 8).

In control hemocytes, Actin flows are highly organised, and flow into a focussed region I termed the primary streamline sink, that is highly correlated to cell directionality (see section 4.3.4.2). I applied this sink analysis to the *zip*[1] mutant flow fields to assess whether there was any change to this organising centre, especially in light of the findings that hemocyte migration is severely disrupted in *zip*[1] mutant embryos (Figure 5.1 A, D). This analysis revealed that while the control cells have a coherent flow and a major contractile organizing centre, with ~60% of the streamlines terminating in one specific region, *zip*[1] mutants exhibit weaker sinks with fewer streamlines contributing to them (Figure 5.2 B). The reduced intensity of these streamline sinks highlights the inability of the *zip*[1] mutant to organise its flow field effectively. This data demonstrates that Myosin II is required for cell scale organisation of Actin flows in hemocytes.

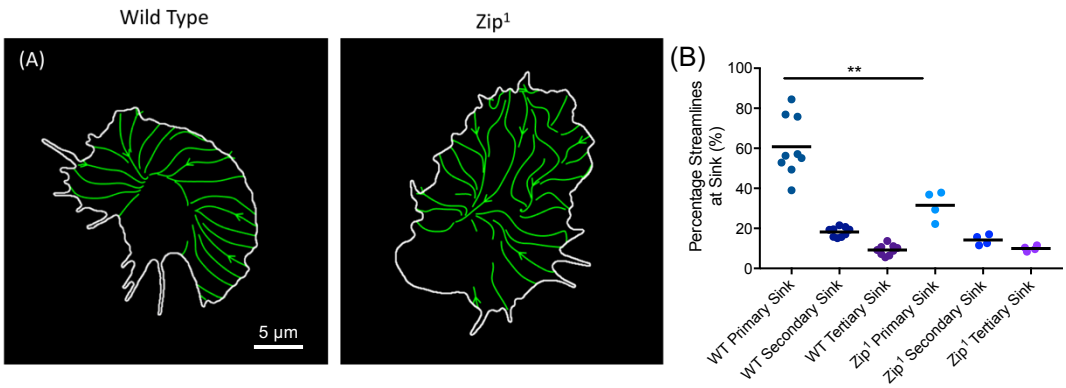

Figure 5.2 Myosin is required for the organised flow of the Actin network.

(A) Images highlighting an analysis of streamlines through the Actin flow field in *wild-type* and *zip*[1] mutant cells. Note the disorganized streamlines in the mutants. **(B)** Quantification of the percentage of streamlines that end at the primary sink in wild-type and *zip*[1] mutant cells. Note that *zip*[1] mutants (n=4

cells) show a significant reduction in their streamline confluence compared to *wild-type* cells (n=9 cells). **P < 0.01, Kruskal-Wallis test and Dunn's multiple comparison test.

5.3.1.3 Hemocyte migration and Actin flows is dependent on Cofilin

From analysis of freely moving hemocytes I have shown that stable regions of network compression and depolymerisation are highly correlated with cell directionality (see section 4.3.4.2). As such I am interested in the regulators of these two processes, and the impacts that disrupting compression or depolymerisation has on cell motion. Through analysing Actin flows in zygotic mutants for *myosin II heavy chain* (*zip^{1}*) I have shown that network organisation mediated through the activity of Myosin II is required for effective migration. Following this, I investigated how network organisation is mediated through depolymerisation, and how this impacts cell migration. For this purpose, I analysed Drosophila embryos that are hypomorphs for Twinstar (*tsr^{1}*) the Drosophila ortholog for Cofilin. Cofilin is a known regulator of the Actin network through depolymerisation (Pollard and Borisy, 2003). Initially, I set out to highlight whether there were any apparent migratory defects in *tsr^{1}* embryonic hemocytes. This was achieved through low magnification imaging of Drosophila embryonic development in *tsr^{1}* embryos and controls. This analysis revealed that a homozygous mutation in Cofilin results in defective embryonic hemocyte dispersal. As with *zip^{1}* mutant hemocytes (Figure 5.2 A), few *tsr^{1}* cells are visible on the ventral surface of the embryo (Figure 5.3 A).

Following the finding that there is disrupted embryonic dispersal of hemocytes in *tsr*^{1} mutant embryos, I next analysed high magnification time-lapses of *tsr*^{1} hemocytes. These cells were imaged at a temporal resolution of 5 seconds in order to assess whether there was any difference in Actin flow behavior or cell speed (Figure 5.3 B). This analysis revealed that cell speed was significantly reduced from approximately 3 μm min^{-1} in controls, to 2.2 ± 0.1 μm min^{-1} in *tsr*^{1} hemocytes (Figure 5.3 D). Analysis of Actin retrograde flow speeds also revealed a significant difference in *tsr*^{1} mutant hemocytes from approximately 4 μm min^{-1} in controls, to 3 ± 0.1 μm min^{-1} (Figure 5.3 C, E, Movie 7). Actin flow field dynamics appeared qualitatively similar however despite the reduced flow speeds, with an absence of the discorded flows seen in *zip*^{1} hemocytes (Figure 5.3 C, Movie 7).

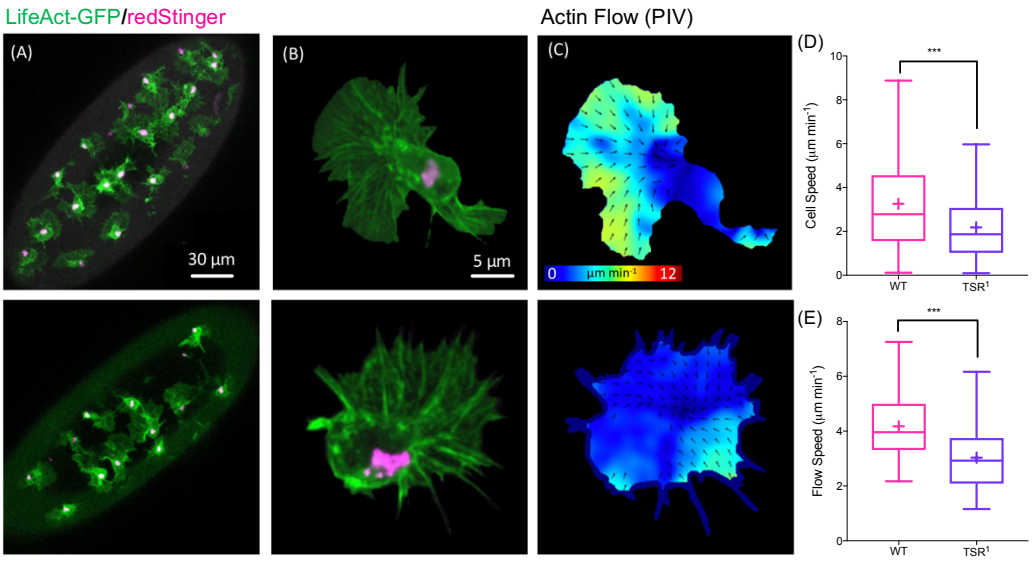

Figure 5.3: Loss of Cofilin leads to reduced Actin flow and cell speed. **(A)** Images of hemocytes on the ventral surface of *Drosophila* embryos in *wild-type* and *tsr*^{1} mutant embryos. **(B)** High magnification images of *wild-type*, and *tsr*^{1} mutant hemocytes. **(C)** Representative PIV heat maps of Actin flow in *wild-*

type and *tsr[1]* mutant cells. **(D)** Quantification of mean cell speed in *wild-type* and mutant cells. Cell speed in *tsr[1]* mutant hemocytes (n=513 data points, from 7 cells) are slower than *wild-type* cells (n=443 data points, from 9 cells). ***P < 0.001, Kruskal-Wallis test and Dunn's multiple comparison test. **(E)** Quantification of mean Actin flow speed in *wild-type* and mutant cells. Actin flows in *tsr[1]* mutant hemocytes are slower than wild-type cells. ***P < 0.001, Kruskal-Wallis test and Dunn's multiple comparison test.

5.3.1.4 Cofilin is dispensable for Actin flow coherence

To confirm the qualitative observation that Actin flows in *tsr[1]* mutant hemocytes are organised, I analysed their Actin flow fields using streamline analysis (Figure 5.4 A, Movie 8). This analysis demonstrated that the Actin network flows in a stable fashion, which is represented by streamlines that retain a straight path between the cell boundary and their termination point. While the *zip[1]* mutant hemocytes feature streamlines following tortuous paths through the flow field (Figure 5.2 A, Movie 8), *tsr[1]* mutant hemocytes more closely resemble the Actin dynamics of controls in the context of flow directionality (Figure 5.4 A, Movie 8). I also analysed the intensity of the streamline sinks by quantifying the number of streamlines that terminate in defined locations in the lamella. This quantification showed no significant difference in the intensity of the primary streamline sink (Figure 5.4 B). This finding establishes Myosin II, which remains active in *tsr[1]*, as a primary component of streamline sink formation, and potentially as the coordinator of cell-scale organisation of Actin network flows.

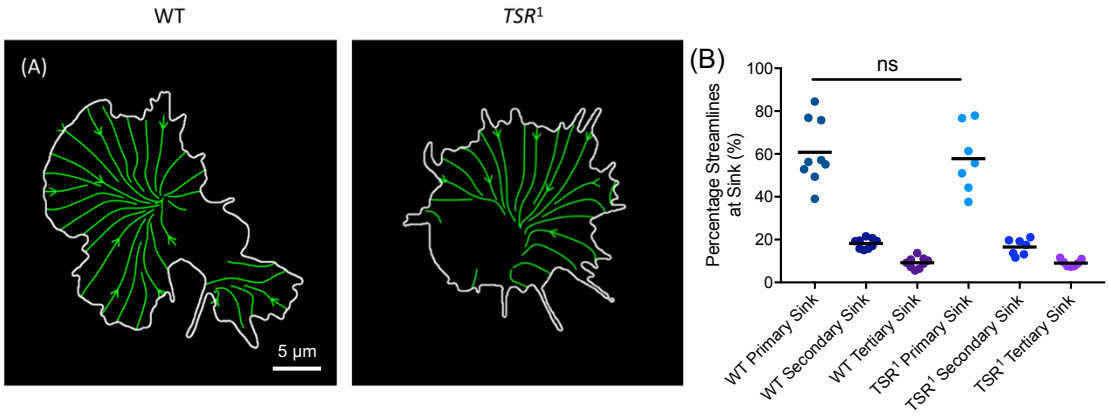

Figure 5.4: Cofilin mutants retain their Actin network organisation. **(A)** Images highlighting an analysis of streamlines through the Actin flow field in *wild-type* and *tsr[1]* mutant cells. Note the organised streamlines in the *wild-type* and *tsr[1]* mutant. **(B)** Quantification of the percentage of streamlines that end at the primary sink in *wild-type* (n=9 cells) and *tsr[1]* mutant cells (n=7 cells). Note that *tsr[1]* mutants show no significant difference in their streamline confluence compared to *wild-type* cells. Kruskal-Wallis test and Dunn's multiple comparison test.

Streamline analysis has revealed that there is a significant difference between the disorganised flows of the *zip[1]* mutant hemocytes and the organised and stable Actin flows observed in wild-type controls and *tsr[1]* mutant hemocytes. To quantify this flow organisation further, I used an alignment parameter (described in section 2.3.7) which analyses the average local organisation of the velocity fields in control hemocytes as well as *zip[1]* and *tsr[1]* mutants (Figure 5.5).

Alignment parameter analysis also revealed that the Actin flow field in *zip[1]* mutant hemocytes are disordered, with large variance in the local

directions of Actin flow velocity vectors (Figure 5.1 C, Figure 5.2 A). Wild-type controls and *tsr*[1] mutants hemocytes display very low variance of flow

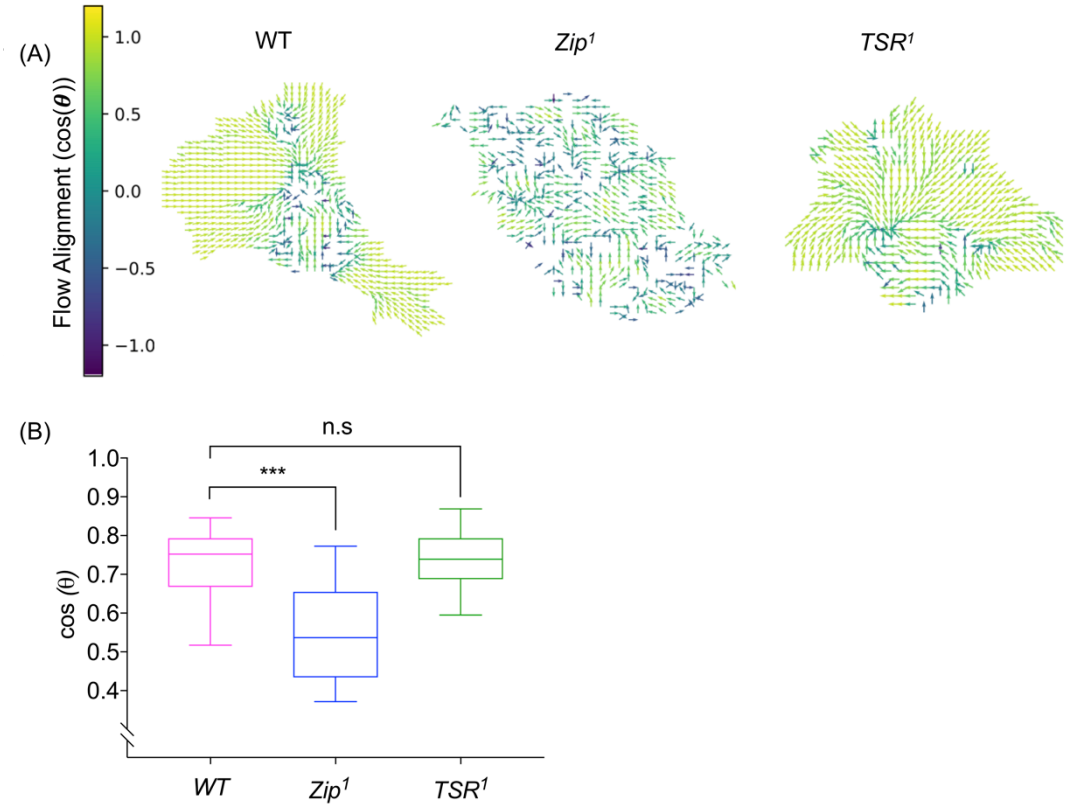

Figure 5.5: Local order of the Actin network is determined by Myosin II but not cofilin. **(A)** Actin flow field colour coded to the degree of local order within *wild-type* and mutant cells. A value of 1 represent perfect alignment between neighbours. **(B)** Box plot representing the averaged alignment across the Actin flow field. Note that the flow in *zip*[1] mutant cells (n=4 cells) is more highly disorganized than either *wild-type* (n=9 cells) or *cofilin* mutant cells (n=7 cells). ***P < 0.001, Kruskal-Wallis test and Dunn's multiple comparison test.

5.3.2 Actin flows are driven by a combination of contraction and disassembly

My observations so far highlight that Myosin II is indispensable for the organisation of Actin flows, and that organisation is mediated by compression and depolymerisation (see sections 4.3.2.1 and 4.3.2.2). As Myosin II is one of principle generators of compression in the Actin network, and Cofilin is fundamental to Actin network turnover through depolymerisation, I next examined the divergence of the Actin flows as well as depolymerisation activity of the *zip*^{1} and *tsr*^{1} mutant hemocytes. Analysing the divergence of the Actin flows in *zip*^{1} and *tsr*^{1} revealed a significant reduction in the intensity of negative divergence compared to control hemocytes (Figure 5.6 A, Movie 9). The strong band of negative divergence that is observed around the cell body in control hemocytes, has dissipated in the *zip*^{1} and *tsr*^{1} mutant hemocytes. I next assessed the gradients of divergence present in these hemocytes. For this, I sampled the divergence field using line scans that originated at the body boundary, traversed the lamellae, and terminated at the cell edge. This analysis revealed that in controls there is a gradient of negative network divergence which peaks approximately 2 μm from the cell body and reduces in intensity closer to the cell edge (Figure 5.6 A, B, Movie 4). In *zip*^{1} and *tsr*^{1} mutant hemocytes, the gradient of negative divergence is not present (Figure 5.6 B). However, there is a spike in the intensity of negative divergence in all experimental conditions at the boundary between the lamella and cell body (Figure 5.6 B).

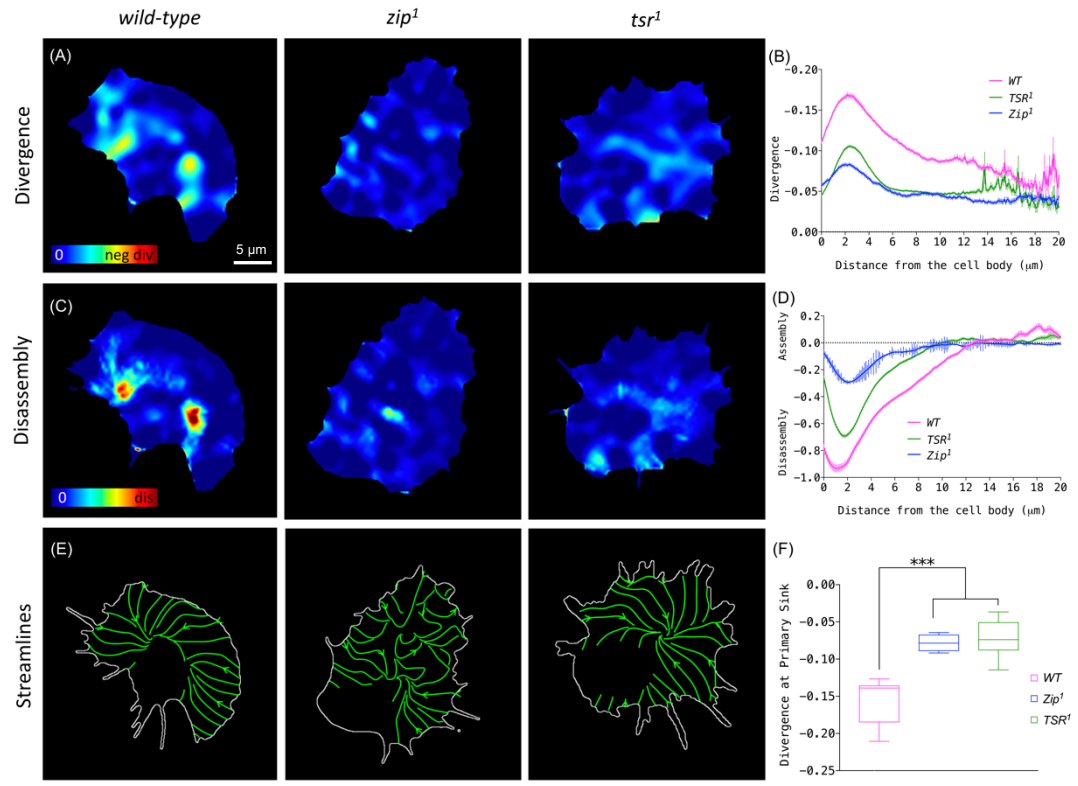

Figure 5.6: A gradient of Myosin II driven contraction is essential for global organization of Actin flow. **(A)** Heatmaps comparing the quantification of divergence in wild-type and mutant hemocytes. **(B)** Quantification of the mean divergence from the cell body to the leading edge in *wild-type* and mutant cells. Data was attained through line scans through the lamella. Error bars = SEM. **(C)** Heatmaps comparing the quantification of Actin disassembly in wild-type and mutant cells. **(D)** Quantification of the mean assembly/disassembly values across a cell in *wild-type*, *zip¹,* and *tsr¹* mutants calculated by drawing line-scans from the cell body to the leading edge. Error bars = SEM. **(E)** Images highlighting an analysis of streamlines in the Actin flow field in *wild-type*, *zip¹* and *tsr¹* mutant cells. Note the disorganized streamlines in *zip¹* mutants. **(F)** Quantification of the mean divergence at maximum streamline sinks in *wild-type*, *zip¹* and *tsr¹* mutant cells, which

reveals that mutants have an increase in divergence values highlighting a reduction in network compression. ***P < 0.001, ordinary one-way ANOVA and the Dunnett's multiple comparison test.

Interestingly, through quantifying the intensity profiles of Actin network turnover I observed a differential contribution to network disassembly between Myosin II and Cofilin. In wild-type controls, line scans of Actin network turnover revealed that disassembly of filaments occurs in hemocytes at the rear of lamella (Figure 5.6 C, D). This peak is similar in location to the observed spike in negative divergence and aligns with my earlier findings that show a spatial correlation between divergence and disassembly (see section 4.3.2.2). As would be expected with the *tsr*^{1} mutants, overall network disassembly was reduced when compared to controls (Figure 5.6 D, Movie 10). However, the initial profile of disassembly resembled that of controls with a significant peak in network turnover just inside the lamella. In *zip*^{1} mutant hemocytes overall network turnover was also reduced, and the gradient of disassembly seen in controls had all but dissipated. Although it should be noted that there is a peak in Actin network disassembly at the rear of the lamella in the *zip*^{1} hemocytes (Figure 5.6 D). With the reduction in overall rates of disassembly both Myosin II and Cofilin appear to be required for destruction of the network either through network contraction, or filament severing respectively. The data suggests that the baseline levels of Actin depolymerisation in hemocytes is controlled by Cofilin, while the graded destruction is mediated by Myosin II. I have also quantified the intensity of divergence that colocalises with the primary sink derived from streamline analysis (Figure 5.6 E, F). This analysis has revealed

that in controls the primary sinks are highly negatively divergent, which is suggestive of a site of Actin remodelling through compression and depolymerisation. However, the primary sinks in both the *tsr[1] and zip[1]* mutant hemocytes feature a significantly reduced intensity of Actin remodelling at these sites (Figure 5.6 F).

5.3.2.1 Negatively divergent regions are an emergent property of the Actin flow field

Following the observation that Myosin II mediates the graded destruction of the Actin network, and the experimentally demonstrated gradient of Myosin II in cells *in vitro* (Svitkina *et al.*, 1997; Wilson *et al.*, 2010), I was interested in visualising how the compressive regions localised with Myosin II. In order to test this, I examined the divergence fields in hemocytes that had the relevant cytoskeletal components labelled; this included Actin (UAS-Moesin-mCherry) and the heavy chain of Myosin II (Zipper-GFP) (Figure 5.7 A, Movie 11).

Initially I examined the passage of Myosin II puncta using temporal projections of the migrating hemocytes in order to visualise the spatial distribution of Myosin II (Figure 5.7 A). This showed an elevated density of Myosin II at the rear of the lamella. This was then quantified through line scan analysis, which demonstrated how the concentration of Myosin II is greatest immediately outside of the lamella and reduces towards the cell edge (Figure 5.7 B). When analysing the divergence in these cells I have found it difficult to map focused regions of negative network divergence to specific puncta of

Myosin II (Figure 5.7 C, D, Movie 12). This finding is particularly surprising given that myosin is a key factor in Actin network organisation, putatively creating the negatively divergent regions of the Actin network in previous analyses (Vallotton *et al.*, 2004; Wilson *et al.*, 2010). By analysing the flowing Myosin II puncta and the divergence of the Actin flow field, I observed negative divergence zones in the network between Actin fibres and adjacent to Myosin II puncta. Previous analysis demonstrated that these regions of negative divergence are time persistent on the order of minutes (see section 4.3.2), however Myosin II puncta are transient here, appearing to flow through these regions, and do not obviously contribute to the formation of these sinks (Figure 5.7 D, Movie 12). As such these sinks could be thought of as an emergent property of a network that undergoes chemical severing through the activity of Cofilin and is under a stable gradient of strain through Myosin II mediated compression.

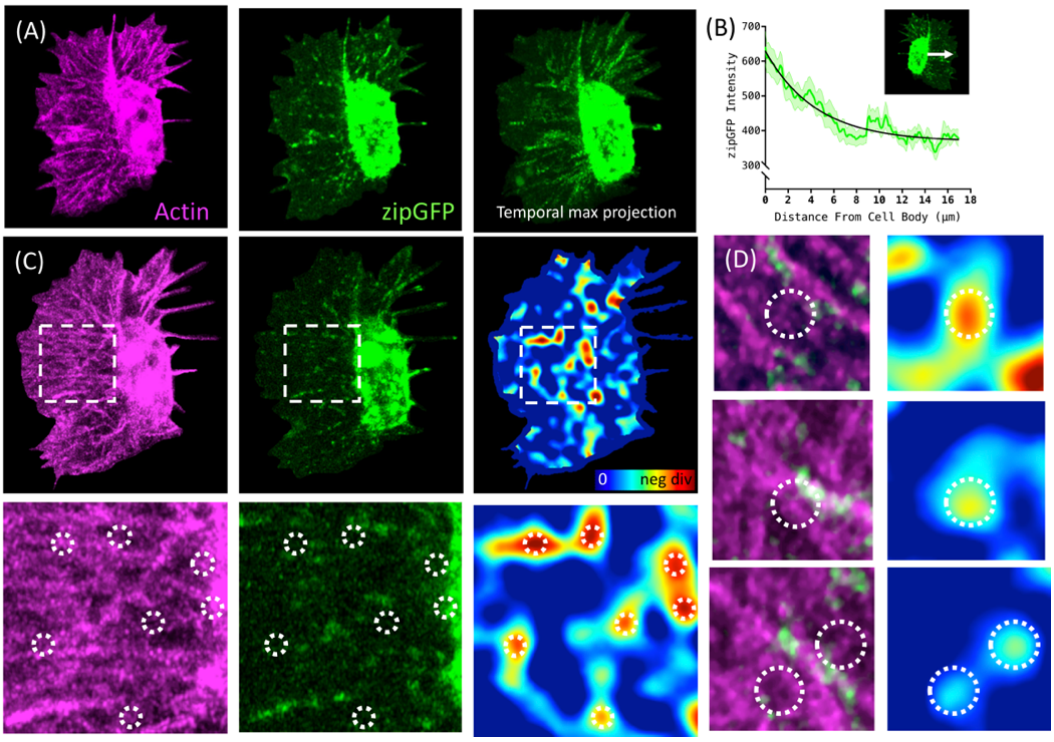

Figure 5.7: Actin network sinks do not colocalise with Myosin II. **(A)** Image of a hemocyte containing labelled Actin (Moesin-mCherry) and Myosin II (zipGFP), in panel 1 and 2 respectively. Panel 3 is a temporal max projection of 5 frames highlighting that Myosin II puncta within the lamellae are predominantly toward the rear of the network surrounding the cell body. **(B)** Line-scan analysis of Myosin II localisation within hemocytes. The plot profile of Myosin II fluorescence intensity was performed on randomly chosen lines within the lamellae of migrating cells from the cell body towards the cell edge (see insert). Note that the average intensity of Myosin II is high toward the cell body and decreases in a gradient as you approach the cell edge. Error bars = SEM. **(C)** Comparison of Actin and Myosin II localisation with the measurement of Actin flow divergence. Bottom panels are high magnification images of the boxes outlined in upper panels. Circles highlight regions of strong negative divergence, which show no obvious colocalisation with Myosin II. **(D)** Time-lapse series comparing Actin and Myosin II localization with the measurement of Actin flow divergence. Circles highlight example regions of strong negative divergence. Note that the negatively divergent regions are adjacent to Myosin II puncta and only transiently associated with Myosin II flow within the network.

5.3.2.2 Myosin II and Cofilin cooperatively control global organisation of Actin flows

This data suggests that the contraction and depolymerisation of the Actin network creates an environment in which stable sinks can emerge, and these are controlled by the expression of *myosin II* and *cofilin*. As a consequence, I was interested in seeing if there was a synergistic effect

between these two genes. In order to examine whether there is a genetic interaction between *myosin II* and *cofilin*, I analysed Actin flow dynamics of hemocytes in trans-heterozygous embryos, that is to say embryos that were heterozygous mutants for both *zip*^{1} and *tsr*^{1}.

Initially, I analysed the dispersal of hemocytes in embryos heterozygous for *zip*^{1} and *tsr*^{1} (Figure 5.8 A). This revealed that hemocyte dispersal was equivalent to controls, forming the stereotypical three-line pattern on the ventral surface of the nerve cord. However, hemocyte dispersal in trans-heterozygous embryos was highly disrupted and featured large patches of the ventral surface unoccupied by hemocytes (Figure 5.8 A). Following this, I analysed Actin dynamics with hemocytes heterozygous for *zip*^{1} and *tsr*^{1}, while also analysing the trans-heterozygous hemocytes (Figure 5.8 B, C). Qualitatively Actin dynamics were similar in the heterozygous mutants when compared to controls through assessment of flow heatmaps (Figure 5.8 C). While a noticeable reduction in Actin flow speed is seen in the trans-heterozygous mutant hemocytes (Figure 5.8 C). Further to this, I quantified the average Actin flow speed, which revealed a significant reduction in the trans-heterozygous mutants (approximately 4 μm min^{-1} in controls to 2.1 ± 0.2 μm min^{-1} in the trans-heterozygous mutants) (Figure 5.8 D).

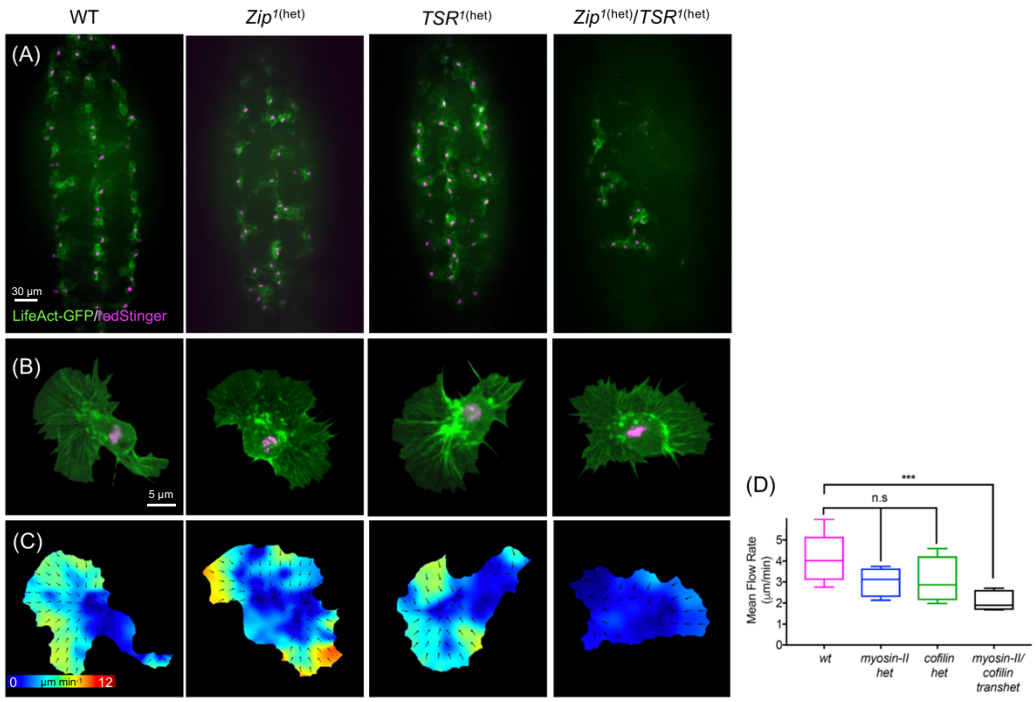

Figure 5.8: Myosin II and Cofilin work synergistically to coordinate global Actin organisation. Comparison of *wild-type*, *zip[1],* and *tsr[1]* heterozygous mutations, with *zip[1],* and *tsr[1]* trans-heterozygous mutations. **(A)** shows images of hemocytes on the ventral surface of *Drosophila* embryos. Note the disrupted dispersal of hemocytes in the trans-heterozygous mutant embryo **(B)** shows high magnification images of hemocytes. **(C)** Bottom panels show representative heatmaps of PIV analysis of Actin flow. Note the reduction in Actin flow dynamics in the trans-heterozygous mutant hemocyte. **(D)** Quantification of mean Actin flow speed in *wild-type*, heterozygous mutants, and trans-heterozygous mutant cells. Note that the cells containing trans-heterozygous mutant alleles for *myosin II* and *cofilin* have a strong reduction in Actin flow speed compared to *wild-type* or heterozygous mutants. ***P < 0.001, ordinary one-way ANOVA and Dunnett's multiple comparison test.

5.4 **Discussion**

In this chapter I have shown that Actin flow organisation, which is required for effective random migration in hemocytes is dependent on the activity of both Myosin II and Cofilin. I have also shown that Myosin II and Cofilin are synergistic regulators of Actin network turnover. My data has shown that Drosophila zygotic mutant embryos for Myosin II (*zip*^{1}) exhibit highly disrupted embryonic dispersal of the hemocytes. In control embryos, hemocytes migrate along stereotypical pathways and form a characteristic three-line pattern on the surface of the ventral nerve cord. This inability to disperse throughout the embryo is likely a result of reduced cell speed as my data has shown, as well as the inability for *zip*^{1} hemocytes to undergo contact inhibition of locomotion as has been previously reported (Davis *et al.*, 2015). The process of contact inhibition requires a mechanical linkage between cells, which requires massive reorganisation of the Actin network mediated by the contractile activity of Myosin II (Davis *et al.*, 2015). As such, it is known that disruption of Actin flow dynamics through Myosin II mutations, can negatively impact the migratory characteristics of hemocytes. Previous investigations into how Actin network flows are regulated have demonstrated that Myosin inhibition leads to a reduction in Actin flow speed, as I observe in these hemocytes (Ponti *et al.*, 2005; Ji, Lim and Danuser, 2008; Wilson *et al.*, 2010; Davis *et al.*, 2015). This flow speed data combined with the disrupted cell motility highlights that hemocyte motion is dependent on the forces generated by Myosin II, and that polymerisation at the cell boundary is insufficient on its own to promote normal cell motion. This finding is contrary to examinations of migrating cells within 2D *in vitro* conditions (Doyle *et al.*, 2012). However, it should be noted that cell

motion that independent of Myosin II in *in vitro* assays does not extend to either 1D or 3D environments.

I have also examined other parameters that describe the ways in which Actin flows are perturbed when Myosin II is absent, beyond measures of Actin flow speed. These other parameters measure the ability for Actin to flow in an aligned fashion through streamline analysis, and the localisation of Actin network remodelling by measuring the gradients of network divergence and turnover. My data also indicates that Myosin II is required for cell-scale organisation of the Actin flow field. This was revealed through streamline analysis which describes the gross directionality. This method when applied to control hemocytes highlighted a polarity to the Actin flow field with respect to cell motion that is mediated by compression and disassembly. However, in *zip*^{1} hemocytes this flow polarity is absent and Actin flows were highly disordered. With transient vortices, and tortuous paths, the streamlines suggest a process by which Myosin II regulates flow organisation by pulling the Actin network into alignment. In control hemocytes a sharp transition between anterograde flow and retrograde flow exists and appears to direct cell motion, which is not present in *zip*^{1} hemocytes. This transition zone represents a state change between regions of the flow that are engaged with the migratory substrate, and regions of the flow that have been disengaged. This transition region has been hypothesised to be mediated by the contractile activity of Myosin II in epithelial cells (Vallotton *et al.*, 2004; Ji, Lim and Danuser, 2008). In *zip*^{1} mutant hemocytes strong band of negative divergence is lost, that in controls is constituted of compressive activity and network depolymerisation.

By removing Myosin II, hemocytes are no longer able to produce the traction forces seen in controls, and the hemocytes are not able to present with the frictional asymmetry that is seemingly required for effective cell motion.

I have also demonstrated that Myosin II works in synergy with the protein Cofilin in order to regulate Actin network organisation, in analysis of hemocytes trans-heterozygous mutants for *zip*^{1} and *tsr*^{1}. While Actin flows are organised in the absence of Cofilin as observed through the regular patterning of streamlines, both flow speed and the overall amount of depolymerisation and compression is reduced in these cells. Which highlights that it is not just the contractile activity of Myosin II that is required for driving Actin flows but Cofilin is also required. It has been established in other systems that Myosin II contraction can be dependent on the filament severing ability of Cofilin (Mendes Pinto *et al.*, 2012). Cofilin is known as a protein inextricably linked with the destruction of the network however its effects are amplified through Myosin II. Cofilin acts to soften the network, reducing local filament density, which enhances Myosin II's compression and filament breaking capabilities (Taylor, Fechheimer and Shotton, 1982). Cofilin is also able to sever filaments more efficiently when the filaments are under strain (Schramm *et al.*, 2017). Interestingly, analysis of the localisation of Myosin II puncta in migrating hemocytes and regions of Actin network sinks revealed that they were not spatially correlated. This suggests that Myosin II is not specifically causing the local contractions that can lead to these network sinks. As such I hypothesise that these sinks are an emergent property of an Actin network that is under a

gradient of tension and depolymerisation as confirmed from the line scans of divergence and network turnover.

Cofilin's effect on cell directionality has not been explored here. For instance, it has been hypothesised that localised activation of Cofilin severs filaments that provide G-Actin monomers, which can be incorporated at the leading edge and thus direct cell motion (Pollard and Borisy, 2003; Ghosh *et al.*, 2004). While my findings in Chapter 3 bring into question the assumption of a leading edge that directs cell motion, however it would be interesting to examine the edge dynamics in these *tsr*^{1} hemocytes. For instance, given the reduction in depolymerisation I see from analysing Actin network turnover, it is possible that the protrusive velocity of the cell edge is highly reduced as well in hemocytes, owing to a reduction in free barbed end of polymerisation.

6 Hemocytes Adopt Different Steering Strategies in the Presence of External Cues

6.1 Introduction

Previously I have shown that Drosophila embryonic hemocytes, despite migrating persistently *in vivo*, also migrate inefficiently. I have also shown that while the standard model of cell migration is that of a stepwise cyclical process there is little evidence to support this concept. This is derived from analysis of the fluctuating leading edge, that protrudes and retracts with minimal relationship to the direction of travel, and at recording speeds of 5 seconds per image, there was no leading-edge activity that informed changes in the cellular trajectory. In fact, it appears as if the migratory behaviour exhibited by Drosophila embryonic macrophages is somewhat of a compromise between the consistent organisation of the Actin network, and the unstable edge behaviour.

However, all previous analysis has been conducted in cells that are random and freely migrating in the embryo. Which is to say that they are not stimulated or motivated to move in a directed fashion through any particular chemical or stress gradient nor are they contacting with other cells in their environment. We can activate directed hemocyte migration in vivo through ablating the embryonic epithelia and imaging the resulting wound response that hemocytes undergo. Much analysis of migrating cells involves chemical stimulation in vitro and I was curious to determine whether the characteristic

of migratory inefficiency of freely migrating cells still applied in this setting. I performed the same fundamental analysis, relating to the detecting of regions of edge extension, as well as measuring the persistence characteristics of hemocytes during directed migration. I was also keen to probe whether hemocytes during directed migration exhibited altered Actin flow conditions such as changes in flow speed, cellular persistence, or network organisation.

6.2 Contributions

I analysed edge dynamics in randomly migrating hemocytes and in hemocytes undergoing directed migration. The library of directed migration movies was produced by Dr Mubarik Burki.

6.3 Results

6.3.1 Hemocytes exhibit efficient migration in response to a wound

In order to investigate how hemocyte migratory behavior changes during a state of directed migration effects, I utilised laser ablation of the embryo epithelial layer. This ablation causes a wound in the embryo that hemocytes rapidly respond to (Figure 6.1, Movie 13). Hemocytes are attracted to epithelial wounds with a putative role in the clearing of cellular debris, however they are not required for the process of wound healing (Stramer *et al.*, 2005).

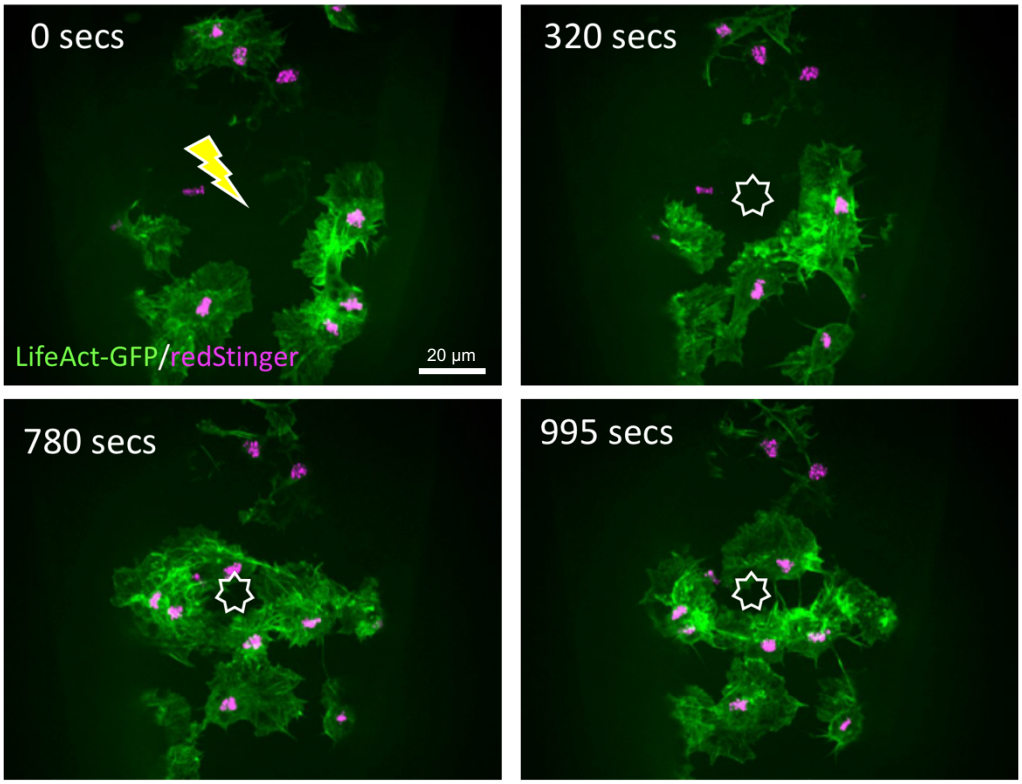

Figure 6.1: Hemocytes migrate rapidly towards wound sites. Time-lapse series featuring hemocytes migrating directionally to a laser wound (star) in the embryo.

6.3.1.1 Extensions are produced in the direction of cell travel

With the observation in control hemocytes that the leading edge does not inform cell directionality, I was interested in whether there were any clear changes in the mechanics of the cellular edge. To investigate this, I analysed hemocytes immediately after epithelial wounding, imaged a temporal resolution of 5 seconds per timepoint. The dynamics of the cell edge was assessed by application of an edge extension and retraction assay (a detailed description of this process can be found in section 2.4.1). This analysis highlights where regions of the cell edge are extending and retracting. In

randomly moving control hemocytes I have observed extensions and retractions presenting around the cell boundary (Figure 6.2 A, Movie 2 & 14). However, during directed migration, a consistent region of edge extensions can be found in the direction of travel and the direction of the wound site (Figure 6.2 A, Movie 14). Further to this I quantified the number of extensions produced around the cell body. This was motivated by the question of whether the disparate extensions seen in freely moving controls, converge into larger extensions in the direction of the wound site. Interestingly however, I found no significant difference between the number of extensions in freely moving controls and hemocytes undergoing directed migration (Figure 6.2 B). As such it is only the largest extensions that appear to be focussed at the front of the cell.

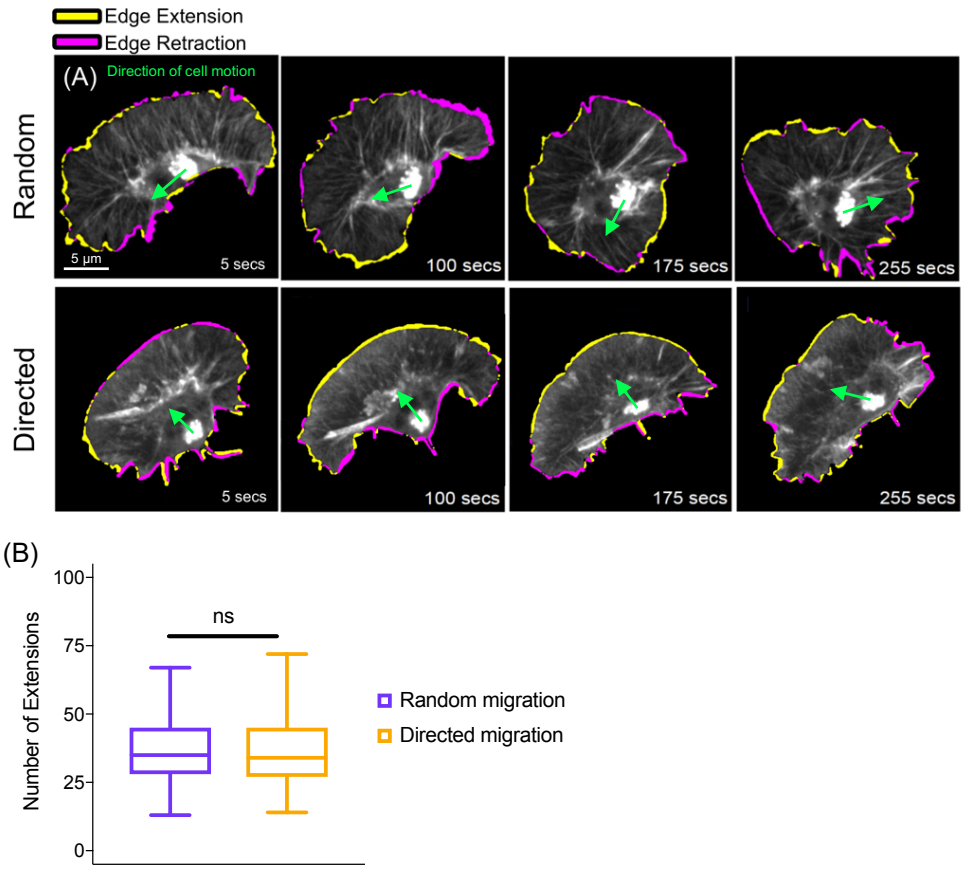

Figure 6.2: Hemocytes during directed migration exhibit large stable extensions. **(A)** Visualisation of hemocyte edge extensions (yellow) and retractions (magenta) during random and directed migration. Extensions and retraction during random migration fluctuate across the cell boundary. During directed migration these edge dynamics, appear to be more focussed, fluctuating spatially at a reduced frequency. **(B)** Despite the presence of a stable large extension in the direction of cell motion for directed cell migration (n=258 data points, from 5 cells), there is no significant difference in the average number of extensions produced across the cell boundary in comparison to cells undergoing random migration (n=443 data points, from 9 cells).

The observation of a focussed region of edge extension at the front of the hemocyte, drove further investigation into the protrusive characteristics of hemocytes responding to epithelial wounds. I quantified the location of these edge extensions by constructing position vectors between the nucleus and their centroid. This analysis was performed on all extensions and the region of largest contiguous extension. Following this, the angle between these position vectors and the vector of cell travel was calculated. With the earlier observation of streamline sinks that direct cell motion I also analysed position vectors to the primary sink. This allowed me to assess the changes in organisation of Actin flows which control directionality in freely moving cells.

This data revealed that in both the freely moving controls, and in hemocytes migrating towards a wound, that edge extensions are produced in

a wide distribution around the cell boundary (Figure 6.3 B, Movie 14). This initially was a surprising finding given the different requirements of the hemocytes in these different modes of migration. While freely moving, hemocytes are able to sample their local environment and as such the migration can be less efficient with regards to the activity of the cell edge. In directed migration however, the response to a dominant external cue might be thought to induce a particular directional bias into the cell edge. This directional bias was observed when analysed the region of largest extension, which features a stronger bias towards the direction of travel compared to freely moving hemocytes (Figure 6.3 A, C). This data suggests that hemocyte edge dynamic change significantly between direction and random hemocyte migration. However, analysis of the directions of primary sinks remain equally coupled to cell directionality in both experimental conditions (Figure 6.3 A, D).

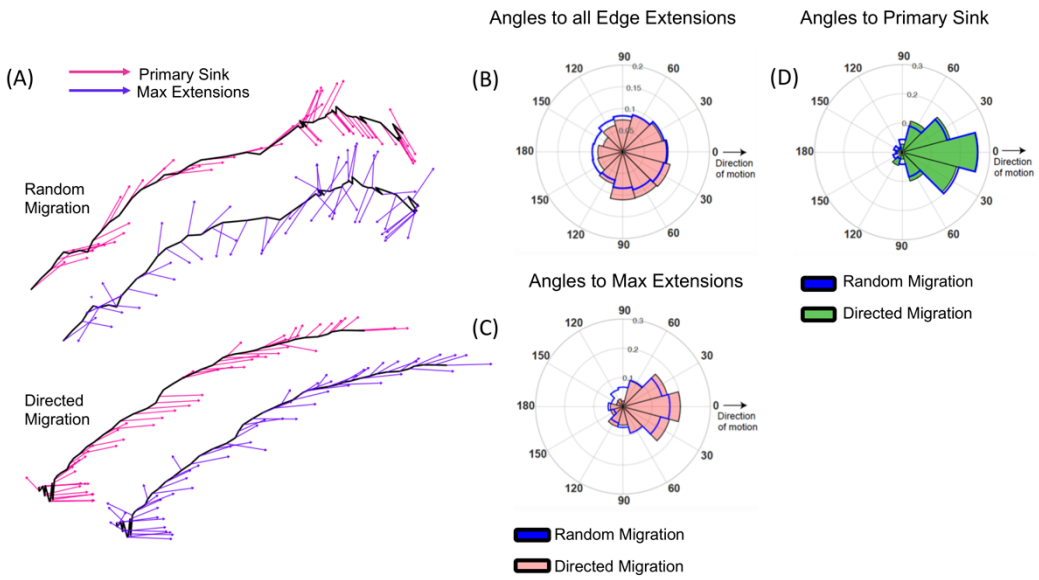

Figure 6.3: During directed migration large regions of edge extension are produced in the direction of travel. **(A)** Example cell tracks of a randomly

migrating hemocyte in which the unit vectors of the largest edge extension and the primary sink are superimposed. A track from a hemocyte undergoing directed migration is represented by the lower two tracks and displays that same vectoral information. Note that the direction to the primary sink is well correlated with the direction of cell motion in both random and directed migration, while the max extension is tightly coupled to the cell track only in the directed migration case. **(B)** Upper panel shows a rose plot of the direction to all extensions normalized to the direction of motion. Both random migration (blue outline) and directed motion (red) are represented. Note the similar angle distribution between the peripheral extensions in random and directed migration. **(C)** Rose plot showing the direction of max extensions normalized to the direction of motion. Random migration (blue outline) and directed motion (red) are represented. Note the increase in angles focussed about the direction of motion during directed migration. **(D)** Rose plot showing the direction of primary sink normalised to the direction of cell motion comparing random migration (blue outline) to directed motion (green). Note the similar angle distribution between the primary sinks in random and directed migration.

As we have seen many edge extensions are produced radially around the cell edge with no obvious relationship in the direction of travel (Figure 6.3 B). This highlights that these extensions may not be contributing to cell directionality. Extension position vector analysis quantifies the location of the edge extensions with respect to the heading of the cell, however the velocities of edge dynamics themselves have been unexplored. In order to analyse the directions of edge displacement I used morphodynamic analysis of the cell

boundary (see section 2.4.2 for more details on this method). Using these edge velocity vectors, I calculated the edge resultant vector, which is attained by summing all edge velocities, this gives a principle direction in which the edge is displacing. The resultant of all edge extensions was compared against the direction of cell travel in both directed and randomly migrating cells using the cosine similarity between these vectors (Figure 6.4 A, C). If the edge resultant vector is aligned with cell directionality this analysis would demonstrate an integrated contribution from the edge towards cell motion. I also performed this analysis on the velocity vectors constrained within the largest contiguous region of extensions (Figure 6.4 B, C).

What this revealed is that the overall directionality of the cell edge is significantly biased in the direction of cell travel during directed migration. This significant difference holds when considering the entire edge, or the largest extension (Figure 6.4). The most interesting result here is that the resultant velocity of all the extensions in the directed migration case is the most aligned with cell travel. This highlights some as yet unresolved ability to integrate all extension velocities into cell motion. As such in directed migration the activity of large regions of extension appear to be less important for cell directionality than holistic protrusive activity across the cell boundary.

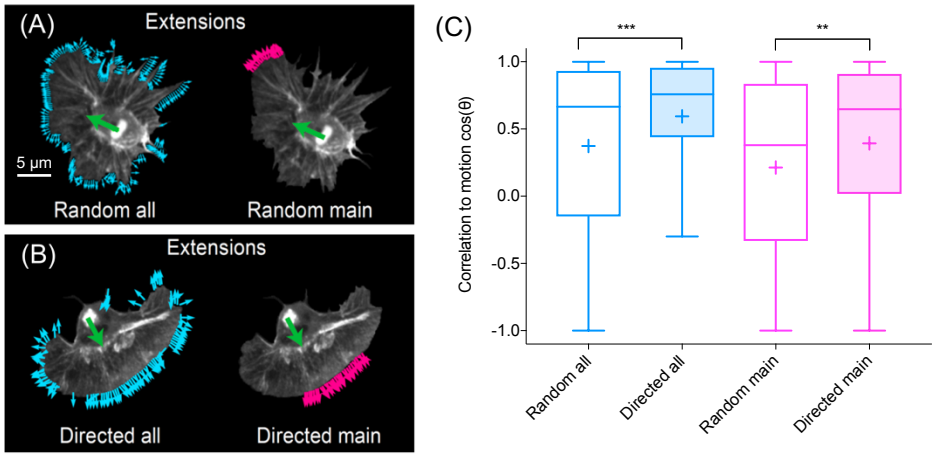

Figure 6.4: During directed migration the whole cell boundary is coherent and acts to extend in the direction of motion. **(A)** Quantification of the velocity vectors of the cell edge in a representative randomly migrating hemocyte. In the image either all edge extension unit vectors (left panel) or the unit vectors of the edge within the largest contiguous protrusion (right panel) are shown. **(B)** Quantification of the velocity vectors of the cell edge in a representative hemocyte responding to a wound. In the image either all edge extension unit vectors (left panel) or the unit vectors of the edge within the largest contiguous protrusion (right panel) are shown. **(C)** Correlation of the direction of cell motion to the direction of the resultant velocities of the edge extensions. Note that the correlation is stronger when comparing either all extensions or the main extension in cells migrating towards a wound. ***P < 0.001 and **P < 0.01, Kruskal-Wallis test and Dunn's multiple comparison test.

6.3.1.2 Edge extensions are directionally persistent

A common observation of cells undergoing chemotaxis is that they are more directionally persistent than those cells migrating using their intrinsic

directionality alone (Petrie, Doyle and Yamada, 2009). As such I wanted to investigate the difference in directional persistence between hemocytes migrating towards a wound, and freely moving hemocytes. This was achieved by analysing the directional autocorrelation of the cell trajectories in these different experimental conditions. I also used this method on the directions of the largest extensions, and the direction of the primary streamline sink, to examine how Actin dynamics change in the presence of external cues.

In freely moving hemocytes, the autocorrelation profiles of the edge, cell motion, and streamline sink are hierarchical. With the primary sink (point of Actin flow asymmetry), as the most persistent, while the largest extension is the least directionally persistent (Figure 6.5 A). As such cell motion could be considered a compromise between these two migratory parameters: the fluctuating edge and the organisation of the Actin flows. However, in directed migration all migratory parameters become more directionally persistent (Figure 6.5 B). The most dramatic difference is seen in the directional persistence of the cell edge (Figure 6.5 D). This data suggests that the presence of an external cue stabilizes the leading edge of migrating hemocytes. As such it is likely that the cell edge is disruptive of efficient cell motion, and must be stabilised in order to increase cellular persistence (Leithner *et al.*, 2016).

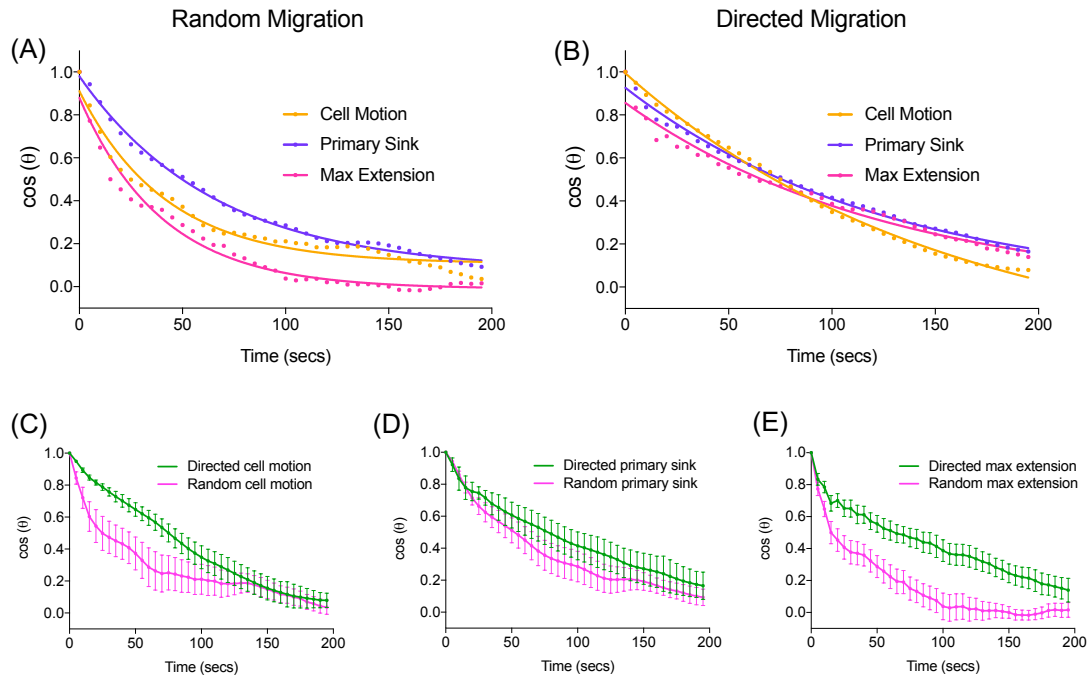

Figure 6.5: Edge dynamics are dramatically stabilised during directed migration. **(A-B)** Directional autocorrelations comparing the persistence of cell motion, maximum edge extension and the maximum streamline endpoint during directed migration. Dotted lines are real data and solid lines are fits to an exponential decay. Note the slower decay in these parameters during directed migration compared to random migration in 'A'. This slower decay suggests an increase in directional persistence of these parameters. **(C-E)** Directional autocorrelations of each migratory parameter (max extension, primary sink, and cell motion). This analysis was performed in random migration (magenta curves) and compared to their counterpart data derived from analysis of cells responding to a wound (green curves). Error bars = SEM.

6.4 **Discussion**

In this chapter I have investigated the organisation and behaviour of Actin retrograde flow within migrating hemocytes as well as the mechanics of

the fluctuating edge during directed migration. In order to perform this analysis, I have taken advantage of the hemocyte role as immune regulators that rapidly respond to wounds (Wood and Martin, 2017). While these cells aren't actually required for wound closure, as Drosophila embryos that lack all hemocytes feature the stereotypical wound re-epithelialisation (wound closure), hemocytes do effectively migrate towards the wound site (Stramer *et al.*, 2005). For an appropriate wound response to occur, chemotactic cues should be released in order to bias a cell's migration to the wound site. It has become clear that hemocytes require specific signalling and a chemotactic gradient to respond to chemotactic cues emanating from epithelial wounds (Wood, Faria and Jacinto, 2006). The preeminent candidate is H_20_2, with this signal Acting to overpower other local influences (Niethammer *et al.*, 2009; Moreira *et al.*, 2010). These influences can include apoptotic debris or developmental cues such as PVF.

Previous analysis of Actin dynamics during wound response have shown a common hemocyte behaviour contact inhibition of locomotion, is inactivated, with cell crowding a wound site without individual cells repelling from each other (Stramer *et al.*, 2005). What I have observed is that there are significant other significant changes in the Actin dynamics of hemocytes during a wound response. This includes dramatic changes in the size and directional persistence of the protruding edge, which are more aligned with in the direction of cell travel. I have also observed an increase in the directional persistence of hemocytes during wound response through assessing the directional autocorrelation of tracked hemocyte nuclei. Directional migration can be

thought of comprising the "*intrinsic cell directionality and external regulation*" and it is this regulation that manifests as more efficient cell movement during a wound response (Petrie, Doyle and Yamada, 2009).

The role of the leading edge during chemotaxis in hemocytes has been elucidated in previous studies (Wood, Faria and Jacinto, 2006). Here, Drosophila embryos were implanted with beads treated with Actin polymerisation inhibitors Latrunculin B or Cytochalasin D. The consequence of this was the inhibition of the immune response, where hemocytes did not chemotact towards the bead and featured a minimized area of edge extensions. Pi3K, which has been associated with cell polarisation and directionality was also shown to be required during hemocyte chemotaxis, but not during developmental dispersal (Weiner *et al.*, 2002; Wood, Faria and Jacinto, 2006). The importance of Pi3K during chemotaxis highlights that stable and efficient edge dynamics that define cell polarity are indeed required for effective migration as my data also shows.

While there are large changes in the mechanics of the cell edge as it extends and retracts, I observe minimal changes in the organisation of the flow field. Through streamline analysis I was able to compare the location of the streamline sink to the direction of travel. This revealed that the primary sink leads cell migration during chemotaxis and in random migration, with a mild enhancement of the directional persistence. As such, it appears that Actin flow organisation is a constant that allows cells to translocate effectively, however

directed migration clearly has different demands, and requires an efficient and stable cell edge.

It would be interesting to develop the process of imaging and analysing directed migration further by tracking cells before and after wounding of the epithelium. This would provide insight into the transition between a freely moving hemocyte, exploring its environment, to a hemocyte responding to the wound. Unfortunately, due to experimental constraints, this was not attainable in this project as the system used to perform the epithelial wounds required the halting of imaging during laser ablation. This meant that movies of freely moving hemocytes and movies of hemocytes responding to wounds were produced independently. However, through utilising an alternate imaging system this kind of analysis could be envisioned. Previous studies have imaged hemocytes migrating on the midline and during lateral migration (Wood, Faria and Jacinto, 2006). These two-distinct migratory behaviours were independently analysed for their respective velocities and their directionality parameters. In our hypothetical wounding case, imaging throughout the wounding process would allow for the observation of the shift between freely moving protrusion independent migration, and protrusion dependent directed migration.

7 Discussion

In this work I have shown that the migration of freely moving hemocytes is governed by the organisation of the flowing Actin network, which is mediated by the synergistic destructive activity of Myosin II and Cofilin. I have also shown that freely moving hemocytes do not depend strongly on the edge protrusions for their directionality. I have found that the random migration of hemocytes is in actuality a compromise between the stability of the flowing Actin network and the noisy and unstable cell boundary. This is surprising given the predominant conception of cell migration which elevates the role of the cell edge and the polymerisation activity that causes. This model is defined by a cyclical step-wise process whereby migrating cells protrude their membrane through the polymerisation of Actin filaments in the direction of travel. The cell then strongly associates with the migratory substrate in order to build traction for translocation. Intracellular contraction then acts to pull the rear of the cell forward, by way of disengaging adhesions at the rear. My data however suggests that the largest areas cell membrane extension, i.e. those that should have the greatest capacity to direct motion, are not highly correlated with cell motion through a comprehensive series of analysis. Initially I found that the location of large membrane extensions at the cell boundary indicate only a weak bias with respect to the direction of travel. The speed of protrusion is significantly different to cell speed in the direction of travel highlighting a disconnect between the activity at the boundary and the motion of the cell. Through directional autocorrelation analysis of the largest extension's position vectors, I have determined that these extensions are less

persistent than the cell they are purported to direct. Finally, I investigated whether there was any temporal hierarchy whereby the cell follows a path dictated by the orientation of large extensions and did not find any preceding behaviours.

The findings in this thesis highlight that during freely moving random migration much effort is afforded to the production of the extensions at the cell boundary. Through analysis of the locations of all of the edge extensions I have determined that these extensions are produced radially, in a wide distribution around the cell boundary, with no obvious bias towards the direction of travel. This concept of cellular 'effort' in the context of producing peripheral protrusions that aren't immediately utilised in the process of cell migration has been called in the literature 'inefficient' migration (Dunn, Weber and Zicha, 1997; Hermans *et al.*, 2013). It is important to note however that during freely moving random migration, hemocytes *in vivo* have a number of important tasks to perform that would be dependent on the rapid fluctuations of the cell boundary both directly and indirectly. For instance, the ability to sample and explore their migratory environment could be dependent on producing protrusions in a wide angular distribution in order to cover as much of the local surroundings as possible. This is likely as hemocytes have been implicated in immune surveillance (Wood and Jacinto, 2007). Hemocytes also have an integral role in the deposition of extracellular matrix components onto the ventral nerve cord as well as the engulfing of apoptotic debris, both roles would require a dynamic cell edge (Wood and Jacinto, 2007; Matsubayashi *et al.*, 2017; Sánchez-Sánchez *et al.*, 2017).

My findings have directly brought into question the nomenclature used to describe the region of the cell boundary purported to be responsible for cell motility, namely the leading edge (Ridley, 2011). Not only do I not observe hemocytes being directed by large edge extensions instantaneously but through directional cross-correlation analysis, I also do not observe any temporal hierarchy that would highlight a gross cellular reorientation with respect to the direction of the largest extensions. The 'leading edge' naming, may in fact be inappropriate, presupposing an unearned role in its directing capabilities. The naming may also be a function of the cell's that are often investigated in migration assays, specifically the fish keratocytes. These cells are able to maintain a constant coherent canoe-like morphology and as such the front of the cell is necessarily always the leading edge of the cell (Verkhovsky, Svitkina and Borisy, 1999; Keren *et al.*, 2008). Interestingly only when exploring the mechanical changes of hemocytes during directed migration does the cell boundary appear to stabilise and connect to the direct of cell motion. In these experiments, I exploited laser ablation of the drosophila epithelium, to stimulate hemocytes towards a cue, i.e. the wound site. In these directed migration cases there was a dramatic increase in the stability of the largest regions of extensions. I also observed an increase in the directional bias of the largest extensions, which suggests a more 'efficient' method of migration is being employed, however interestingly the number of extensions was unchanged between experimental conditions. Models developed to describe the process of cellular chemotaxis, show that steering towards a chemical cue is a stochastic process (Arrieumerlou and Meyer, 2005). This process is determined by the local frequency of binding events of the signalling

molecules, with the assumption that more receptors will be occupied closer to the chemical cue, providing a signalling asymmetry. This asymmetry then promotes localised lamellipodial extension in the direction of the chemical cue, as such the noise of the cell edge is effectively damped by environmental cues. Other studies into the edge activity of chemotacting cells suggest that extensions can be preferentially selected for or against, from the current pool of extension locations and orientations. This highlights that initially extensions themselves do not predetermine and lead migration, they're a consequence of some as yet unresolved 'decision' process (Andrew and Insall, 2007).

Through particle image velocimetry I have been able to determine that the Actin network displays a high degree of cell-scale organisation. This organisation could provide hemocytes with an ability adapt to environmental influences mechanically, in a way that an incoherently organised Actin cytoskeleton would not provide. Stability of the Actin flow field itself is provided by compressive sinks in the network. These regions described in this thesis through divergence analysis are apparent hemocyte analogues to the convergence zones described in a number of other studies (Vallotton *et al.*, 2004; Okeyo *et al.*, 2009). These regions are highly stable in time which is in stark contrast to the fluctuating nature of the cell edge. A previous description of the 'geography' of the flowing Actin network has reported four kinetically and kinematically distinct regions of the cytoskeleton (Vallotton *et al.*, 2004). These regions are the fast-flowing branched Actin network of the lamellipodia at the cell edge; the cross-linked Actin network of the lamella; a region of network flow that moves anterograde with respect to the cell front; and a region

of transition and convergence between retrograde and anterograde flows, reportedly mediated by network contraction (Vallotton *et al.*, 2004; Ji, Lim and Danuser, 2008). I was also able to identify this transition region in migrating hemocytes through the first use of streamline analysis in the study of cell migration.

This transition region as denoted by the streamline primary sink is highly correlated with the direction of cell motion. Interestingly when I examined the temporal cross correlation of this primary sink to the direction of motion, I found no preceding behaviour. With the finding that extension directionality, flow polarity, and cell motion are tightly coordinated in time, this indicates that mechanical coupling must be in place in order for transmission of this information to be possible. These migratory components are significant distances apart, as such signalling molecules would take too long given the flow speed we observe, for such a tight coordination between the interior of the cell and the cell periphery. There is currently evidence to suggest that mechanical coupling in migrating cells can be mediated by membrane tension (Ofer, Mogilner and Keren, 2011). However, it could also be mediated through coherent Actin network that spans from the cell boundary and links to the nucleus, through nuclear anchoring proteins such as ANC (Starr, 2003; Gomes, Jani and Gundersen, 2005).

Further analysis of Actin flows with streamlines, determined that streamline confluence intensifies at the boundary between directionally distinct domains of the Actin flow field. These regions are defined by their polarity with

respect to the direction of cell motion. Actin flows that move antiparallel to cell motion are retrograde, while Actin flows that move parallel to cell motion are anterograde. Transition regions between retrograde and anterograde flow domains are what defines convergence zones in other cell types (Vallotton *et al.*, 2004; Okeyo *et al.*, 2009). I have observed a significant flow speed difference between these domains, with retrograde regions exhibiting much slower average flow speeds than the average anterograde flow speed which is in line with earlier findings (Schaub, Bohnet, Laurent, J. J. Meister, *et al.*, 2007; Fournier *et al.*, 2010; Wilson *et al.*, 2010). This flow speed difference was predicted in previous studies where it was suggested that retrograde flowing Actin is strongly associated with the migratory substrate (in a gripping state), while the process of transitioning into an anterograde flow pattern towards the rear of the cell acts to weaken and eventually disengages the network from the substrate causing slippage as per the molecular clutch (Shao, Levine and Rappel, 2012). This transition region between gripping and slipping has also been observed in migrating Nematode Spermatozoa suggesting a highly conserved component of migrating cells (Zajac *et al.*, 2008).

Convergence zones in hemocytes are not just constrained to this transition region as in epithelial cells but are located around the cell body as in fish keratocytes (Vallotton *et al.*, 2004; Ji, Lim and Danuser, 2008; Okeyo *et al.*, 2009). However, the mechanism by which these convergence zones arise has been unclear, these regions are often sites of network turnover, observed through reduction in Actin network intensity (Vallotton *et al.*, 2004; Huber, Käs

and Stuhrmann, 2008). In epithelial cells these convergence zones have been hypothesised to arise from contractile activity, following observations that flow domains on either side of the convergence zones are mechanically coupled (Vallotton *et al.*, 2004). Other studies have shown that they are sites of significant network depolymerisation in fish keratocytes (Wilson *et al.*, 2010). Through analysis of Actin network convergence data, I have explored the contributions that both network compression and turnover have in forming these convergence zones.

In order to assess network compression, I calculated the principal strains within the flowing Actin network. This analysis revealed how the network is under elevated compression deep inside the network around the cell body and spatially correlates to the convergence zones. I have, through quantifying this spatial correlation found that approximately half of the network convergence consists of compressive behaviour. I also examined the Actin network turnover through published methods (Vallotton *et al.*, 2004; Wilson *et al.*, 2010) (Wilson 2010, Vallotton 2004). This analysis showed how in hemocytes convergence zones are significantly comprised of network depolymerisation as well. In previous studies, depolymerisation in migrating cells has been shown to be driven by the contractile activity of Myosin II (Wilson *et al.*, 2010). Where Myosin II localisation coincides with the spatial distribution of Actin disassembly, with a Myosin II gradient that peaks at the rear of the cell. I also observe a similar gradient upon analysis of the distribution of Myosin II puncta in hemocytes which has also been observed in *Dictyostelium* (Yumura, Mori and Fukui, 1984). It has been suggested that

Myosin II is capable of network disassembly through contraction and mechanical buckling of the filaments, as well as through a surprising mechanism of F-Actin unbundling (Haviv *et al.*, 2008; Murrell and Gardel, 2012). As such it was perhaps unsurprising to see through analysis of Actin flows in hemocytes mutant for *myosin II* (zip^1) that there is a significant reduction in the intensity of network convergence, and the global organisation of the Actin flows. Interestingly however I did not find Myosin II puncta specifically colocalising to regions of negative divergence, and as such these regions may be motor-independent.

I also examined hemocytes mutant for *cofilin* (tsr^1), which revealed a reduction in the intensity of the disassembly in the Actin network. Cofilin is considered a primary driver of Actin turnover, severing filaments and providing free barbed ends for polymerisation activity (Pollard and Borisy, 2003). I have found that hemocytes with a tsr^1 mutation feature profoundly disrupted Actin flow dynamics and cell migration behaviour. As such hemocyte migration is dependent on Cofilin for effective migration. We are currently unable to assess the spatial distribution of Cofilin in hemocytes, and as such are not able to determine whether sites of network disassembly collocate with sites of high Cofilin activity. In fact, in fish keratocytes active cofilin is located near the leading edge, which is opposed to the gradient of Myosin II that peaks at the rear of the lamella (Svitkina and Borisy, 1999; Dawe *et al.*, 2003). In keratocytes Cofilin density is elevated in the lamellipodia but posterior to the extreme distal edge, considered to be an exclusion zone (Svitkina and Borisy, 1999). This region excludes Cofilin activity as the Actin filaments here are not

in the preferred phosphorylation state (these filaments are either ATP-F-Actin or ADP-Pi-F-Actin) for Cofilin to bind and sever (Pollard 2009). With this current understanding of Cofilin localisation it would be difficult to suggest a direct spatial relationship to turnover and Cofilin activity (turnover activity occurs primarily at the rear in hemocytes), despite a clear role controlling network depolymerisation.

One hypothesis to explain the lack of spatial colocalisation between Myosin II or Cofilin with sites of network remodelling arises through an understanding of the synergy between these proteins. Through analysis of Actin flow dynamics and migration behaviours in hemocytes trans-heterozygous for *cofilin* and *myosin II*, I have shown that these two genes work synergistically to carry out the network remodelling required for coordinated cell motion. As such I hypothesise that network disassembly is dependent on both contractions mediated by Myosin II and severing from Cofilin. Specifically, these regions of turnover are an emergent property network both under graded tension and featuring a baseline of filament disassembly.

This synergistic behavior has been observed in other experimental settings, namely the study of Actin ring contraction in budding yeast (Mendes Pinto *et al.*, 2012). Here it was revealed upon depletion of Myosin II, that the rate of depolymerisation of the Actin ring was markedly reduced alongside a reduction in contractility. In hemocytes it is perhaps a likely hypothesis that Myosin II mediated contraction and Cofilin mediated severing cooperatively work together in a mechanism reminiscent of the solation-contraction model

(Taylor, Fechheimer and Shotton, 1982; Janson, Kolega and Taylor, 1991; Kolega, Janson and Taylor, 1991). In this model, efficient contraction of a crosslinked Actin gel can only take place once structure of the gel has been reduced, which is to say it has undergone a transition from the gel state to the sol state (solation). Gels that are highly structured are antagonistic to contraction but weakening of this structure can occur from crosslinker dissociation or Actin severing (Taylor, Fechheimer and Shotton, 1982). Once the structure is weakened, the gel is more amenable to contraction and this process of weakening could be mediated by severing of the filaments by Cofilin. This synergistic behaviour of Actin network contraction and destruction results in a mechanical gradient that unlike the fluctuating hemocyte edge has the capacity to provide stability, through the persistence of global Actin flows. Destruction of the network is known to replenish the pool of Actin monomers, that are available to be incorporated into the cell edge for the purpose of producing new protrusions (Ghosh *et al.*, 2004). This replenishment is important to maintain homeostasis in the context of cell shape, otherwise these cells would indefinitely contract, and would be incapable of migrating due to a loss in the cell asymmetry required for cell motion. There is also evidence that depolymerisation alone can cause contraction. In one motility study of *Ascaris suum* sperm cells, it was shown that network retraction could occur in a Myosin II independent manner (Miao *et al.*, 2003). Here, depolymerisation weakens the structure of the network, and coupled with motor-independent filament remodelling shortens the gel causing retraction of the cell rear. In another study, an investigation into *Nematode Spermatozoa*, revealed that an anisotropic cytoskeleton can contract through the process of

disassembly (Zajac *et al.*, 2008). This disassembly-based contraction may be relevant in the provision of forces that move the cell body. In this hemocyte system strong sites of depolymerisation are located around the cell body with a primary sink situated in the peri-nuclear region which is highly correlated with cell travel. This primary sink is defined by the greatest intensity of streamline confluence in a specific region and as previously discussed represents the transition between retrograde flow and anterograde flow. I have also observed a narrow corridor of slow Actin flow speeds in the direction of travel. Slow flows are associated with a region of the Actin network that is engaged with the migratory substrate, providing the required friction for cell translocation (Jurado, 2004). This slow flow corridor may act to align cell body retraction through an axis that is defined by the location of the primary streamline sink, that is remodelling the Actin network.

In this work I have shown that Actin flows are able to provide a stable polarity of which the cell uses to guide cell motion. However, I was unable to verify one hypothesis that is often linked to the role of cell motion and Actin flows, in that there is a linear coupling to the speed of Actin retrograde flows and the speed of cell migration (Jurado, 2004; Maiuri *et al.*, 2015). Other studies have attempted to analyse this relationship, through a variety of means. Often the Actin flows are analysed in limited ways through tools such as kymography, which do not provide information of the global flow field (Jurado, 2004; Maiuri *et al.*, 2015). However, one study that used flurescence speckle microscopy, a methodology that provides a flow data across the lamella did not find a relationship between the rates of Actin flows and cell

migration. I have also not been able to find and correlation between these two parameters, which I hypothesise is not valid and rapid temporal resolutions. It may be the case that other measures are required to quantify displacements of the nucleus. For instance, measuring the jerk (the second derivative of velocity) may reveal sudden jumps of the nucleus that represent a change in cytoskeletal tension upon engagement and disengagement of the substrate.

One element of the modern cell biologist's toolkit that has gone unmentioned thus far in this work is the development of a mathematical model of the Actin flow system. Building a model of this hemocyte actin flow system would allow for the integration of published quantitative data, as well as offer insight into the key molecular actors in the system. Given the system described in this thesis is multiple factors, specifically the synergistic interactions of Cofilin and Myosin, it would be useful to develop a mathematical model that can also elucidate these multifactorial behaviours and reproduce specific migratory characteristics. While it is important to note that cell motion is a phenomenon regulated by multiple factors operating on different orders of temporal and spatial description, it can be useful to construct a minimal physical model that contains the fewest amount of required biological features, in order to reconstitute the migratory behaviour. With the model in hand, the information could be easily implemented within open source cytoskeletal simulation software such as Cytosim. While the development of such a model is beyond the purview of this work, the reader may consolidate the following information. The model to be outlined would need to incorporate an Actin network, Myosin motors for network contraction, and the Actin disassembling

capacity of Cofilin. The first step to consider is that the theoretical cell is polarised, that is to say it has a definable front and back. Polarisation can be defined by the density of the Actin network, in that Actin is most dense towards the front and undergoes an exponential decrease in density as a function of distance from the front of the cell. Myosin however exhibits the opposite density profile; an exponential increase in Myosin density is observed as a function of distance from the front of the cell. Cofilin localisation is poorly understood in hemocytes, and while published data locates active cofilin at the leading edge (Svitkina and Borisy, 1999) the important thing to consider, with respect to the data produced in this work, is that there is a constant level of background disassembly mediated by Cofilin. One important feature of the model involves the maintenance of a constant volume of this theoretical cell. As a consequence, if the density of the Actin network is increasing deep inside the cell, it must be reducing at the cell edge and vice versa. An emergent property of the Actin flow system observed in this work is the formation of intense regions of network disruption, i.e. Actin network sinks. These sinks appear to arise from a synergistic interaction of Cofilin and Myosin. In this model Cofilin is providing a baseline of network disassembly, and once the Actin network density reaches a hypothetical low-density value Myosin is able to not only contract the meshwork but also contribute to disassembly. While this work has been unable to associate specific regions of network disassembly to the locations of Myosin puncta, it may be the case that these sinks occur within a network that is undergoing a gradient of strain while also becoming less stable as a result of Cofilin mediated severing.

Through this work I have attempted to build the most comprehensive picture of the flowing Actin network available and I have introduced new tools to the field, that will hopefully shed light on the biomechanics of cell motion. These tools have been developed to be easily accessible and adaptable to new cell systems. I have also been conscious of addressing directly some long held conceptions of cell motility. For instance, my data does not provide much confidence for the idea that cell migration is leading edge driven, nor does it appear to be fair to describe the process as stepwise or cyclical. The complexity of cell migration may mean it is still conceptually useful to navigate the cell migration landscape with discrete terms such as the leading edge. However, it should not be lost on the reader that this process is a mechanically integrated one, that operates across spatial and temporal descriptions. As such the tools that we build and use to analyse cell motion should reflect this, with more attention being paid to the integrated whole and less to the minutiae.

7.1 **Future Work**

The ability to build a coherent picture of the internal Actin dynamics of cells and make reasonable comparisons to cell motion, is a beneficial property of the cell system I have employed, as hemocytes in these experimental settings migrate well and have trackable flows over experimentally convenient timescales. A significant challenge in understanding the underlying processes behind cell migration is to bridge the gap between phenomena that occur on vastly different levels of temporal and spatial description (Rafelski and Theriot, 2004). However, with a newly developed understanding of single cell motion it

would be interesting to investigate other cell types. I have begun to analyse the organisation of Actin flows in different cell types, including B16 melanoma cells and Retinal Pigment Epithelial cells. In B16 Melanoma cells, I have examined Actin flows using Particle Image Velocimetry and have begun to characterise this data. I have also investigated the organisation of the Actin network using streamline analysis.

This preliminary data has proved promising, revealing a similar point of organisation, as seen in hemocytes, through the primary sink. Using these cells also has the advantage of investigating cell types that have identifiable lamella and lamellipodia, the latter of which is not obviously present in hemocytes. Investigating Actin flows in fish keratocytes using streamline analysis would also prove valuable. Actin flows in these cells have been investigated thoroughly and are well characterised, and as such would be a good cell system to investigate further, by utilising the techniques developed here for hemocytes. In the context of streamline sinks it would interesting to observe where the sinks are located in the keratocyte system. From assessing the published analysis of keratocyte flows, it seems as if there are multiple candidate locations for streamline sinks (Schaub, Bohnet, Laurent, J. Meister, *et al.*, 2007; Yam *et al.*, 2007; Adachi *et al.*, 2009; Wilson *et al.*, 2010). My data suggests that in hemocytes, the primary sink is located in the perinuclear region, in the direction of travel. This sink is also a site of significant network remodelling through compression and disassembly. In fish keratocytes however, these regions of compression and disassembly have been observed to be located in two foci that flank the cell body (Wilson *et al.*, 2010). There is

also a transition between keratocyte lateral and retrograde flows, that could, as it does in hemocytes colocalise with the primary sink (Wilson *et al.*, 2010; Shao, Levine and Rappel, 2012). This transition point in keratocytes is also notable in studies of traction stresses, whereby pliable substrates are compressed and folded at this transition point, along the axis of cell motion (Oliver, Dembo and Jacobson, 1999). Given this open question as to the location of streamline sinks in other cell systems, it would be useful to use the streamline analysis in these keratocyte cells, in order to further validate the primary sink as a cytoskeletal marker of cell polarity. It would also be valuable to see whether in hemocytes or in other migrating cells if the primary sink denotes a site of elevated traction forces. The reduced flow in the direction of travel, and the finding that the primary sink is a site of intense network contraction would imply a coupling of this region and the substrate. External to this project I have contributed to works that have suggested that hemocytes are contracting the extracellular matrix upon which they are migrating (Matsubayashi *et al.*, 2017). This was achieved by using Particle Image Velocimetry to track the local displacement of the basement membrane, caused by hemocytes interactions.

One notable component of cell motion that went unaddressed in this thesis was the role of Microtubules. Freely moving hemocytes feature stable, Microtubule ‘arms’ which are formed in the direction of travel (Stramer *et al.*, 2010). During directed migration (wound response), hemocytes overexpressing the Microtubule severing protein Spastin, are significantly less persistent than controls, and hemocytes also require Microtubules during other

migratory processes such as contact inhibition of locomotion (Stramer *et al.*, 2010; Davis *et al.*, 2015). As a consequence, I would examine the effects of microtubule organisation in light of the new Actin flow data presented in this thesis. My analysis of Actin flow speed for instance demonstrates that there is a corridor of slow Actin flows in the direction of travel. As such I would be interested in seeing whether Microtubule bundles preferentially use this region to extend through, and whether they are stabilised within this corridor. It would also be interesting to examine whether the primary sink locates near the site of Microtubule organisation. Microtubules polymerise from α and β tubulin dimers from microtubule organising centres (MTOCs) (Etienne-Manneville, 2013). It is known that these MTOCs can be used as markers of migratory polarity and as such there may be a spatial relationship between the sinks and Microtubule organisation (Gant-Luxton and Gundersen, 2011). For instance, the slow Actin flows coupled with a decrease in network density at the sink may provide a more stable environment for the polymerisation of microtubules to occur. However, it should be noted that little is known about MTOCs in hemocytes and as such more work is required to elucidate the role these might play in hemocyte migration.

Appendix

Movie Legends

Movie 1: Centroid and nuclear tracking in hemocytes. Automatic tracking of hemocytes at 5 seconds per timepoint using the centroid of the cell and the nucleus as a fiducial marker. The nucleus was labelled with UAS-RedStinger and Actin was labelled using UAS-LifeAct-GFP. Note how the track of the centroid (magenta) does not reflect cell motion in contrast to the track of the nucleus (green). The centroid measure is highly responsive to significant morphological changes, with displacements of the centroid occurring along the axis of large cell extensions. The nucleus however is stable in shape, and its translation reflects whole cell translation.

Movie 2: Analysis of edge extensions. Regions of extension are revealed by subtraction of consecutive binarized images of hemocytes from time-lapse movies. Position vectors can be constructed between the nucleus and the centroid of the regions of edge extension (yellow arrows). These position vectors can be compared to the direction of cell motion (magenta arrow). Note how many peripheral extensions are produced around the perimeter of the hemocyte during migration (left panel), and that the largest region of extension is often uncorrelated to cell motion (right panel).

Movie 3: Quantification of Actin flows in freely moving hemocytes. Actin flows are tracked using Particle Image Velocimetry (PIV). The initial Actin displacement vectors derived from the PIV (centre panel) must be filtered in order to remove spurious vectors. The velocity field (right panel) is colour

coded with respect to the speed of the flow (from 0 to 12 μm min^{-1}), with the directions of the flow denoted by black unit vectors.

Movie 4: Time persistent sinks in the Actin network consist of compression and disassembly. The left panel shows a heatmap of the Actin flow divergence in a migrating hemocyte. Note the similar localisation of compressive activity (centre panel) and sites of network disassembly (right panel).

Movie 5: Actin flow coherence can be measured using streamlines. Time-lapse movie of a freely moving hemocyte labelled with UAS-RedStinger (nuclear marker) and UAS-LifeAct-GFP (Actin). Streamlines seeded at equidistant point along the cell boundary (green lines) are overlaid showing where the Actin network flows to (left panel). Streamlines are highly confluent, often terminating in common streamline sinks, which can be tracked (magenta spots) (right panel).

Movie 6: Streamline sinks are better correlated to cell motion that edge extensions. Regions of edge extension are revealed by subtraction of consecutive binarized images of hemocytes from time-lapse movies (left panel). Position vectors can be constructed between the nucleus and the centroid of the regions of edge extension (yellow arrows). A streamline sink (magenta spot) is calculated by computing the number of streamlines converging in a singular region of the Actin network (centre panel). Position vectors can be constructed between this sink and the nucleus. Note how the sinks appears to be coupled to cell motion while the largest region of extension exhibits exploratory behavior around the cell boundary (right panel).

Movie 7: Quantification of Actin flows in Myosin II and Cofilin mutant hemocytes. Time-lapse movie showing example of an Actin flow heatmap in a freely moving randomly migrating hemocyte (left panel). Note the variability in flow speeds across the lamella, as represented by colour fluctuations in the heatmap. Myosin II mutant hemocytes. Myosin II mutant hemocytes feature disrupted Actin dynamics, represented by low flow speeds and high variability in the directions of Actin flows, demonstrated reduced network coherence (centre panel). Cofilin mutant hemocytes feature disrupted Actin dynamics, represented by low flow speeds (right panel).

Movie 8: Actin flow coherence depends on Myosin II. Time-lapse movies showing the streamline representation of Actin flows in wild-type control (left panel), Myosin II mutants (centre panel), and Cofilin mutant hemocytes (right panel). Note the highly disorganised streamlines in the Myosin II mutant, which represent a loss in network coherence in the lamella.

Movie 9: Actin flow divergence is driven by Myosin II and Cofilin. Representative time-lapse movies showing divergence heatmaps of the Actin flow field in wild-type controls (left panel), Myosin II mutant (centre panel), and Cofilin mutant hemocytes (right panel). Note that in the mutant heatmaps, the overall intensity of Actin flow divergence is significantly reduced compared to controls.

Movie 10: Disassembly of the Actin network is driven by Myosin II and Cofilin. Representative time-lapse movies showing disassembly heatmaps of the Actin flow field in wild-type controls (left panel), Myosin II mutant (centre

panel), and Cofilin mutant hemocytes (right panel). Note that in the mutant heatmaps, the overall intensity of Actin network disassembly is significantly reduced compared to controls.

Movie 11: Quantification of Myosin II during migration. Time-lapse movie of a hemocyte labelled with UAS-Moesin-mCherry (Actin, left panel) and UAS-ZipperGFP (Myosin II heavy chain, centre panel). Puncta of Myosin II flows often decorate large Actin fibers, and flow centripetally beginning at the cell periphery (centre panel).

Movie 12: Analysing the colocalisation of Myosin II puncta and flow divergence. Time-lapse movie of a hemocyte labelled with UAS-Moesin-mCherry (Actin, left panel) and UAS-ZipperGFP (Myosin II heavy chain, centre panel). Images have been zoomed to highlight the activity of specific Myosin II puncta. Note that regions of intense negative divergence (right panel) do not coincide with Myosin II puncta.

Movie 13: Hemocytes rapidly respond to embryonic wounds. Time-lapse movie of freely moving hemocytes labelled with UAS-RedStinger (nuclear marker) and UAS-LifeAct-GFP (Actin) (left panel). Hemocytes occupy the ventral surface of the nerve cord during developmental dispersal. Directed migration in hemocytes can be stimulated by laser ablation of the embryonic epithelium (right panel). Here, hemocytes respond rapidly, migrating towards the wound site. Note that hemocyte no longer under contact inhibition of locomotion during a wound response.

Movie 14: Quantification of edge dynamics during random and directed migration. Regions of extension are revealed by subtraction of consecutive binarized images of hemocytes from time-lapse movies. Position vectors can be constructed between the nucleus and the centroid of the regions of edge extension (yellow arrows) and compared to the direction of cell motion. In random migration large edge extensions are uncorrelated with cell directionality (left panel). During directed migration large extensions directionally persistent and are often in the direction of cell travel (right panel). The wound site is highlighted by the white asterisk (right panel).

Bibliography

Abercrombie, M., Heaysman, J. E. M. and Pegrum, S. M. (1970) 'The locomotion of fibroblasts in culture. III. Movements of particles on the dorsal surface of the leading lamella', *Experimental Cell Research*, 62(2–3), pp. 389–398. doi: 10.1016/0014-4827(70)90570-7.

Adachi, T. *et al.* (2009) 'Strain field in actin filament network in lamellipodia of migrating cells: Implication for network reorganization', *Journal of Biomechanics*, 42(3), pp. 297–302. doi: 10.1016/j.jbiomech.2008.11.012.

Alexandrova, A. Y. *et al.* (2008) 'Comparative dynamics of retrograde actin flow and focal adhesions: Formation of nascent adhesions triggers transition from fast to slow flow', *PLoS ONE*, 3(9), pp. 1–9. doi: 10.1371/journal.pone.0003234.

Allard, J. and Mogilner, A. (2013) 'Traveling waves in actin dynamics and cell motility', *Current Opinion in Cell Biology*. Elsevier Ltd, 25(1), pp. 107–115. doi: 10.1016/j.ceb.2012.08.012.

Andrew, N. and Insall, R. H. (2007) 'Chemotaxis in shallow gradients is mediated independently of PtdIns 3-kinase by biased choices between random protrusions', *Nature Cell Biology*, 9(2), pp. 193–200. doi: 10.1038/ncb1536.

Arrieumerlou, C. and Meyer, T. (2005) 'A local coupling model and compass parameter for eukaryotic chemotaxis', *Developmental Cell*, 8(2), pp. 215–227. doi: 10.1016/j.devcel.2004.12.007.

Bangasser, B. L. *et al.* (2017) 'Shifting the optimal stiffness for cell migration', *Nature Communications*, 8(May), pp. 1–10. doi: 10.1038/ncomms15313.

Bard, L. *et al.* (2008) 'A Molecular Clutch between the Actin Flow and N-Cadherin Adhesions Drives Growth Cone Migration', *Journal of Neuroscience*, 28(23), pp. 5879–5890. doi: 10.1523/JNEUROSCI.5331-07.2008.

Barnhart, E. *et al.* (2015) 'Balance between cell−substrate adhesion and myosin contraction determines the frequency of motility initiation in fish keratocytes', *Proceedings of the National Academy of Sciences*, 112(16), pp. 5045–5050. doi: 10.1073/pnas.1417257112.

Barnhart, E. L. *et al.* (2011) 'An adhesion-dependent switch between mechanisms that determine motile cell shape', *PLoS Biology*, 9(5). doi: 10.1371/journal.pbio.1001059.

Benhamou, S. (2004) 'How to reliably estimate the tortuosity of an animal's path: Straightness, sinuosity, or fractal dimension?', *Journal of Theoretical Biology*, 229(2), pp. 209–220. doi: 10.1016/j.jtbi.2004.03.016.

Beningo, K. A. *et al.* (2001) 'Nascent Focal Adhesions Are Responsible for the Generation of Strong Propulsive Forces in Migrating Fibroblasts', 153(4), pp. 881–887.

Betz, T. (2007) *Actin Dynamics and Forces of Neuronal Growth*, *Physics*. Fakultat fur Physik und Geowissenschaften der Universitat at Leipzig.

Betz, T. *et al.* (2009) 'Stochastic actin polymerization and steady retrograde flow determine growth cone advancement', *Biophysical Journal*, 96(12), pp. 5130–5138. doi: 10.1016/j.bpj.2009.03.045.

Betz, T. *et al.* (2011) 'Growth cones as soft and weak force generators', *Proceedings of the National Academy of Sciences*, 108(33), pp. 13420–13425. doi: 10.1073/pnas.1106145108.

Betz, T., Lim, D. and Kas, J. A. (2006) 'Neuronal growth: A bistable stochastic process', *Physical Review Letters*, 96(9), pp. 1–4. doi: 10.1103/PhysRevLett.96.098103.

Blanchoin, L. *et al.* (2014) 'Actin dynamics, architecture, and mechanics in cell motility.', *Physiological reviews*, 94(1), pp. 235–63. doi: 10.1152/physrev.00018.2013.

Blanchoin, L. and Pollard, T. D. (1999) 'PROTEIN CHEMISTRY AND STRUCTURE : Mechanism of Interaction of Acanthamoeba Mechanism of Interaction of Acanthamoeba Actophorin (ADF / Cofilin) with Actin Filaments *', *The Journal of biological chemistry*, 274(22), pp. 15538–15546.

Bravo-Cordero, J. J. *et al.* (2013) 'Functions of cofilin in cell locomotion and invasion', *Nature Reviews Molecular Cell Biology*. Nature Publishing Group, 14(7), pp. 405–417. doi: 10.1038/nrm3609.

Brown, A. F. and Dunn, G. A. (1989) 'Microinterferometry of the movement of dry matter in fibroblasts', pp. 26–29.

Brückner, K. *et al.* (2004) 'The PDGF/VEGF receptor controls blood cell survival in Drosophila', *Developmental Cell*, 7(1), pp. 73–84. doi: 10.1016/j.devcel.2004.06.007.

Bugyi, B. and Carlier, M.-F. (2010) 'Control of Actin Filament Treadmilling in Cell Motility', *Annual Review of Biophysics*, 39(1), pp. 449–470. doi: 10.1146/annurev-biophys-051309-103849.

Burnett, M. M. and Carlsson, A. E. (2012) 'Quantitative analysis of approaches to measure cooperative phosphate release in polymerized actin', *Biophysical Journal*. Biophysical Society, 103(11), pp. 2369–2378. doi: 10.1016/j.bpj.2012.10.032.

Cant, K. *et al.* (1994) ‘Singed, a Fascin Homolog, Is Required for Actin Bundle Formation during Oogenesis and Bristle Extension’, *Journal of Cell Biology*, 125(2), pp. 369–380.

Case, L. B. *et al.* (2015) ‘Molecular mechanism of vinculin activation and nanoscale spatial organization in focal adhesions’, *Nature Cell Biology*, 17(7), pp. 880–892. doi: 10.1038/ncb3180.

Caspi, A. *et al.* (2001) ‘A new dimension in retrograde flow: Centripetal movement of engulfed particles’, *Biophysical Journal*. Elsevier, 81(4), pp. 1990–2000. doi: 10.1016/S0006-3495(01)75849-3.

Chan, C. E. and Odde, D. J. (2008) ‘Traction dynamics of filopodia on compliant substrates’, *Science*, 322(5908), pp. 1687–1691. doi: 10.1126/science.1163595.

Chen, W. T. (1979) ‘Induction of Spreading During Fibroblast Movement’, *Journal of Cell Biology*, 81(3), pp. 684–691.

Courson, D. S. and Rock, R. S. (2010) ‘Actin cross-link assembly and disassembly mechanics for ??-actinin and fascin’, *Journal of Biological Chemistry*, 285(34), pp. 26350–26357. doi: 10.1074/jbc.M110.123117.

Cramer, L. P., Kay, R. R. and Zatulovskiy, E. (2018) ‘Repellent and Attractant Guidance Cues Initiate Cell Migration by Distinct Rear-Driven and Front-Driven Cytoskeletal Mechanisms’, *Current Biology*. Elsevier Ltd., 28(6), p. 995–1004.e3. doi: 10.1016/j.cub.2018.02.024.

Dang, I. *et al.* (2013) ‘Inhibitory signalling to the Arp2/3 complex steers cell migration’, *Nature*, 503(7475), pp. 281–284. doi: 10.1038/nature12611.

Dang, I. *et al.* (2017) ‘The Arp2/3 inhibitory protein Arpin is dispensable for chemotaxis’, *Biology of the Cell*, 109(4), pp. 162–166. doi:

10.1111/boc.201600064.

Davis, J. R. *et al.* (2012) ‘Emergence of embryonic pattern through contact inhibition of locomotion’, *Development*, 139(24), pp. 4555–4560. doi: 10.1242/dev.082248.

Davis, J. R. *et al.* (2015) ‘Inter-cellular forces orchestrate contact inhibition of locomotion’, *Cell*. The Authors, 161(2), pp. 361–373. doi: 10.1016/j.cell.2015.02.015.

Dawe, H. R. *et al.* (2003) ‘ADF/cofilin controls cell polarity during fibroblast migration’, *Current Biology*, 13(3), pp. 252–257. doi: 10.1016/S0960-9822(03)00040-X.

Delorme, V. *et al.* (2007) ‘Cofilin Activity Downstream of Pak1 Regulates Cell Protrusion Efficiency by Organizing Lamellipodium and Lamella Actin Networks’, *Developmental Cell*, 13(5), pp. 646–662. doi: 10.1016/j.devcel.2007.08.011.

DesMarais, V. (2004) ‘Synergistic interaction between the Arp2/3 complex and cofilin drives stimulated lamellipod extension’, *Journal of Cell Science*, 117(16), pp. 3499–3510. doi: 10.1242/jcs.01211.

Doyle, A. D. *et al.* (2012) ‘Micro-environmental control of cell migration--myosin IIA is required for efficient migration in fibrillar environments through control of cell adhesion dynamics.’, *Journal of cell science*, 125(Pt 9), pp. 2244–56. doi: 10.1242/jcs.098806.

Duchek, P. *et al.* (2001) ‘Guidance of cell migration by the Drosophila PDGF/VEGF receptor’, *Cell*, 107(1), pp. 17–26. doi: 10.1016/S0092-8674(01)00502-5.

Dunn, G., Weber, I. and Zicha, D. (1997) ‘Protrusion, Retraction and the

Efficiency of Cell Locomotion', pp. 33–46.

Dunn, K. W., Kamocka, M. M. and McDonald, J. H. (2011) 'A practical guide to evaluating colocalization in biological microscopy', *Am J Physiol Cell Physiol*, 300, pp. 723–742. doi: 10.1152/ajpcell.00462.2010.

Elosegui-Artola, A., Trepat, X. and Roca-Cusachs, P. (2018) 'Control of Mechanotransduction by Molecular Clutch Dynamics', *Trends in Cell Biology*. Elsevier Ltd, 28(5), pp. 356–367. doi: 10.1016/j.tcb.2018.01.008.

Etienne-Manneville, S. (2013) 'Microtubules in Cell Migration', *Annual Review of Cell and Developmental Biology*, 29(1), pp. 471–499. doi: 10.1146/annurev-cellbio-101011-155711.

Euteneuer, U. and Schliwa, M. (1984) 'Persistent, directional motility of cells and cytoplasmic fragments in the absence of microtubules', *Nature*, 310(5972), pp. 58–61. doi: 10.1038/310058a0.

Evans, C. J., Hartenstein, V. and Banerjee, U. (2003) 'Thicker than blood: Conserved mechanisms in Drosophila and vertebrate hematopoiesis', *Developmental Cell*, 5(5), pp. 673–690. doi: 10.1016/S1534-5807(03)00335-6.

Evans, I. R. *et al.* (2010) 'Interdependence of macrophage migration and ventral nerve cord development in Drosophila embryos', *Development*, 137(10), pp. 1625–1633. doi: 10.1242/dev.046797.

Falzone, T. T. *et al.* (2012) 'Assembly kinetics determine the architecture of α-actinin crosslinked F-actin networks', *Nature Communications*. Nature Publishing Group, 3(May), pp. 861–869. doi: 10.1038/ncomms1862.

Forscher, P. and Smith, S. J. (1988) 'Actions of Cytochalasins on the Organization of Actin-Filaments and Microtubules in a Neuronal Growth

Cone', *Journal of Cell Biology*, 107(4), pp. 1505–1516. doi: DOI 10.1083/jcb.107.4.1505.

Fournier, M. F. *et al.* (2010) 'Force transmission in migrating cells', *The Journal of Cell Biology*, 188(2), pp. 287–297. doi: 10.1083/jcb.200906139.

Fritz-Laylin, L. K. *et al.* (2017) 'Actin-Based protrusions of migrating neutrophils are intrinsically lamellar and facilitate direction changes', *eLife*, 6, pp. 1–25. doi: 10.7554/eLife.26990.

Gant-Luxton, G. W. and Gundersen, G. G. (2011) 'Orientation and Function of the Nuclear Centrosomal Axis During Cell Migration', *Current Opinion in Cell Biology*, 23(5), pp. 579–588. doi: 10.1016/j.ceb.2011.08.001.Orientation.

Gardel, M. L. *et al.* (2008) 'Traction stress in focal adhesions correlates biphasically with actin retrograde fl ow speed', *Journal of Cell Biology*, 183(6), pp. 999–1005. doi: 10.1083/jcb.200810060.

Ghosh, M. *et al.* (2004) 'Cofilin Promotes Actin Polymerization and Defines the Direction of Cell Motility', *Science*, 304(5671), pp. 743–746. doi: 10.1126/science.1094561.

Giannone, G. *et al.* (2007) 'Lamellipodial Actin Mechanically Links Myosin Activity with Adhesion-Site Formation', *Cell*, 128(3), pp. 561–575. doi: 10.1016/j.cell.2006.12.039.

Giannone, G., Mege, R. M. and Thoumine, O. (2009) 'Multi-level molecular clutches in motile cell processes', *Trends in Cell Biology*, 19, pp. 475–486. doi: 10.1016/j.tcb.2009.07.001.

Gomes, E. R., Jani, S. and Gundersen, G. G. (2005) 'Nuclear movement regulated by Cdc42, MRCK, myosin, and actin flow establishes MTOC polarization in migrating cells', *Cell*, 121(3), pp. 451–463. doi:

10.1016/j.cell.2005.02.022.

Goodrich, H. (1924) ‘Cell Behavior in Tissue Cultures’, *Biological Bulletin*, 46(5), pp. 252–262.

Gorelik, R. and Gautreau, A. (2014) ‘Quantitative and unbiased analysis of directional persistence in cell migration.’, *Nature protocols*. Nature Publishing Group, 9(8), pp. 1931–43. doi: 10.1038/nprot.2014.131.

Gorelik, R. and Gautreau, A. (2015) ‘The Arp2/3 inhibitory protein arpin induces cell turning by pausing cell migration’, *Cytoskeleton*, 72(7), pp. 362–371. doi: 10.1002/cm.21233.

Gunsalus, K. C. *et al.* (1995) ‘Mutations in twinstar, a Drosophila gene encoding a cofilin/ADF homologue, result in defects in centrosome migration and cytokinesis’, *Journal of Cell Biology*, 131(5), pp. 1243–1259. doi: 10.1083/jcb.131.5.1243.

Guo, X. *et al.* (2015) ‘The galvanotactic migration of keratinocytes is enhanced by hypoxic preconditioning’, *Scientific Reports*. Nature Publishing Group, 5, pp. 1–13. doi: 10.1038/srep10289.

Haviv, L. *et al.* (2008) ‘A Cytoskeletal Demolition Worker: Myosin II Acts as an Actin Depolymerization Agent’, *Journal of Molecular Biology*, 375(2), pp. 325–330. doi: 10.1016/j.jmb.2007.09.066.

Heinemann, F., Doschke, H. and Radmacher, M. (2011) ‘Keratocyte lamellipodial protrusion is characterized by a concave force-velocity relation’, *Biophysical Journal*. Biophysical Society, 100(6), pp. 1420–1427. doi: 10.1016/j.bpj.2011.01.063.

Henson, J. H. *et al.* (1999) ‘Two components of actin-based retrograde flow in sea urchin coelomocytes.’, *Molecular biology of the cell*, 10(12), pp. 4075–

90. doi: 10.1091/mbc.10.12.4075.

Herant, M. and Dembo, M. (2010) ‘Form and function in cell motility: From fibroblasts to keratocytes’, *Biophysical Journal*. Biophysical Society, 98(8), pp. 1408–1417. doi: 10.1016/j.bpj.2009.12.4303.

Hermans, T. M. *et al.* (2013) ‘Motility efficiency and spatiotemporal synchronization in non-metastatic vs. metastatic breast cancer cells’, *Integrative Biology*, 5(12), p. 1464. doi: 10.1039/c3ib40144h.

Holz, A. *et al.* (2003) ‘The two origins of hemocytes in Drosophila.’, *Development (Cambridge, England)*, 130(20), pp. 4955–4962. doi: 10.1242/dev.00702.

Hu, K. *et al.* (2007) ‘Differential transmission of actin motion within focal adhesions’, *Science*, 315(5808), pp. 111–115. doi: 10.1126/science.1135085.

Huber, F., Käs, J. and Stuhrmann, B. (2008) ‘Growing actin networks form lamellipodium and lamellum by self-assembly’, *Biophysical Journal*, 95(12), pp. 5508–5523. doi: 10.1529/biophysj.108.134817.

Isambert, H. *et al.* (1995) ‘Flexibility of actin filaments derived from thermal fluctuations. Effect of bound nucleotide, phalloidin, and muscle regulatory proteins.’, *Journal of Biological Chemistry*, 270(19), pp. 11437–44.

Ishikawa, R. *et al.* (2003) ‘Polarized actin bundles formed by human fascin-1: Their sliding and disassembly on myosin II and myosin V in vitro’, *Journal of Neurochemistry*, 87(3), pp. 676–685. doi: 10.1046/j.1471-4159.2003.02058.x.

Janson, L. W., Kolega, J. and Taylor, D. L. (1991) ‘Modulation of contraction by gelation/solation in a reconstituted motile model’, *Journal of Cell Biology*,

114(5), pp. 1005–1015. doi: 10.1083/jcb.114.5.1005.

Ji, L., Lim, J. and Danuser, G. (2008) 'Fluctuations of intracellular forces during cell protrusion', *Nature Cell Biology*, 10(12), pp. 1393–1400. doi: 10.1038/ncb1797.

Jiang, G. *et al.* (2003) 'Two-piconewton slip bond between fibronectin and the cytoskeleton depends on talin', *Nature*, 424(6946), pp. 334–337. doi: 10.1038/nature01805.

Jurado, C. (2004) 'Slipping or Gripping? Fluorescent Speckle Microscopy in Fish Keratocytes Reveals Two Different Mechanisms for Generating a Retrograde Flow of Actin', *Molecular Biology of the Cell*, 16(2), pp. 507–518. doi: 10.1091/mbc.E04-10-0860.

Kanchanawong, P. *et al.* (2010) 'Nanoscale architecture of integrin-based cell adhesions', *Nature*. Nature Publishing Group, 468(7323), pp. 580–584. doi: 10.1038/nature09621.

Kasza, K. E. *et al.* (2010) 'Actin filament length tunes elasticity of flexibly cross-linked actin networks', *Biophysical Journal*. Biophysical Society, 99(4), pp. 1091–1100. doi: 10.1016/j.bpj.2010.06.025.

Keren, K. *et al.* (2008) 'Mechanism of shape determination in motile cells', *Nature*, 453(7194), pp. 475–480. doi: 10.1038/nature06952.

Koestler, S. A. *et al.* (2008) 'Differentially oriented populations of actin filaments generated in lamellipodia collaborate in pushing and pausing at the cell front', *Nature Cell Biology*, 10(3), pp. 306–313. doi: 10.1038/ncb1692.

Kolega, J., Janson, L. W. and Taylor, D. L. (1991) 'The role of solation-contraction coupling in regulating stress fiber dynamics in nonmuscle cells', *Journal of Cell Biology*, 114(5), pp. 993–1003. doi: 10.1083/jcb.114.5.993.

Krause, M. and Gautreau, A. (2014) ‘Steering cell migration: Lamellipodium dynamics and the regulation of directional persistence’, *Nature Reviews Molecular Cell Biology*. Nature Publishing Group, 15(9), pp. 577–590. doi: 10.1038/nrm3861.

Krummel, M. F., Bartumeus, F. and Gerard, A. (2016) ‘T-cell Migration, Search Strategies and Mechanisms’, 16(3), pp. 193–201. doi: 10.1038/nri.2015.16.T-cell.

Lauffenburger, D. A. and Horwitz, A. F. (1996) ‘Cell migration: A physically integrated molecular process’, *Cell*, 84(3), pp. 359–369. doi: 10.1016/S0092-8674(00)81280-5.

Lee, J. *et al.* (1994) ‘Traction Forces Generated by Locomting Keratocytes’, *Journal of Cell Biology*, 127(6, Part 2), pp. 1957–1964. doi: 10.1083/JCB.127.6.1957.

Leithner, A. *et al.* (2016) ‘Diversified actin protrusions promote environmental exploration but are dispensable for locomotion of leukocytes’, *Nature Cell Biology*, 18(11), pp. 1253–1259. doi: 10.1038/ncb3426.

Lewis, J. P. (Industrial L. & M. (1995) ‘Fast Normalized Cross-Correlation Template Matching by Cross-’, *Vision Interface*, 1995(1), pp. 1–7. doi: 10.1007/s00034-009-9130-7.

Lin, C. H. *et al.* (1996) ‘Myosin drives retrograde F-actin flow in neuronal growth cones’, *Neuron*, 16(4), pp. 769–782. doi: 10.1016/S0896-6273(00)80097-5.

Lin, C. H. and Forscher, P. (1995) ‘Growth cone advance is inversely proportional to retrograde F-actin flow’, *Neuron*, 14(4), pp. 763–771. doi: 10.1016/0896-6273(95)90220-1.

Lomakin, A. J. *et al.* (2015) ‘Competition for actin between two distinct F-actin networks defines a bistable switch for cell polarization’, *Nature Cell Biology*, 17(11), pp. 1435–1445. doi: 10.1038/ncb3246.

Lowery, L. A. and Vactor, D. V (2009) ‘The trip of the tip : understanding the growth cone machinery’, *Nature Reviews Molecular Cell Biology*, 10(5), pp. 332–343. doi: 10.1038/nrm2679.The.

Machacek, M. *et al.* (2009) ‘Coordination of Rho GTPase activities during cell protrusion’, *Nature*. Nature Publishing Group, 461(7260), pp. 99–103. doi: 10.1038/nature08242.

Machacek, M. and Danuser, G. (2006) ‘Morphodynamic profiling of protrusion phenotypes.’, *Biophysical journal*. Elsevier, 90(4), pp. 1439–1452. doi: 10.1529/biophysj.105.070383.

Maiuri, P. *et al.* (2012) ‘The first World Cell Race’, *Current Biology*. Elsevier, 22(17), pp. R673–R675. doi: 10.1016/j.cub.2012.07.052.

Maiuri, P. *et al.* (2015) ‘Actin flows mediate a universal coupling between cell speed and cell persistence’, *Cell*, 161(2), pp. 374–386. doi: 10.1016/j.cell.2015.01.056.

Matsubayashi, Y. *et al.* (2017) ‘A Moving Source of Matrix Components Is Essential for De Novo Basement Membrane Formation’, *Current Biology*, 27(22), p. 3526–3534.e4. doi: 10.1016/j.cub.2017.10.001.

McCullough, B. R. *et al.* (2008) ‘Cofilin Increases the Bending Flexibility of Actin Filaments: Implications for Severing and Cell Mechanics’, *Journal of Molecular Biology*, 381(3), pp. 550–558. doi: 10.1016/j.jmb.2008.05.055.

McGough, A. *et al.* (1997) ‘Cofilin changes the twist of F-actin: Implications for actin filament dynamics and cellular function’, *Journal of Cell Biology*,

138(4), pp. 771–781. doi: 10.1083/jcb.138.4.771.

Mendes Pinto, I. *et al.* (2012) 'Actin Depolymerization Drives Actomyosin Ring Contraction during Budding Yeast Cytokinesis', *Developmental Cell*, 22(6), pp. 1247–1260. doi: 10.1016/j.devcel.2012.04.015.

Mendoza, M. C. *et al.* (2015) 'ERK reinforces actin polymerization to power persistent edge protrusion during motility', *Science Signaling*, 8(377), p. ra47. doi: 10.1126/scisignal.aaa8859.

Miao, L. *et al.* (2003) 'Retraction in Amoeboid Cell Motility Powered by Cytoskeletal Dynamics', *Science*, 302(5649), pp. 1405–1407. doi: 10.1126/science.1089129.

Mitchison, T. J. and Cramer, L. P. (1996) 'Actin-based cell motility and cell locomotion', *Cell*, 84(3), pp. 371–379. doi: 10.1016/S0092-8674(00)81281-7.

Mitchison, T. and Kirschner, M. (1988) 'Cytoskeletal dynamics and nerve growth.', *Neuron*, 1(9), pp. 761–772. doi: 0896-6273(88)90124-9 [pii].

Mogilner, A. and Oster, G. (1996) 'Cell motility driven by actin polymerization', *Biophysical Journal*. Elsevier, 71(6), pp. 3030–3045. doi: 10.1016/S0006-3495(96)79496-1.

Mogilner, A. and Oster, G. (2003a) 'Force generation by actin polymerization II: The elastic ratchet and tethered filaments', *Biophysical Journal*. Elsevier, 84(3), pp. 1591–1605. doi: 10.1016/S0006-3495(03)74969-8.

Mogilner, A. and Oster, G. (2003b) 'Polymer motors: Pushing out the front and pulling up the back', *Current Biology*, 13(18), pp. 721–733. doi: 10.1016/j.cub.2003.08.050.

Mogilner, A. and Rubinstein, B. (2010) 'Actin disassembly "clock" and membrane tension determine cell shape and turning: A mathematical model',

Journal of Physics Condensed Matter, 22(19). doi: 10.1088/0953-8984/22/19/194118.

Moreira, S. *et al.* (2010) 'Prioritization of Competing Damage and Developmental Signals by Migrating Macrophages in the Drosophila Embryo', *Current Biology*. Elsevier Ltd, 20(5), pp. 464–470. doi: 10.1016/j.cub.2010.01.047.

Murrell, M. P. and Gardel, M. L. (2012) 'F-actin buckling coordinates contractility and severing in a biomimetic actomyosin cortex', *Proceedings of the National Academy of Sciences*, 109(51), pp. 20820–20825. doi: 10.1073/pnas.1214753109.

Nagy, M. *et al.* (2010) 'Hierarchical group dynamics in pigeon flocks', *Nature*, 464(7290), pp. 890–893. doi: 10.1038/nature08891.

Nakata, T. *et al.* (2016) 'The Role of Stress Fibers in the Shape Determination Mechanism of Fish Keratocytes', *Biophysical Journal*. Biophysical Society, 110(2), pp. 481–492. doi: 10.1016/j.bpj.2015.12.014.

Nicholson-Dykstra, S., Higgs, H. N. and Harris, E. S. (2005) 'Actin dynamics: Growth from dendritic branches', *Current Biology*, 15(9), pp. 346–357. doi: 10.1016/j.cub.2005.04.029.

Nicholson-Dykstra, S. M. and Higgs, H. N. (2008) 'Arp2 depletion inhibits sheet-like protrusions but not linear protrusions of fibroblasts and lymphocytes', *Cell Motility and the Cytoskeleton*, 65(11), pp. 904–922. doi: 10.1002/cm.20312.

Niethammer, P. *et al.* (2009) 'A tissue-scale gradient of hydrogen peroxide mediates rapid wound detection in zebrafish', *Nature*. Nature Publishing Group, 459(7249), pp. 996–999. doi: 10.1038/nature08119.

Nishita, M. *et al.* (2005) ‘Spatial and temporal regulation of cofilin activity by LIM kinase and Slingshot is critical for directional cell migration’, *Journal of Cell Biology*, 171(2), pp. 349–359. doi: 10.1083/jcb.200504029.

Nordenfelt, P. *et al.* (2017) ‘Direction of actin flow dictates integrin LFA-1 orientation during leukocyte migration’, *Nature Communications*. Springer US, 8(1), p. 2047. doi: 10.1038/s41467-017-01848-y.

Ofer, N., Mogilner, A. and Keren, K. (2011) ‘Actin disassembly clock determines shape and speed of lamellipodial fragments’, *Proceedings of the National Academy of Sciences*, 108(51), pp. 20394–20399. doi: 10.1073/pnas.1105333108.

Okeyo, K. O. *et al.* (2009) ‘Actomyosin contractility spatiotemporally regulates actin network dynamics in migrating cells’, *Journal of Biomechanics*. Elsevier, 42(15), pp. 2540–2548. doi: 10.1016/j.jbiomech.2009.07.002.

Okeyo, K. O., Adachi, T. and Hojo, M. (2010) ‘Mechanical regulation of actin network dynamics in migrating cells’, *Journal of Biomechanical Science and Engineering*, 5(3), pp. 186–207. doi: 10.1299/jbse.5.186.

Oliver, T., Dembo, M. and Jacobson, K. (1999) ‘Separation of propulsive and adhesive traction stresses in locomoting keratocytes’, *Journal of Cell Biology*, 145(3), pp. 589–604. doi: 10.1083/jcb.145.3.589.

Olofsson, B. and Page, D. T. (2005) ‘Condensation of the central nervous system in embryonic Drosophila is inhibited by blocking hemocyte migration or neural activity’, *Developmental Biology*, 279(1), pp. 233–243. doi: 10.1016/j.ydbio.2004.12.020.

Ono, S. and Ono, K. (2002) ‘Tropomyosin inhibits ADF/cofilin-dependent

actin filament dynamics', *Journal of Cell Biology*, 156(6), pp. 1065–1076. doi: 10.1083/jcb.200110013.

Pankov, R. *et al.* (2005) 'A Rac switch regulates random versus directionally persistent cell migration', *Journal of Cell Biology*, 170(5), pp. 793–802. doi: 10.1083/jcb.200503152.

Park, J. S. *et al.* (2016) 'Directed migration of cancer cells guided by the graded texture of the underlying matrix', *Nature Materials*, 15(7), pp. 792–801. doi: 10.1038/nmat4586.

Parsons, B. and Foley, E. (2016) 'Cellular immune defenses of Drosophila melanogaster', *Developmental and Comparative Immunology*. Elsevier Ltd, 58, pp. 95–101. doi: 10.1016/j.dci.2015.12.019.

Peskin, C. S., Odell, G. M. and Oster, G. F. (1993) 'Cellular motions and thermal fluctuations: the Brownian ratchet', *Biophysical Journal*. Elsevier, 65(1), pp. 316–324. doi: 10.1016/S0006-3495(93)81035-X.

Petrie, R. J., Doyle, A. D. and Yamada, K. M. (2009) 'Random versus directionally persistent cell migration', *Nature Reviews Molecular Cell Biology*. Nature Publishing Group, 10(8), pp. 538–549. doi: 10.1038/nrm2729.

Pollard, T. D. (1986) 'Rate constants for the reactions of ATP-and ADP-actin with the ends of actin filaments', *Journal of Cell Biology*, 103(6), p. 2747. doi: 10.1083/jcb.103.6.2747.

Pollard, T. D. and Borisy, G. G. (2003) 'Cellular motility driven by assembly and disassembly of actin filaments', *Cell*, 112(4), pp. 453–465. doi: 10.1016/S0092-8674(03)00120-X.

Pontes, B. *et al.* (2017) 'Membrane tension controls adhesion positioning at

the leading edge of cells', *Journal of Cell Biology*, 216(9), pp. 2959–2977. doi: 10.1083/jcb.201611117.

Ponti, A. *et al.* (2004) 'Two distinct actin networks drive the protrusion of migrating cells', *Science*, 305(5691), pp. 1782–1786. doi: 10.1126/science.1100533.

Ponti, A. *et al.* (2005) 'Periodic patterns of actin turnover in lamellipodia and lamellae of migrating epithelial cells analyzed by quantitative fluorescent speckle microscopy', *Biophysical Journal*. Elsevier, 89(5), pp. 3456–3469. doi: 10.1529/biophysj.104.058701.

Prass, M. *et al.* (2006) 'Direct measurement of the lamellipodial protrusive force in a migrating cell', *Journal of Cell Biology*, 174(6), pp. 767–772. doi: 10.1083/jcb.200601159.

Prentice-Mott, H. V. *et al.* (2016) 'Directional memory arises from long-lived cytoskeletal asymmetries in polarized chemotactic cells', *Proceedings of the National Academy of Sciences*, 113(5), pp. 1267–1272. doi: 10.1073/pnas.1513289113.

Prochniewicz, E. *et al.* (2005) 'Cofilin increases the torsional flexibility and dynamics of actin filaments', *Journal of Molecular Biology*, 353(5), pp. 990–1000. doi: 10.1016/j.jmb.2005.09.021.

Rafelski, S. M. and Theriot, J. A. (2004) 'Crawling Toward a Unified Model of Cell Motility: Spatial and Temporal Regulation of Actin Dynamics', *Annual Review of Biochemistry*, 73(1), pp. 209–239. doi: 10.1146/annurev.biochem.73.011303.073844.

Raffel, M. *et al.* (2007) *Particle Image Velocimetry: A Practical Guide*. Second. Springer US.

Reymann, A.-C. *et al.* (2012) 'Actin Network Architecture Can Determine Myosin Motor Activity', *Science*, (260678). doi: 10.1126/science.1221708.

Ridley, A. J. *et al.* (2003) 'Cell Migration: Integrating Signals from Front to Back', *Science*, 302(5651), pp. 1704–1709. doi: 10.1126/science.1092053.

Ridley, A. J. (2011) 'Life at the leading edge', *Cell*. Elsevier Inc., 145(7), pp. 1012–1022. doi: 10.1016/j.cell.2011.06.010.

Ridley, A. J. (2015) 'Rho GTPase signalling in cell migration', *Current Opinion in Cell Biology*. Elsevier Ltd, 36, pp. 103–112. doi: 10.1016/j.ceb.2015.08.005.

del Rio, A. *et al.* (2009) 'Stretching Single Talin Rod Molecules Activates Vinculin Binding', *Science*, 323(5914), pp. 638–641. doi: doi: 10.1126/science.1162912.

Sabass, B. *et al.* (2008) 'High resolution traction force microscopy based on experimental and computational advances', *Biophysical Journal*, 94(1), pp. 207–220. doi: 10.1529/biophysj.107.113670.

Sánchez-Sánchez, B. J. *et al.* (2017) 'Drosophila Embryonic Hemocytes Produce Laminins to Strengthen Migratory Response', *Cell Reports*, 21(6), pp. 1461–1470. doi: 10.1016/j.celrep.2017.10.047.

Schaub, S., Bohnet, S., Laurent, V. M., Meister, J., *et al.* (2007) 'Comparative Maps of Motion and Assembly of Filamentous Actin and Myosin II in Migrating Cells', *Molecular Biology of the Cell*, 18, pp. 3723–3732. doi: 10.1091/mbc.E06.

Schaub, S., Bohnet, S., Laurent, V. M., Meister, J. J., *et al.* (2007) 'Comparative Maps of Motion and Assembly of Filamentous Actin and Myosin II in Migrating Cells', *Molecular Biology of the Cell*, 18, pp. 3723–

3732. doi: 10.1091/mbc.E06-09-0859.

Schaub, S., Meister, J.-J. and Verkhovsky, A. B. (2007) ‘Analysis of actin filament network organization in lamellipodia by comparing experimental and simulated images’, *Journal of Cell Science*, 120(8), pp. 1491–1500. doi: 10.1242/jcs.03379.

Schramm, A. C. *et al.* (2017) ‘Actin Filament Strain Promotes Severing and Cofilin Dissociation’, *Biophysical Journal*. Biophysical Society, 112(12), pp. 2624–2633. doi: 10.1016/j.bpj.2017.05.016.

Schwarz, U. S. and Gardel, M. L. (2012) ‘United we stand – integrating the actin cytoskeleton and cell–matrix adhesions in cellular mechanotransduction’, *Journal of Cell Science*, 125(13), pp. 3051–3060. doi: 10.1242/jcs.093716.

Shao, D., Levine, H. and Rappel, W.-J. W.-J. (2012) ‘Coupling actin flow, adhesion, and morphology in a computational cell motility model’, *Proceedings of the National Academy of Sciences of the United States of America*, 109(18), pp. 6851–6856. doi: 10.1073/pnas.1203252109.

Shishika, D. *et al.* (2014) ‘Male motion coordination in anopheline mating swarms’, *Scientific Reports*, 4, pp. 1–7. doi: 10.1038/srep06318.

Sidani, M. *et al.* (2007) ‘Cofilin determines the migration behavior and turning frequency of metastatic cancer cells’, *Journal of Cell Biology*, 179(4), pp. 777–791. doi: 10.1083/jcb.200707009.

Song, X. *et al.* (2006) ‘Initiation of cofilin activity in response to EGF is uncoupled from cofilin phosphorylation and dephosphorylation in carcinoma cells’, *Journal of Cell Science*, 119(14), pp. 2871–2881. doi: 10.1242/jcs.03017.

Stam, S. *et al.* (2017) ‘Filament rigidity and connectivity tune the deformation modes of active biopolymer networks’, *Proceedings of the National Academy of Sciences*, p. 201708625. doi: 10.1073/pnas.1708625114.

Starr, D. A. (2003) ‘ANChors away: an actin based mechanism of nuclear positioning’, *Journal of Cell Science*, 116(2), pp. 211–216. doi: 10.1242/jcs.00248.

Stramer, B. *et al.* (2005) ‘Live imaging of wound inflammation in Drosophila embryos reveals key roles for small GTPases during in vivo cell migration’, *Journal of Cell Biology*, 168(4), pp. 567–573. doi: 10.1083/jcb.200405120.

Stramer, B. *et al.* (2008) ‘Gene induction following wounding of wild-type versus macrophage-deficient Drosophila embryos’, *EMBO Reports*, 9(5), pp. 465–471. doi: 10.1038/embor.2008.34.

Stramer, B. *et al.* (2010) ‘Clasp-mediated microtubule bundling regulates persistent motility and contact repulsion in Drosophila macrophages in vivo’, *Journal of Cell Biology*, 189(4), pp. 681–689. doi: 10.1083/jcb.200912134.

Sun, Z., Guo, S. S. and Fässler, R. (2016) ‘Integrin-mediated mechanotransduction’, *Journal of Cell Biology*, 215(4). doi: 10.1083/jcb.201609037.

Suraneni, P. *et al.* (2012) ‘The Arp2/3 complex is required for lamellipodia extension and directional fibroblast cell migration’, *Journal of Cell Biology*, 197(2), pp. 239–251. doi: 10.1083/jcb.201112113.

Suter, D. M. *et al.* (1998) ‘The Ig superfamily cell adhesion molecule, apCAM, mediates growth cone steering by substrate-cytoskeletal coupling’, *Journal of Cell Biology*, 141(1), pp. 227–240. doi: 10.1083/jcb.141.1.227.

Svitkina, T. M. *et al.* (1997) ‘Analysis of the actin-myosin II system in fish

epidermal keratocytes: Mechanism of cell body translocation', *Journal of Cell Biology*, 139(2), pp. 397–415. doi: 10.1083/jcb.139.2.397.

Svitkina, T. M. and Borisy, G. G. (1999) 'Arp2/3 complex and actin depolymerizing factor/cofilin in dendritic organization and treadmilling of actin filament array in lamellipodia', *Journal of Cell Biology*, 145(5), pp. 1009–1026. doi: 10.1083/jcb.145.5.1009.

Swaminathan, V. *et al.* (2017) 'Actin retrograde flow actively aligns and orients ligand-engaged integrins in focal adhesions', *Proceedings of the National Academy of Sciences*, 114(40), pp. 10648–10653. doi: 10.1073/pnas.1701136114.

Tadokoro, S. *et al.* (2003) 'Talin binding to integrin β tails: A final common step in integrin activation', *Science*, 302(5642), pp. 103–106. doi: 10.1126/science.1086652.

Tanaka, K. *et al.* (2018) 'Structural basis for cofilin binding and actin filament disassembly', *Nature Communications*, 9(1), pp. 1–3. doi: 10.1038/s41467-018-04290-w.

Taylor, D. L., Fechheimer, M. and Shotton, D. M. (1982) 'Cytoplasmic Structure and Contractility: The Solation-Contraction Coupling Hypothesis [and Discussion]', *Philosophical Transactions of the Royal Society B: Biological Sciences*, 299(1095), pp. 185–197. doi: 10.1098/rstb.1982.0125.

Tepass, U. *et al.* (1994) 'Embryonic origin of hemocytes and their relationship to cell death in Drosophila.', *Development (Cambridge, England)*, 120(7), pp. 1829–1837. doi: 8223268.

Thievessen, I. *et al.* (2013) 'Vinculin-actin interaction couples actin retrograde flow to focal adhesions, but is dispensable for focal adhesion

growth', *Journal of Cell Biology*, 202(1), pp. 163–177. doi: 10.1083/jcb.201303129.

Urbano, J. M. *et al.* (2009) 'Drosophila laminins act as key regulators of basement membrane assembly and morphogenesis', *Development*, 136(24), pp. 4165–4176. doi: 10.1242/dev.044263.

Vallotton, P. *et al.* (2003) 'Recovery, visualization, and analysis of actin and tubulin polymer flow in live cells: A fluorescent speckle microscopy study', *Biophysical Journal*, 85(2), pp. 1289–1306. doi: 10.1016/S0006-3495(03)74564-0.

Vallotton, P. *et al.* (2004) 'Simultaneous mapping of filamentous actin flow and turnover in migrating cells by quantitative fluorescent speckle microscopy', *Proceedings of the National Academy of Sciences*, 101(26), pp. 9660–9665. doi: 10.1073/pnas.0300552101.

Verkhovsky, A. B., Svitkina, T. M. and Borisy, G. G. (1999) 'Self-polarization and directional motility of cytoplasm', *Current Biology*, 9(1), pp. 11–20. doi: 10.1016/S0960-9822(99)80042-6.

Vicente-Manzanares, M. *et al.* (2009) 'Non-muscle myosin II takes centre stage in cell adhesion and migration', *Nature Reviews Molecular Cell Biology*. Nature Publishing Group, 10(11), pp. 778–790. doi: 10.1038/nrm2786.

Vinson, V. K. *et al.* (1998) 'Interactions of Acanthamoeba profilin with actin and nucleotides bound to actin', *Biochemistry*, 37(31), pp. 10871–10880. doi: 10.1021/bi980093l.

Waltzer, L. *et al.* (2002) 'Two isoforms of serpent containing either one or two GATA zinc fingers have different roles in Drosophila haematopoiesis', *EMBO*

Journal, 21(20), pp. 5477–5486. doi: 10.1093/emboj/cdf545.

Waterman-Storer, C. M. and Danuser, G. (2002) 'New directions for Fluorescent Speckle Microscopy', *Current Biology*, 12(18), pp. 633–640. doi: 10.1016/S0960-9822(02)01139-9.

Waterman-Storer, C. M. and Salmon, E. D. (1997) 'Actomyosin-based retrograde flow of microtubules in the lamella of migrating epithelial cells influences microtubule dynamic instability and turnover and is associated with microtubule breakage and treadmilling', *Journal of Cell Biology*, 139(2), pp. 417–434. doi: 10.1083/jcb.139.2.417.

Weavers, H. and Wood, W. (2016) 'Creating a Buzz about Macrophages: The Fly as an In Vivo Model for Studying Immune Cell Behavior', *Developmental Cell*. Elsevier Inc., 38(2), pp. 129–132. doi: 10.1016/j.devcel.2016.07.002.

Weiger, M. C. *et al.* (2010) 'Directional persistence of cell migration coincides with stability of asymmetric intracellular signaling', *Biophysical Journal*. Biophysical Society, 98(1), pp. 67–75. doi: 10.1016/j.bpj.2009.09.051.

Weiner, O. D. *et al.* (2002) 'A PtdInsP3 - and Rho GTPase-mediated positive feedback loop regulates neutrophil polarity', *Nature Cell Biology*, 4(7), pp. 509–513. doi: 10.1038/ncb811.A.

Welch, M. D. *et al.* (1997) 'Actin dynamics in vivo', *Current Opinion in Cell Biology*, 9(1), pp. 54–61. doi: 10.1016/S0955-0674(97)80152-4.

Westerweel, J. (1997) 'Fundamentals of digital particle image velocimetry', *Measurement Science and Technology*, 8(12), pp. 1379–1392. Available at: http://iopscience.iop.org/article/10.1088/0957-0233/8/12/002/pdf.

Wilson, C. A. *et al.* (2010) 'Myosin II contributes to cell-scale actin network

treadmilling through network disassembly', *Nature*. Nature Publishing Group, 465(7296), pp. 373–377. doi: 10.1038/nature08994.

Wilson, C. A. and Theriot, J. A. (2006) 'A correlation-based approach to calculate rotation and translation of moving cells', *IEEE Transactions on Image Processing*, 15(7), pp. 1939–1951. doi: 10.1109/TIP.2006.873434.

Wood, W., Faria, C. and Jacinto, A. (2006) 'Distinct mechanisms regulate hemocyte chemotaxis during development and wound healing in Drosophila melanogaster', *Journal of Cell Biology*, 173(3), pp. 405–416. doi: 10.1083/jcb.200508161.

Wood, W. and Jacinto, A. (2007) 'Drosophila melanogaster embryonic haemocytes: Masters of multitasking', *Nature Reviews Molecular Cell Biology*, pp. 542–551. doi: 10.1038/nrm2202.

Wood, W. and Martin, P. (2017) 'Macrophage Functions in Tissue Patterning and Disease: New Insights from the Fly', *Developmental Cell*. Elsevier Inc., 40(3), pp. 221–233. doi: 10.1016/j.devcel.2017.01.001.

Wu, C. *et al.* (2012) 'Arp2/3 is critical for lamellipodia and response to extracellular matrix cues but is dispensable for chemotaxis', *Cell*. Elsevier Inc., 148(5), pp. 973–987. doi: 10.1016/j.cell.2011.12.034.

Yam, P. T. *et al.* (2007) 'Actin-myosin network reorganization breaks symmetry at the cell rear to spontaneously initiate polarized cell motility', *Journal of Cell Biology*, 178(7), pp. 1207–1221. doi: 10.1083/jcb.200706012.

Yamao, M. *et al.* (2015) 'Distinct predictive performance of Rac1 and Cdc42 in cell migration', *Scientific Reports*. Nature Publishing Group, 5, pp. 1–14. doi: 10.1038/srep17527.

Yang, H. W., Collins, S. R. and Meyer, T. (2016) 'Locally excitable Cdc42

signals steer cells during chemotaxis', *Nature Cell Biology*, 18(2), pp. 191–201. doi: 10.1038/ncb3292.

Young, P. E. *et al.* (1993) 'Morphogenesis in Drosophila requires nonmuscle myosin heavy chain function', *Genes Dev*, 7(1), pp. 29–41. doi: 10.1101/gad.7.1.29.

Yumura, S., Mori, H. and Fukui, Y. (1984) 'Localization of actin and myosin for the study of ameboid movement in Dictyostelium using improved immunofluorescence', *Journal of Cell Biology*, 99(3), pp. 894–899. doi: 10.1083/jcb.99.3.894.

Zajac, M. *et al.* (2008) 'Depolymerization-driven flow in nematode spermatozoa relates crawling speed to size and shape', *Biophysical Journal*. Elsevier, 94(10), pp. 3810–3823. doi: 10.1529/biophysj.107.120980.

Zanet, J. *et al.* (2012) 'Fascin promotes filopodia formation independent of its role in actin bundling', *Journal of Cell Biology*, 197(4), pp. 477–486. doi: 10.1083/jcb.201110135.

Zhu, J. *et al.* (2009) 'The structure of a receptor with two associating transmembrane domains on the cell surface: integrin αIIbβ3', 34(2), pp. 234–249. doi: 10.1016/j.molcel.2009.02.022.The.